

**TRANSCRIPTIONAL REGULATION OF TYPE 2 INNATE LYMPHOID CELLS BY  
INTERLEUKIN-7 RECEPTOR SIGNALING**

by

Julia Chi Lam Lu

B.Sc., University of Alberta, 2018

A THESIS SUBMITTED IN PARTIAL FULFILLMENT OF  
THE REQUIREMENTS FOR THE DEGREE OF

MASTER OF SCIENCE

in

THE FACULTY OF GRADUATE AND POSTDOCTORAL STUDIES  
(Microbiology and Immunology)

THE UNIVERSITY OF BRITISH COLUMBIA  
(Vancouver)

August 2022

© Julia Chi Lam Lu, 2022

The following individuals certify that they have read, and recommend to the Faculty of Graduate and Postdoctoral Studies for acceptance, a thesis entitled:

Transcriptional regulation of type 2 innate lymphoid cells by interleukin-7 receptor signaling

submitted by Julia Chi Lam Lu in partial fulfillment of the requirements for

the degree of Master of Science

in Microbiology and Immunology

**Examining Committee:**

Ninan Abraham, Professor, Microbiology & Immunology and Zoology, University of British Columbia

Supervisor

Kelly McNagny, Professor, Medical Genetics, University of British Columbia

Supervisory Committee Member

Maria Tokuyama, Assistant Professor, Microbiology and Immunology, University of British Columbia

Additional Examiner

**Additional Supervisory Committee Members:**

Kelly Brown, Assistant Professor, Pediatrics, University of British Columbia

Supervisory Committee Member

## Abstract

Innate lymphoid cells (ILCs) are a rare population of innate immune cells that are part of the first line of defense against pathogens. These cells arise from the same lymphoid lineage that B cells, T cells, and NK cells belong to. Type 2 ILCs (ILC2s) are a subset of ILCs that reside in the lungs, mucosal layers, and skin, and have roles in clearing helminth infections, triggering allergic responses, and promoting lung tissue repair after Influenza infections. The function of these cells mirrors those of  $T_H2$  cells but lack the ability to recognize antigens. However, their full developmental background is still unknown. It is currently understood that ILC2s develop in the fetal liver and adult bone marrow from common lymphoid progenitors and differentiate into several intermediates before being classified as ILC2 progenitors (ILC2p). ILC2ps express interleukin-7 (IL-7) receptor with the aid of the transcription factor GATA3. Our lab has shown that IL-7 is a critical growth factor for ILC2 development as mutations to the IL-7 receptor showed a reduction in the ILC2 population and GATA-3 expression. Conversely, overexpression of IL-7 resulted in the expansion of the ILC2 population and elevated GATA-3 expression. I hypothesized that IL-7 transcriptionally regulates ILC2 maintenance and immune responses. Using qRT-PCR and high-parameter flow cytometry, I examined ILC2 development dependence on IL-7 and maternal IL-7 influence on offspring ILC2 populations. Through RNA sequencing, I identified the differences in the transcriptional landscapes regulated by IL-7 and thymic stromal lymphopoietin (TSLP) in lung ILC2s. This body of work will not only increase our understanding of a rare but vital cell population, but also contribute novel targets in therapeutic strategies for allergic asthma and viral infections.

## **Lay Summary**

Type 2 innate lymphoid cells (ILC2s) are rare immune cells found in the lungs, gut, and skin and are vital to fighting parasitic worm infection and lung tissue repair after Influenza infection. ILC2s may also cause unwanted effects such as stimulating inflammatory responses during allergic reactions. The development of ILC2s is tied to the expression of DNA regulator “GATA3” and receptor for an essential immune hormone “interleukin-7” (IL-7). I found that when IL-7 signaling was blocked, the total number of ILC2s and their GATA3 expression decreased in fetal and adult tissues. Fetal exposure to high doses of IL-7 was also found to potentially influence ILC2 development. Lastly, I showed that lung ILC2s treated with IL-7 or its related immune hormone “thymic stromal lymphopoietin” affected gene activity in these cells distinctly from each other. These findings will aid in the development of novel treatments for allergic asthma and airway viral infections.



## **Preface**

The research done in this thesis was developed collaboratively by Dr. Ninan Abraham and Julia Lu. All experiments were performed and analyzed by Julia Lu, with guidance from Dr. Abdalla Sheikh. In chapter 4, RNA sequencing was done by UBC Sequencing and Bioinformatics Consortium, and RNA sequencing analysis was done by Dr. Stephane Flibotte (UBC Life Sciences Institute Bioinformatics Facility).

All animal work was performed using protocols approved by the University of British Columbia Animal Care Committee (ACC; experimental protocol A17-0249 and breeding protocols A16-0154 and A20-0190) as per guidelines set by the Canadian Council on Animal Care.

## Table of Contents

<b>Abstract .....</b>	<b>iii</b>
<b>Lay Summary.....</b>	<b>iv</b>
<b>Preface .....</b>	<b>v</b>
<b>Table of Contents.....</b>	<b>vi</b>
<b>List of Tables.....</b>	<b>x</b>
<b>List of Figures .....</b>	<b>xi</b>
<b>List of Abbreviations .....</b>	<b>xiii</b>
<b>Acknowledgements .....</b>	<b>xv</b>
<b>Chapter 1: Introduction.....</b>	<b>1</b>
1.1    Innate lymphoid cells.....	1
1.1.1    Innate lymphoid cell development and tissue establishment.....	4
1.1.2    Importance of ILC2s in immune responses.....	5
1.1.2.1    ILC2s during Influenza infections.....	5
1.1.2.2    ILC2s during respiratory allergic reactions and asthma.....	6
1.2    Interleukin-7 and family cytokines.....	7
1.2.1    Interleukin-7 and thymic stromal lymphopoietin .....	8
1.2.2    Interleukin-7 in ILC development and function.....	8
1.2.3    Interleukin-7 treatments and therapies .....	9
1.3    Hypothesis and aims.....	11
<b>Chapter 2: Materials and Methods.....</b>	<b>12</b>
2.1    Mouse strains, housing, and breeding .....	12

2.1.1	Timed matings .....	13
2.1.1.1	Maternal-fetal IL-7 exposure timed matings .....	13
2.2	Mouse tissue collection and single cell preparation .....	14
2.2.1	Bone marrow .....	14
2.2.2	Lungs .....	15
2.2.3	Thymus, spleen, and fetal liver.....	15
2.2.4	Immunomagnetic cell selection of ILC2s.....	15
2.3	Cytokine stimulation of ILC2s .....	16
2.3.1	<i>In vitro</i> IL-7 stimulation of bone marrow ILC2s.....	16
2.3.2	<i>In vivo</i> intranasal IL-7 and TSLP stimulation of lung ILC2s .....	16
2.4	Influenza infection.....	17
2.5	Flow cytometry.....	17
2.5.1	Cell staining.....	17
2.5.2	Cell sorting for RNA sequencing analysis .....	19
2.6	IL-7 ELISA.....	19
2.7	Lung ILC2 RNA sequencing.....	19
2.7.1	RNA extraction.....	19
2.7.2	RNA sequencing pipeline .....	20
2.8	Bone marrow ILC2 qRT-PCR.....	21
2.9	Statistical analyses.....	21
<b>Chapter 3: The importance of IL-7 receptor signaling and maternal-fetal IL-7 on ILC2</b>		
<b>development and peripheral tissue establishment.....</b>		<b>23</b>
3.1	Introduction .....	23

3.2	IL-7R $\alpha^{Y449F}$ knock-in signaling mutation affects bone marrow ILC2 marker transcripts and ILC2 numbers .....	24
3.2.1	ILC1s and ILC3s are unaffected by the IL-7R $\alpha^{Y449F}$ knock-in signaling mutation .....	30
3.3	IL-7R $\alpha^{Y449F}$ knock-in effects are independent of IL-7 receptor recycling.....	34
3.4	Impaired IL-7 signaling may impede fetal liver ILC2 development.....	37
3.5	Maternal-fetal IL-7 effects on fetal liver ILC2 development.....	41
3.6	Maternal-fetal IL-7 effects on adult offspring bone marrow ILC2s.....	43
3.7	Maternal-fetal IL-7 effects on lung ILC2 establishment and immune response .....	46
3.8	Summary and Discussion .....	53
3.8.1	Summary.....	53
3.8.2	Discussion.....	53
<b>Chapter 4: Transcriptomic analysis of IL-7 and TSLP signaling in lung ILC2s .....</b>		<b>58</b>
4.1	Introduction .....	58
4.2	Optimizing ILC2 surface markers for cell sorting.....	60
4.3	Transcriptional profiling of <i>in vivo</i> IL-7- and TSLP-stimulated lung ILC2s .....	62
4.4	Summary and Discussion .....	79
4.4.1	Summary.....	79
4.4.2	Discussion.....	79
<b>Chapter 5: Conclusion.....</b>		<b>84</b>
5.1	Summary of main findings .....	84
5.2	Implications for human health.....	85
5.3	Future Directions .....	89

5.3.1	Transcriptional effects of IL-7 signaling on fetal liver ILC2s.....	89
5.3.2	Genetic imprinting from maternal IL-7 on offspring bone marrow ILC2s .....	89
5.3.3	<i>Postn</i> and <i>Retnla</i> transcripts and protein expression in lung ILC2s.....	89
5.3.4	Transgenic IL-7 ILC2 immune responses to Influenza infections and airway irritants .....	90
5.3.5	IL-7 signaling during gut ILC2 immune responses.....	90
5.3.6	Signaling pathway analyses in IL-7R $\alpha$ <sup>Y449F</sup> ILC2s.....	90
5.4	Conclusions .....	91
<b>References.....</b>		<b>92</b>
<b>Appendix: 4-day <i>in vivo</i> intranasal IL-7 stimulation of lung ILC2s.....</b>		<b>109</b>

## List of Tables

Table 2.1 Different mouse strains used to study ILC2 development and function. ....	12
Table 2.2 Experimental mouse conditions of offspring mice in maternal-fetal IL-7 exposure experiments.....	14
Table 2.3 Flow cytometry antibodies used for experiments.....	18
Table 2.4 Mouse ILC2 qRT-PCR primer pair sequences.....	21
Table 3.1 Flow cytometry staining panel for bone marrow ILC2s. ....	28
Table 3.2 Flow cytometry staining panel for ILC1, ILC2, and ILC3 populations.....	31
Table 3.3 Flow cytometry staining panel for fetal liver ILC2s. ....	39
Table 3.4 Flow cytometry staining panel for naïve lung ILC2s and <i>in vivo</i> stimulated ILC2s.....	47
Table 3.5 Flow cytometry staining panel for Influenza infected lung ILC2s.....	50
Table 4.1 Flow cytometry staining panel for sorting lung ILC2s for RNA isolation.....	63
Table 4.2 Annotations of differentially expressed genes found in control, IL-7-stimulated, and TSLP-stimulated lung ILC2s.....	69
Table 4.3 Annotations of key genes associated with ILC2s for their development, homeostasis, and immune responses.....	70
Table 4.4 Annotations of differentially expressed genes found in control and IL-7-stimulated lung ILC2s. ....	76

## List of Figures

Figure 3.1 Key ILC2 marker transcripts are downregulated in IL-7R $\alpha^{Y449F}$ bone marrow ILC2s. .....	26
Figure 3.2 Impaired IL-7 signaling reduces adult BM ILC2 population and their GATA3 expression. ....	29
Figure 3.3 The IL-7 signalling defect in IL-7R $\alpha^{Y449F}$ mice only affects ILC2 numbers. ....	32
Figure 3.4 CD127 receptor recycling in IL-7R $\alpha^{Y449F}$ bone marrow ILC2s is similar to WT during a 10-day IL-7 stimulation. ....	36
Figure 3.5 Fetal liver ILC2s appear to be reduced in PLZF <sup>GFPcre</sup> /IL-7R $\alpha^{Y449F}$ mice. ....	38
Figure 3.6 E16.5 fetal liver ILC2s isolated from TgIL7 mothers appear to have higher cell counts and GATA3 expression compared to WT cells. ....	40
Figure 3.7 Fetal exposure to high concentrations of maternal IL-7 shows trends towards elevated offspring adult bone marrow ILC2 development. ....	42
Figure 3.8 Maternal-fetal IL-7 exposure does not impact adult thymic CD4 and CD8 T cells. ...	45
Figure 3.9 Fetal exposure to high doses of maternal IL-7 does not impact offspring adult lung ILC2 maintenance.....	48
Figure 3.10 Lung ILC2 response to PR8 Influenza challenge is unaffected by fetal exposure to high doses of maternal IL-7.....	52
Figure 4.1 Nrpl expression in lung ILC2s is independent of IL-7 signaling. ....	61
Figure 4.2 IL-7- and TSLP-stimulated lung ILC2s RNAseq dataset has good read coverage and clustered closely to published lung and fat ILC2 RNAseq datasets.....	65

Figure 4.3 TSLP-stimulated lung ILC2s have a distinct transcriptional landscape compared to control or IL-7-stimulated lung ILC2s. ....	68
Figure 4.4 Key ILC2 genes were not found to be differentially expressed in IL-7- or TSLP-stimulated lung ILC2s. ....	72
Figure 4.5 Intranasal IL-7-stimulated lung ILC2s downregulate <i>Retnla</i> and <i>Gzmb</i> transcripts in comparison to control lung ILC2s. ....	75
Figure 4.6 Key ILC2 genes were not differentially expressed in IL-7-stimulated lung ILC2s when compared to unstimulated controls. ....	78



## List of Abbreviations

$\gamma$ c	Gamma chain
ANOVA	Analysis of variance
ACK	Ammonium-Chloride-Potassium lysis buffer
BM	Bone marrow
CD	Cluster of differentiation
CHILP	Common helper innate lymphoid precursors
CLP	Common lymphoid cells
dpi	Days post-infection
Ex.x	Embryonic day x.x (x indicating day; ex. E10.5 = embryonic day 10.5)
EILP	Early innate lymphoid progenitor
ELISA	Enzyme-linked immunosorbent assay
FACS	Fluorescence activated cell-sorting
FBS	Fetal bovine serum
FMO	Fluorescence minus one
GFP	Green fluorescent protein
HAU	Hemagglutination unit
HBSS	Hanks' Balanced Salt Solution
IL	Interleukin
IL-7-KO	IL-7eGFP mouse/mice
IL-7R $\alpha$	Interleukin-7 receptor alpha
ILC	Innate lymphoid cell
ILCp	Innate lymphoid cell progenitor

ILC1	Type 1 innate lymphoid cell
ILC2	Type 2 innate lymphoid cell
ILC3	Type 3 innate lymphoid cell
Influenza PR8	Influenza A/PR/8/34
mf-IL7	Maternal-fetal IL-7
mL	Millilitre
NCS	Newborn calf serum
PBS	Phosphate buffered saline
PLZF	Promyelocytic leukemia zinc finger
TgIL7	Transgenic IL-7 mouse/mice
T <sub>H</sub> cells	T-helper cells
WT	Wild-type mouse/mice (C57BL/6J background)
μL	microlitre
μm	micrometer

## Acknowledgements

First and foremost, I would like to thank my supervisor, Dr. Ninan Abraham for his support, guidance, and mentorship. Thank you for pushing me to my maximum potential and sharing your passion for scientific research. You presented me with many invaluable opportunities for public outreach, professional development, and networking. You are an exceptional mentor!

Secondly, I would like to thank members of the Abraham Lab for their support and guidance. A special thank you to Dr. Jung Hee Seo – none of us would be able to do our research without you! Thank you, Dr. Abdalla Sheikh and Etienne Melese, for teaching me experimental techniques, troubleshooting my flow cytometry data, and giving a second opinion on my data.

I would like to thank all my current and past committee members: Dr. Kelly McNaghy, Dr. Kelly Brown, and Dr. Martin Hirst for their guidance and support throughout my studies. Also thank you, Dr. Michael Gold and Dr. Linda Matsuuchi, for their mentorship and giving me the opportunity to co-organize Tri-Lab Journal Club.

Finally, I would like to thank my family and friends. I offer my sincere gratitude to my family for their extended and unconditional support throughout my years of education. A special thank you to my partner, Colton Carlson, for being my personal cheerleader and distracting me with fun outdoor adventures.

*“We keep moving forward, opening new doors, and doing new things,  
because we’re curious and curiosity keeps leading us down new paths.”*

*- Walt Disney*

# Chapter 1: Introduction

## 1.1 Innate lymphoid cells

ILCs were identified in 2008 and 2009 as a heterogeneous cell population involved in immune defense against infection and tissue repair<sup>1</sup>. These cells are derived from the lymphoid lineage and can be considered the innate immune cell counterpart to adaptive CD4<sup>+</sup> T cells<sup>2</sup>. One difference between ILCs and CD4<sup>+</sup> T cells is that ILCs lack antigen recognition, thus solely relies on environmental cues of cytokines and alarmins to respond<sup>3</sup>. This also means ILC immune responses are more rapid and non-specific compared to adaptive T cell responses<sup>4</sup>. ILCs were extensively studied in mouse models and humans, however, there is a lack of ILC research on other mammals and non-mammals<sup>1</sup>. Based on extensive phylogenetic analysis of ILC signature genes, it is thought that ILC-like cell populations exist in lampreys, bony fish, amphibians, reptiles, and birds<sup>1, 5</sup>. Since ILC-like cells were identified in invertebrates and early vertebrates, ILCs are hypothesized to be the evolutionary precursor to T<sub>H</sub> cells due to their shared characteristics and lack of antigen specificity in ILCs<sup>2</sup>.

ILCs are classified into three subsets: type 1 ILCs (ILC1), type 2 ILCs (ILC2), and type 3 ILCs (ILC3)<sup>6</sup>. Each subset has their own distinct functions and expression of transcription factors and surface markers<sup>6, 7</sup>. Consistent with the notion that ILCs are the innate counterpart to T<sub>H</sub> cells, they share important development transcription factors and respond to similar signals<sup>2</sup>. Importantly, all ILCs lack immune cell lineage markers (CD3, CD19, CD56, CD68, CD205; classified as Lin<sup>-</sup>)<sup>6</sup>.

The defining characteristics of ILC1s are their production of IFN- $\gamma$  and inability to release T<sub>H</sub>2 and T<sub>H</sub>17 cytokines, which makes these cells the innate counterpart of T<sub>H</sub>1 cells<sup>6</sup>. ILC1s rely on Tbet as their key transcription factor for their development and function, and

express NK1.1 and NKp46, similar to T<sub>H</sub>1 and NK cells respectively<sup>8,9</sup>. Although they express NK cell markers, these cells are non-cytotoxic and respond to intracellular pathogens and tumours through the detection of interleukin (IL)-12, -15, -18 to activate macrophages and induce production of oxygen radicals<sup>9</sup>. ILC1s are tissue-resident cells primarily found in non-lymphoid tissues such as small intestine mucosa, liver, salivary glands, and female reproductive tract<sup>10</sup>. Unlike other ILC subsets, adult tissue-resident ILC1s are maintained through self-renewal rather than recruitment<sup>10</sup>.

ILC2s were first identified in 2006 as “non-B, non-T” cells that release IL-13 in response to IL-25 production<sup>6,11</sup>. Later, it was discovered that these cells can produce T<sub>H</sub>2 specific cytokines in response to IL-25, IL-33 and TSLP<sup>12</sup>. During parasitic infections, ILC2s have been shown to release IL-5, IL-6, and IL-9 to aid in infection clearance<sup>11,13</sup>. ILC2s also rely on GATA3 and ROR $\alpha$  transcription factors for their function and development, thus are the innate counterpart to T<sub>H</sub>2 cells<sup>14-17</sup>. ILC2s may remain in adult bone marrow and become tissue-residents or migrate into peripheral tissues such as the lungs where they can exacerbate allergic lung inflammation or promote tissue repair and homeostasis following influenza infections<sup>11,18-20</sup>. Lung ILC2s also express high neuropilin-1 (Nrp1) which is not seen in other mature ILC2 subsets<sup>21</sup>. Transfers of non-lung ILC2s into the lung environment resulted in the manifestation of Nrp1 expression on these cells indicating its tissue-induced and tissue-specific expression. New studies have shown that ILC2s may be involved in immune surveillance in tumour environments and are important in controlling tumor metastasis<sup>22</sup>. It is debated whether ILC2s were seeded during development and remained as tissue-residents or were activated and trafficked to sites where they were needed<sup>23,24</sup>. These contradictory findings suggest there may be two ILC2 subpopulations<sup>25</sup>.

The last subset are ILC3s that are defined by their ability to produce IL-17A IL-22, and IFN $\gamma$ . Similar to T<sub>H</sub>17 cells, ILC3s rely on ROR $\gamma$ t for their development and function<sup>26, 27</sup>. Characterization of ILC3s is much more complex because there are two subpopulations of ILC3s: lymphoid tissue-inducing cells (LTi cells) and natural cytotoxicity receptor (NCR) +/- ILC3s<sup>6, 28</sup>. LTi cells are required for secondary lymphoid organ development such as the spleen and lymph nodes during embryogenesis<sup>6</sup>. NCR+ and NCR- ILC3s differ in their production of IL-22 and IL-17A; NCR+ ILC3s only produce IL-22 while NCR- ILC3s can produce both cytokines<sup>3, 29, 30</sup>. NCR expression is associated with NKp46 expression and NK cell phenotype, which makes ILC3s similar to ILC1s<sup>28</sup>. ILC3s can be found at barrier tissues such as the skin, lung, and gastrointestinal tract, and their production of IL-22 is important for generating intestinal immune responses against pathogens<sup>28</sup>. Due to the diverse nature of ILC3s, they are thought to be tissue-resident sentinels and act as a communications hub for intestinal immunity<sup>28</sup>.

Although ILCs are classified under 3 different subsets for universal nomenclature purposes, it bears iterating that ILCs demonstrate plasticity between subsets<sup>31-33</sup>. For example, when treated *in vitro* with IL-1 $\beta$  and IL-12, ILC2s will convert into ILC1s and produce IFN $\gamma$ <sup>33</sup>. Using ST2-GFP reporter mice that tags IL-33-stimulated ILC2s with GFP, *in vivo* conversion of lung ILC2s to ILC1s has been shown during Influenza infection<sup>34</sup>. The induction of ROR $\gamma$ t expression in ILC2s will convert these cells into IL-17 producing ILC3s under conditions of papain-induced inflammation<sup>35</sup>. Similar changes also occur in ILC2s during *Nippostrongylus brasiliensis* helminth infections<sup>31</sup>. This plasticity observed in ILCs allows them to be highly adaptable to all immune stimuli but can exhibit conflicting immune responses. Under certain conditions, ILCs may exacerbate the pathology while in others, they aid in disease resolution, making them a complex immune cell subset to characterize.

### 1.1.1 Innate lymphoid cell development and tissue establishment

ILC development occurs in the fetal liver and adult BM of both humans and mice<sup>24, 36, 37</sup>. All ILCs begin as common lymphoid progenitors (CLPs) which can develop into B cells and T cells<sup>36, 38</sup>. CLPs upregulate Notch and Id2 to promote ILC development and block T and B cell development<sup>39, 40</sup>. At this stage, there is a heterogeneous cell population of common helper innate lymphoid precursors (CHILPs; also called common ILC progenitor) and NK cell precursors (NKps)<sup>39, 41</sup>. NKps have the capability to develop into NK cells through an independent developmental pathway while CHILPs progress onto ILC development by upregulating promyelocytic leukemia zinc finger (PLZF) and integrin  $\alpha_4\beta_7$  expression to become ILC progenitors (ILCps)<sup>36, 41, 42</sup>. PLZF is an excellent marker to use to study ILC development as its expression is halted prior to the commitment of ILCps into specific lineages<sup>36, 42</sup>. IL-7 receptor is also upregulated on all ILCps as it is required for their development<sup>43</sup>. During this stage of ILC development, ILCps commit to their lineage through the expression of subset specific transcription factors: Tbet for ILC1, GATA3 for ILC2, and ROR $\gamma$ t for ILC3<sup>41, 44</sup>. Once these cells commit to their lineage, they become subset progenitors (ILC1p, ILC2p, and ILC3p) and are ready to enter into the periphery from the fetal liver to complete maturation<sup>39</sup>.

It was recently discovered that the adult BM ILC2 pool continuously expanded and established themselves as tissue-resident cells within the first 6 months after birth<sup>20</sup>. Using a tamoxifen-induced fate-mapping model, it was observed that fate-mapped BM ILC2s were steadily diluted by newly generated unlabelled cells over a period of 4 months after tamoxifen removal. However, the examination of fate-mapped peripheral ILC2s in the lungs and small intestine revealed that the majority of these ILC2s remained tagged indicating that peripheral



ILC2s are stable, long-lived cells and few ILC2s seeded from the bone marrow during adulthood<sup>20</sup>.

It is still unclear what drives ILCp commitment to one of the three ILC subsets and how mature ILCs demonstrate subset plasticity. Current literature suggests there are complex transcription factor networks between GATA3 and Runx3 that regulate this<sup>44</sup>. If GATA3 is highly expressed, Runx3 expression is repressed to prevent expression of ILC1 and ILC3 transcription factors and Bcl11b expression is reinforced to promote ILC2 selection<sup>44-46</sup>. Conversely, if Runx3 is highly expressed, GATA3 expression is repressed to block the expression of ILC2 transcription factors and promote ILC1 and ILC3 selection through increased Rorc expression<sup>44, 47</sup>.

### **1.1.2 Importance of ILC2s in immune responses**

Although ILC2s are a rare innate immune cell subset that make up 0.4% to 1% of the total live cells in the lungs<sup>41, 48</sup>, they make a large contribution to immune responses to viral and parasitic infections as well as airway allergens and asthma. ILC2s stimulate T<sub>H</sub>2 immune responses when activated, however, these responses may not always benefit the host or patient. For instance, ILC2s are required for early innate responses to Influenza infection and tissue repair post-infection (see section 1.1.2.1) but can cause substantial pro-inflammatory responses in asthma patients upon encountering stimuli (see section 1.1.2.2).

#### **1.1.2.1 ILC2s during Influenza infections**

Influenza infections are conventionally known to induce T<sub>H</sub>1 immune responses; however, recent publications have shown that T<sub>H</sub>2 immune responses are required for full recovery<sup>18, 19, 49, 50</sup>. Upon the infiltration of Influenza virus in the lungs, infected lung epithelial cells rapidly release pro-inflammatory cytokines induced by NF-κB to enable recruitment of

innate immune cells such macrophages, NK cells, and dendritic cells. Recruited macrophages will release IL-33 which activates resident lung ILC2s and induces their IL-5 and IL-13 release. The release of these cytokines regulates eosinophil recruitment and mucous secretion<sup>50</sup>. It has been shown that the release of IL-13 by ILC2s can induce airway hyperreactivity in asthmatic patients during flu, a response independent of adaptive immunity<sup>19</sup>. IL-5 and IL-13 release by ILC2s has been shown to be regulated by IL-7 signaling as IL-7 signaling deficient mice have diminished cytokine release upon acute Influenza infection<sup>51</sup>. It has also been determined that ILC2 responses to Influenza infection are independent of CD4<sup>+</sup> T cells, despite both promoting T<sub>H</sub>2 immunity through the release of IL-5 and IL-13<sup>49</sup>.

In addition to releasing IL-5 and IL-13, ILC2s are also responsible for tissue repair and homeostasis once infection has cleared. In mouse models, when ILC2s are depleted or IL-33 signaling is blocked during an Influenza infection, mice showed reduced lung function and hampered airway tissue remodelling when the infection cleared<sup>18</sup>. It was shown that lung ILC2 accumulation occurred after infection had cleared and that amphiregulin release by ILC2s was a key promoter for lung tissue remodelling and rebuilding airway epithelial integrity<sup>18</sup>. Genome-wide transcriptional profiling showed lung ILC2s expressed genes related to wound healing, immune defense responses, and cell proliferation<sup>18</sup>.

#### **1.1.2.2 ILC2s during respiratory allergic reactions and asthma**

Eosinophilic inflammation, excessive mucous and IgE production, and presence of pro-inflammatory cytokines IL-4, IL-5, IL-9, and IL-13 are all key characteristics of respiratory allergic responses<sup>52, 53</sup>. Prior to the discovery of ILCs, it was thought that T<sub>H</sub>2 cells and mast cells were the main orchestrators of allergic reactions<sup>54</sup>. ILC2s were later found to have dominant roles in orchestrating these responses as well. Since ILC2s lack antigen receptors, their

responses to allergens are solely based on the release of IL-25, IL-33, TSLP released by surrounding epithelial cells<sup>7, 12</sup>. When ILC2s become activated indirectly by allergens, similar to Influenza infections, they release large amounts of IL-5 and IL-13 to drive pro-inflammatory responses<sup>53, 55</sup>. ILC2-deficient mice (ROR $\alpha$ -deficient model) have impaired T<sub>H</sub>2 responses to papain allergen due to deficiency of IL-13, which is needed to activate T<sub>H</sub>2 T cells and recruit dendritic cells<sup>54, 56</sup>. Adoptive transfer of ILC2s from WT to ILC2-deficient mice was sufficient to restore this defect.

Asthma is a chronic, T<sub>H</sub>2-skewed inflammatory disease of the lungs with a broad range of triggers and severities<sup>57</sup>. Since the discovery of ILC2s, it has been shown that asthmatic patients have increased numbers of peripheral blood ILC2s and T<sub>H</sub>2 cytokine levels<sup>58</sup>. Inhaled steroids are a common prescribed treatment for asthmatic patients as it suppresses the activation of inflammatory cells and release of inflammatory cytokines and chemokines<sup>59</sup>. However, TSLP-activated ILC2s are found to be resistant to corticosteroid (dexamethasone) treatment and were elevated post-treatment in patients indicating they may be the cause of severe or refractory asthma<sup>60, 61</sup>. Treatment with TSLP blockage or STAT5 signaling was shown to eliminate corticosteroid resistance in ILC2s.

## **1.2 Interleukin-7 and family cytokines**

IL-7 is a growth-promoting cytokine required for B cell, T cell, and ILC development. It is produced by stromal cells in the BM and thymus under homeostatic conditions<sup>62</sup>. IL-7 is a member of the common  $\gamma$ -chain cytokines which also includes IL-2, IL-4, IL-9, IL-15, and IL-21. Defects in IL-7 or its receptor results in severe immunodeficiencies which has resulted in IL-7 being one of the most extensively studied cytokines<sup>63</sup>. Conversely, when IL-7 is elevated above physiological levels, it can lead to the development of rheumatoid arthritis, psoriasis, and

inflammatory bowel disease<sup>64</sup>. IL-7 is not only critical for the development of key immune cells but is also important for thymic development (thymopoiesis) and CD8 T cell priming during Influenza infections<sup>63, 65</sup>.

### **1.2.1 Interleukin-7 and thymic stromal lymphopoietin**

The IL-7 receptor is a heterodimer consisting of IL-7R $\alpha$  (CD127) and the common  $\gamma$ -chain ( $\gamma_c$ ; CD132)<sup>66</sup>. Upon the binding of IL-7 to its receptor, Jak1 and Jak3 are activated and phosphorylated, which then recruits and phosphorylates STAT5. Phosphorylated STAT5 will translocate to the nucleus to regulate cell proliferation, homeostasis, and function. IL-7R $\alpha$  can also form a heterodimer with the TSLP receptor subunit (TSLPR) to allow for TSLP signaling. TSLP is produced by epithelial cells in the intestines, lungs, and skin<sup>67</sup>. In contrast to IL-7 signaling, the binding of TSLP to its receptor results in Jak1 and Jak2 activation to phosphorylate STAT5. Although the receptor for TSLP uses IL-7R $\alpha$ , it's signaling promotes the expression of non-essential genes for hematopoietic processes and genes for pro-inflammatory responses<sup>68, 69</sup>.

### **1.2.2 Interleukin-7 in ILC development and function**

Current literature suggests that IL-7 is indispensable for the development of ILCs and that specifically, ILC2s are heavily dependent on IL-7 signaling<sup>42, 43, 70, 71</sup>. The receptor for IL-7 appears on ILC2s during early development with transient expression, then remains highly expressed throughout the lifespan of these cells<sup>43, 70</sup>. There is evidence that IL-7 and Notch signals are key regulators of ILC differentiation from T cell development. When CLPs experience strong IL-7 and moderate Notch signaling in the fetal liver, ILC development is favoured, whereas low IL-7 and high Notch signaling promotes T cell development<sup>43, 72</sup>. Recent findings from our lab identified that IL-7 signaling was required for GATA3 expression in ILC2s during their development in adult BM<sup>51</sup>. When IL-7R signaling was impaired, BM ILC2s and

their GATA3 expression was significantly reduced<sup>51</sup>. Others have shown that deletion of IL-7 receptor resulted in the absence of ILC2s, suggesting IL-7 has roles in determining ILC2 fate in ILCps<sup>44, 70</sup>.

Current research on ILC2s and their requirement for IL-7 is heavily focused on developmental relevance, however, there is evidence that supports a requirement for IL-7 in ILC2 function. In a *Trichinella spiralis* infection study in Tbet-deficient mice, there was an increased number of ILC2s responding to such infection and elevated IL-5 and IL-13 production<sup>73</sup>. It was also determined that these ILC2s had higher expression of IL-7R $\alpha$ , suggesting IL-7 regulates ILC2 function<sup>73</sup>. IL-7 is also important for proper lung ILC2 responses to Influenza infections since a reduction in IL-5, IL-13, and amphiregulin was observed when IL-7 signaling was impaired<sup>51</sup>. Since amphiregulin is needed for tissue remodelling and homeostasis post-infection, loss of IL-7 may result in poorer Influenza infection outcomes with greater lung tissue damage.

### **1.2.3 Interleukin-7 treatments and therapies**

Due to the effects that IL-7 has on immune cell development and establishment of immune responses, it is an attractive candidate for immunotherapies and treatments. Early clinical trials focused on using recombinant human IL-7 (rhIL7) to improve vaccine efficacies. Numerous studies found that rhIL7 treatment near time of vaccination expanded the pool of antigen-specific effector and memory T cells and had long-lasting effects on the memory T cell<sup>74-78</sup>. IL-7 was also found to increase TCR repertoire diversity which may be beneficial for aging individuals with progressive immune deficiencies<sup>77</sup>. Other applications of IL-7 therapies include HIV infections, idiopathic CD4 T cell lymphopenia, congenital immunodeficiency, and post-hematopoietic stem cell transplantation<sup>77, 79</sup>. During early clinical trials of IL-7 therapy,

there were concerns over the potential of inducing lymphopenia and autoimmunity, but no adverse side effects were observed in these trials<sup>78</sup>. With the recent COVID-19 pandemic, it was discovered that rhIL-7 administered to critically ill COVID-19 patients helped reverse the pathologic hallmarks of COVID-19 without worsening inflammation or pulmonary injury<sup>80, 81</sup>. These findings are consistent with other studies that showed IL-7 restored lymphocyte numbers and synergistically improved antiviral treatments. This is relevant to ILC2s and their contribution to lung diseases since SARS-CoV2 utilizes Nrp1, a marker of lung ILC2s, as one of its cellular entry receptors<sup>82</sup>.

Clinical trials were later expanded into examining rhIL7 efficacy in cancer immunotherapies<sup>78, 83, 84</sup>. It was shown that chimeric antigen receptor (CAR) T cells treated with IL-7 expanded more robustly compared to IL-4 treatment and mediated potent antitumour immunity in mouse breast cancer models<sup>85, 86</sup>. IL-7 treatment has also been shown in metastatic melanoma and sarcoma patients to boost naïve T cell populations but not regulatory T cells (Tregs). This is a promising finding since Tregs contribute to tumour growth and abnormal immune responses to tumours<sup>79</sup>. Based on the benefits of combining vaccines with rhIL7 to expand TCR repertoires, prostate cancer vaccine Provenge was combined with rhIL7 and showed a doubling of prostate cancer-specific T cells that are likely to benefit patients<sup>79, 87</sup>.

### 1.3 Hypothesis and aims

Given that IL-7 is crucial to the development and function of ILC2s, **I hypothesized that IL-7 transcriptionally regulates ILC2 maintenance and immune responses.** I aim to answer the following questions in this study: What role does IL-7 play in ILC function and maintenance? How does IL-7 promote ILC2 maintenance and function in peripheral tissues? What are the downstream transcriptional effects of IL-7 and TSLP signaling in ILC2s? I first examined IL-7 signaling regulation of developing ILC2s in fetal liver and adult BM through analysis of GATA3 and key ILC2 surface markers. Next, I examined the long-term effects of IL-7 on functional responses to influenza infections. Lastly, the effects of IL-7 and TSLP signaling on mature lung ILC2s were examined through RNA sequencing of these cells following *in vivo* stimulation with IL-7 or TSLP. This study gained insights on a rare but vital cell population, but also contributed novel targets such as periostin and RELM- $\alpha$  for therapeutic strategies to treat immune-related diseases and infections.

## Chapter 2: Materials and Methods

### 2.1 Mouse strains, housing, and breeding

Mice were housed at the University of British Columbia (UBC) in the Center for Disease Modelling (CDM), a specific-pathogen-free facility. Mouse strains used and a brief description of them are listed in Table 2.1. Mice were housed till 6- to 8-weeks old before tissue isolation for experiments.

Strain	Brief description
C57BL/6J	Control, wild-type mice. Jackson Laboratory sourced.
IL-7eGFP (IL-7-KO)	IL-7 knock-out mouse in which IL-7 gene is replaced with GFP (homozygous expression) <sup>88</sup> . These mice were a gift from Dr. J. Mike McCune (UCSF).
IL-7R $\alpha$ <sup>Y449F</sup> (B6.129S7- <i>Il7r1m11mx</i> /J)	Knock-in hypomorph mouse with mutation from tyrosine to phenylalanine at motif 449 on IL-7R $\alpha$ ; B6 background <sup>89</sup> .
Transgenic IL-7 (TgIL7)	Transgenic mouse with IL-7 inserted at E $\mu$ promoter for high expression of IL-7; B6 background <sup>90, 91</sup> . These mice were a gift from Dr. Philip Leder (Harvard Medical School, Boston, MA).
TSLPR <sup>-/-</sup>	TSLPR knock-out mouse; B6 background <sup>92</sup> . These mice were a gift from Dr. James Ihle (St. Jude Children's Research Hospital, Memphis, TN).
PLZF <sup>GFPcre</sup>	Reporter mouse that incorporates an IRES-EGFPcre fusion protein expressed from the mouse PLZF/ <i>Zbtb16</i> promoter; B6 background <sup>36</sup> .
PLZF <sup>GFPcre</sup> /IL-7R $\alpha$ <sup>Y449F</sup>	PLZF <sup>GFPcre</sup> mouse crossed with IL-7R $\alpha$ <sup>Y449F</sup> mice; B6 background.

**Table 2.1 Different mouse strains used to study ILC2 development and function.**



### **2.1.1 Timed matings**

8 to 10 adult female mice of the same strain were housed together in a cage for 10 days to sync estrous cycles before separation, then paired with a male mouse between 4:00-5:00PM. Sunflower seeds were added to timed mating cages to optimize conditions for mating. Plugs were checked visually and with a metal probe before 8:00AM the next day to confirm successful mating. If a plug is found on the female mouse, that day was scored embryonic day 0.5 (E0.5). Plugged females were then singly housed and fed a high-fat diet. On E14.5, pregnancies were confirmed through visual check (i.e., rounded belly, enlarged nipple patches).

#### **2.1.1.1 Maternal-fetal IL-7 exposure timed matings**

TgIL7 female mice were mated with male WT mice following the protocol described in section 2.1.1. This breeding set-up differs from conventional TgIL7 breeding in that the female is TgIL7 rather than the male to allow for the transfer of IL-7 to the fetuses through the placenta but may result in poorer breeding outcomes as TgIL7 females have historically shown in our lab. Fetal overexpression of IL-7 does not occur as the IL-7 transgene in this mouse model is controlled by E $\mu$  heavy chain, which is only expressed in mature B and T cells<sup>90, 91</sup>. Tissues from offspring mice were not collected until 6 to 8 weeks after birth. Each experimental mouse condition and a brief description are provided in Table 2.2.

Experimental mouse condition	Brief description
WT	C57BL/6J mice with no exposure to maternal-fetal IL-7 (mf-IL7); control for WT+mf-IL7 mice. On C57BL/6J background.
WT + mf-IL7	WT offspring from female TgIL7 and male WT timed matings; have been exposed to mf-IL7 during fetal development.
TgIL7	TgIL7 mice with no exposure to mf-IL7; control for TgIL7+mf-IL7 mice. Overexpression of IL-7 does not occur until after birth.
TgIL7 + mf-IL7	TgIL7 offspring from female TgIL7 and male WT timed matings; have been exposed to mf-IL7 during fetal development and overexpress IL-7 after birth.

**Table 2.2 Experimental mouse conditions of offspring mice in maternal-fetal IL-7 exposure experiments.**

## **2.2 Mouse tissue collection and single cell preparation**

For all experiments, mice were anesthetized using 3% isoflurane carried through 1L/min oxygen before euthanasia. For bone marrow, thymus, and spleen tissues, CO<sub>2</sub> was then delivered at a flow rate of 12L/min before cervical dislocation to finalize euthanasia. For lungs and fetal liver tissues, 5% isoflurane in 1L/min oxygen was used to anesthetize mice before cervical dislocation to euthanize mice. Isopropanol was used to sterilize the animal before using scissors and tweezers to excise desired tissue(s). All tissues were placed in individually labelled sterile tubes with sterile ice-cold PBS on ice before cell isolation.

### **2.2.1 Bone marrow**

To isolate bone marrow, all excess muscle is scraped off femurs and tibias using scissors then the ends were cut off. Using a 27-gauge needle, 10mL ice-cold HBSS supplemented with 10% FBS or NCS was used to flush bone marrow from prepped femurs and tibias (10mL per bone). Samples were then centrifuged at 400G for 5 minutes at 4°C. ACK lysis buffer was used

to lyse red blood cells. Samples were resuspended in ice-cold HBSS supplemented with 10% FBS or NCS before cell counting with trypan blue.

### **2.2.2 Lungs**

To make single cell lung suspensions, lungs were minced with scissors followed with enzymatic digestion with 180 units/mL Collagenase IV and 20µg/mL DNase I in 5mL RPMI medium. Samples were placed in a shaking incubator at 37°C for 45 minutes before filtering through 70µm cell strainers. Cells were collected in conical tubes then centrifuged at 400G for 5 minutes at 4°C before using ACK lysis buffer to lyse red blood cells. Samples were resuspended in ice-cold HBSS supplemented with 10% FBS or NCS before cell counting with trypan blue.

### **2.2.3 Thymus, spleen, and fetal liver**

To collect fetal liver, the uterus was first isolated then washed with 15mL sterile ice-cold PBS before gently removing the fetuses. Each fetus was then decapitated before isolating for the liver with tweezers.

To make single cell suspensions, tissue of interest was filtered through 70µm cell strainers with ice-cold HBSS supplemented with 10% FBS or NCS. Filtered samples were then centrifuged at 400G for 5 minutes at 4°C. ACK lysis buffer was used to remove red blood cells. Cells were resuspended in ice-cold HBSS supplemented with 10% FBS or NCS for cell counting with trypan blue.

### **2.2.4 Immunomagnetic cell selection of ILC2s**

EasySep™ Mouse Streptavidin RapidSpheres™ Isolation Kits and EasySep™ Mouse ILC2 Enrichment Kits were purchased from StemCell Technologies (Vancouver, BC Canada) to aid in the enrichment of ILC2s from various tissue sources. For isolation of BM ILC2s for qRT-

PCR, EasySep™ Mouse ILC2 Enrichment Kit was used. For isolation of lung ILC2s post-stimulation with IL-7 or TSLP, EasySep™ Mouse Streptavidin RapidSpheres™ Isolation Kit was used after staining with biotin-labelled lineage antibodies to deplete Lineage+ cells (see section 2.4.1 for full list of lineage antibodies used).

## **2.3 Cytokine stimulation of ILC2s**

### **2.3.1 *In vitro* IL-7 stimulation of bone marrow ILC2s**

After preparing BM single cell suspensions,  $6 \times 10^6$  cells were seeded into 6-well plates in 2.5mL RPMI media. Cells were rested under serum starvation for 2 hours prior to stimulation. IL-7 (Peprotech, catalog #217-17) was prepared in RPMI media supplemented with 10% FBS, 1% penicillin-streptomycin, and 50μM 2-mercaptoethanol at a concentration of 20ng/mL. To stimulate the cells, 2.5mL of the prepared IL-7 was added to each well to create a final concentration of 10ng/mL IL-7. Controls were given same volume of RPMI media supplemented with 10% FBS, 1% penicillin-streptomycin, and 50μM 2-mercaptoethanol. Cells were incubated for 16 hours before collection for antibody staining and analysis by flow cytometry. Samples were collected at various timepoints over a 10-day period and supplemented with additional media (0.5-1mL) if phenol red indicated high acidity at later timepoints.

### **2.3.2 *In vivo* intranasal IL-7 and TSLP stimulation of lung ILC2s**

Recombinant mouse IL-7 (carrier-free) was purchased from Biolegend (catalog #577804) and TSLP was purchased from R&D (catalog #555-TS/CF). IL-7 was diluted to 2μg in 30μL sterile PBS before intranasal delivery. TSLP was first diluted to 10μg/mL with sterile PBS as a stock solution then prepared to 500ng in 30μL sterile PBS. Mice were put under shallow anesthesia with isoflurane before intranasal delivery of cytokines. Cytokine delivery was split

into two-15µL doses, one dose per nostril to prevent suffocation. Sterile PBS was used in the control mice. After intranasal cytokine delivery, mice were gently placed back in their cages and monitored until they behaved normally. Mice were then monitored daily until day of tissue collection. No pathologies were expected or occurred during these experiments.

## **2.4 Influenza infection**

Influenza A/PR/8/34 (PR8) was purchased from Charles River Laboratories (Wilmington, MA, USA). Mice were put under anesthesia with isoflurane before infection with 500 Hemagglutinin Units (HAU) of Influenza PR8 in 12.5µL of sterile PBS. Control/uninfected mice were given 12.5µL of sterile PBS alone. Infection lasted for 6 days before experimental endpoint. Infected mice were monitored daily following guidelines set by University of British Columbia ACC and Canadian Council on Animal Care.

## **2.5 Flow cytometry**

All flow cytometry data presented in this thesis were acquired on Attune NxT Flow Cytometer (Thermo Fisher Scientific; Waltham, MA) or CytoFlex Flow Cytometer (Beckman Coulter, California) offered by ubcFLOW single cell flow analytics core (Vancouver BC, Canada). Data were analyzed using FlowJo software (FlowJo LLC; Ashland, Oregon).

### **2.5.1 Cell staining**

All cell staining steps were done at 4°C in the dark using HBSS supplemented with 10% FBS or NCS. Mouse anti-2.4G2/Fc receptor (AbLab) was preincubated with cells at a 1:400 dilution prior to surface and intracellular staining steps to prevent non-specific antibody binding. Table 2.3 is a comprehensive list of all antibodies used and the titrated working dilution.

	Antibody	Company	Titred working dilution
Lineage markers	Anti-CD3 $\epsilon$ [2C11], biotin	AbLab	1/200
	Anti-B220 [RA-6B2], biotin	AbLab	1/200
	Anti-NK1.1 [PK136], biotin	AbLab	1/200
	Anti-CD11b [M1/70], biotin	AbLab	1/200
	Anti-CD11c [N418], biotin	AbLab	1/200
	Anti-Gr-1 [RB6-8C5], biotin	AbLab	1/200
	Anti-Ter119 [Ter119], biotin	AbLab	1/200
	Anti-CD11c [N418], biotin	AbLab	1/200
	Anti-CD45.1 [A20], biotin	AbLab	1/200
	Anti-TCR- $\beta$ [H57-597], biotin	Biolegend	1/200
	Anti-TCR- $\gamma\delta$ [UC-13D5], biotin	Biolegend	1/200
	Anti-CD4 [RM4-5], biotin	BD Biosciences	1/200
	Streptavidin, Brilliant Violet 650	BD Biosciences	1/100
Surface markers	Anti-ST2 [DJ8], FITC	MD Bioproducts	1/100
	Anti-ST2 [RMST2-2], PE	ThermoFisher Scientific	1/50
	Anti-CD127 [ebioSB/199], PerCP-eFluor 710	ThermoFisher Scientific	1/100
	Anti-Nrp1 [3DS304M], PE-Cy7	ThermoFisher Scientific	1/200
	Anti- $\alpha 4\beta 7$ [DATK32], PE	ThermoFisher Scientific	1/100
	Anti-Sca-1 [D7], APC	ThermoFisher Scientific	1/200
	Anti-CD4 [GK1.5], APC	ThermoFisher Scientific	1/200
	Anti-NK1.1 [PK136], FITC	Biolegend	1/100
	Anti-ICOS [C398.4A], PE/Dazzle 594	Biolegend	1/200
	Anti-CD45 [30- F11], Pacific Blue	Biolegend	1/400
	Anti-NKp46 [29A1.4], Brilliant Violet 605	Biolegend	1/100
	Anti-CD90.2 [30-H12], Alexa Fluor 700	Biolegend	1/400
Intracellular markers	Anti-CD8a, Alexia Fluor 488	AbLab	1/200
	Anti-IL-13 [eBio13A], PE/ PE-Cy7	ThermoFisher Scientific	1/200
	Anti-IL-5 [TRFK5], APC	Biolegend	1/200
	Anti-GATA3 [TWAJ], PE/ eFluor 660	ThermoFisher Scientific	1/50
	Anti-Tbet [4B10], PE-Cy7	ThermoFischer Scientific	1/100
	Anti-ROR $\gamma$ t [B2D], PE	ThermoFisher Scientific	1/100
	Anti-phospho-STAT5 [pY694], Alexa Fluor 647	BD Biosciences	1/50
	Rabbit anti-GATA3 [D13C9], primary monoclonal	Cell Signaling Technologies	1/100
	Donkey anti-Rabbit IgG (H+L), secondary antibody, PE	ThermoFisher Scientific	1/4000

**Table 2.3 Flow cytometry antibodies used for experiments.**

Viability stain [catalog #L34957 and #65-0865-14] (ThermoFisher Scientific) was used according to manufacturer's instructions. eBioscience Foxp3/Transcription Factor staining buffer set was purchased from ThermoFisher Scientific for intracellular marker staining except for phospho-STAT5 detection where cell fixation and permeabilization was done using 90% methanol (diluted with PBS) at -20°C overnight.

### **2.5.2 Cell sorting for RNA sequencing analysis**

Single lung cell suspensions were stained then enriched with immunomagnetic cell selection kit before using BD Influx Cell Sort to sort for Lineage- CD45<sup>+</sup> Thy1.2<sup>+</sup> ST2<sup>+</sup> Nrp1<sup>+</sup> cells (see Table 2.3 for Lineage antibodies used). Cells were directly sorted into RNAlater Stabilization Solution (ThermoFisher Scientific) for RNA isolation.

## **2.6 IL-7 ELISA**

Mouse IL-7 ELISA kits were purchased directly from Abcam (catalog #ab100714). Supernatants from 10-day IL-7 stimulation assays of bone marrow cells were collected and frozen at -80°C. Before running the protein assay, samples were thawed and diluted 1:2 with cell culture media. TgIL7 spleen lysates were also collected and used as a positive control. Manufacturer's instructions were followed for the ELISA assay.

## **2.7 Lung ILC2 RNA sequencing**

Tissues and cells for RNAseq were isolated following protocols as described in sections 2.2.2, 2.2.4, and 2.4.2.

### **2.7.1 RNA extraction**

RNeasy Micro Kit was purchased from Qiagen (catalog #74004) to process sorted lung cells. Briefly, lung single cell suspensions were made as described in section 2.2.2 then sorted as detailed in section 2.4.2. Sorted cells were then lysed with RLT lysis buffer included in RNeasy

Micro Kit then frozen at -80°C for storage. Manufacturer's instructions were followed for RNA isolation from lysed cells.

### **2.7.2 RNA sequencing pipeline**

RNA samples were analyzed on an Agilent Bioanalyzer RNA 6000 Nano chip for quality assessment before using SMART-Seq v4 Ultra Low Input RNA kit (catalog #634888) to amplify low-input RNAs. Samples were then sent to UBC Sequencing and Bioinformatics Consortium for library preparation and sequencing. Extracted DNA was quantified using Qubit fluorometry. Sequencing libraries were prepared using the Illumina DNA prep library preparation kit (formerly known as Nextera DNA Flex), according to manufacturer's instructions (Illumina, San Diego, CA, USA). Libraries were pooled and loaded onto a single NextSeq Mid output flow cell, generating paired-end 150 bp reads (260 million paired-end reads). Raw base call data (bcl) were converted into FastQ format using the bcl2fastq conversion software from Illumina. RNA sequencing analysis

RNAseq analysis was performed by Dr. Stephane Flibotte (UBC/Life Sciences Institute Bioinformatics Facility, University of British Columbia, Vancouver, BC Canada). The multiple pipelines for the analysis were taken from Vuilleumier *et al.*<sup>93</sup>. Briefly, sequencing reads were first put through FASTP<sup>94</sup> to remove duplicate and low-quality reads then quality checked with FASTQC<sup>95, 96</sup>. Adaptors were trimmed then reads were aligned against whole mouse genome (NCBI mm10) using STAR<sup>97</sup> and HISAT2<sup>98</sup>. Matrices of counts were created using STAR<sup>97</sup>, STAR-RSEM<sup>99</sup>, kallisto<sup>100</sup>, salmon<sup>101</sup>, and HISAT2-Stringtie<sup>98, 102, 103</sup>. DESeq2<sup>104</sup> and edgeR<sup>105-107</sup> was then used to calculate for differential expression of transcript reads. Scatterplots of read counts were created in RStudio<sup>108</sup> with ggplot2<sup>109</sup> using results calculated by kallisto and



DESeq2. Heatmaps of z-scores were created in RStudio with pheatmap<sup>110</sup> using results calculated by DESeq2.

## 2.8 Bone marrow ILC2 qRT-PCR

Tissues and cells for qRT-PCR were isolated following protocol described in sections 2.2.1 and 2.2.4. Qiagen RNeasy Micro Kit (catalog #74004) was used to isolate RNA. All RNA samples were stored at -80°C until needed. cDNA was generated using All-In-One 5X RT MasterMix purchased from Applied Biological Materials (catalog #G592) and stored at -20°C. PerfeCTa SYBR Green SuperMix purchased from QuantaBio (catalog #95054-500) was used for qRT-PCR master mixes. Primer sequences for mouse *Rora*, *Tbx21*, and *Il13* were collected from PrimerBank and listed in Table 2.4<sup>111-113</sup>. Mouse *Gata3* primer was purchased from Millipore Sigma (KiCqStart Primer, gene ID 14462, RefSeq ID NM\_008091; proprietary sequences).

Primer	Direction	Sequence (5'→3')
<i>Rora</i>	Forward	GTGGAGACAAATCGTCAGGAAT
	Reverse	TGGTCCGATCAATCAAACAGTTC
<i>Tbx21</i>	Forward	AGCAAGGACGGCGAATGTT
	Reverse	GGGTGGACATATAAGCGGTTC
<i>Il13</i>	Forward	CAGCCTCCCCGATACCAAAT
	Reverse	GCGAAACAGTTGCTTTGTGTAG

**Table 2.4 Mouse ILC2 qRT-PCR primer pair sequences.**

## 2.9 Statistical analyses

Statistical analyses and graphical data representation were done using Graphpad Prism 9 (version 9.4.0, San Diego, CA, USA). Data presented in this thesis are presented as mean ± SEM

and analyzed by unpaired Student's  $t$ -test or one-way ANOVA with Tukey's post-test as appropriate. Results giving a  $p$ -value of less than 0.05 were significant. Outliers were identified and removed using the robust regression and outlier removal (ROUT) method with  $Q=1\%$  (maximum false discovery rate).

## **Chapter 3: The importance of IL-7 receptor signaling and maternal-fetal IL-7 on ILC2 development and peripheral tissue establishment.**

### **3.1 Introduction**

During an Influenza infection in the lungs, innate immune cells are the first responders to the infection site to control spread until adaptive immune cells arrive and establish a more specific response<sup>114</sup>. Type 2 innate lymphoid cells (ILC2s) are one population of innate immune cells recruited that produce IL-5 and IL-13 in response to alarmins (IL-33, IL-25, TSLP) produced by damaged epithelial cells, macrophages, and dendritic cells<sup>18, 115</sup>. One unique characteristic of ILC2s is that they closely resemble T<sub>H</sub>2 cells in their induction of similar type 2 immune responses, GATA3 expression and requirement for IL-7 for development and function<sup>14-17</sup>. What differs between these cell types are their site of development and specificity of immune responses generated. Developing ILC2s are found in the fetal liver (FL) and adult bone marrow (BM). Unlike T cells, ILC2s develop fully in the FL and BM before migration to peripheral tissues. Lastly, ILC2s do not detect antigens so the immune responses produced are generic, unlike T cells which fine-tune their responses depending on the antigen they encounter.

Both developing and mature ILC2s heavily rely on IL-7 which conveys signals for homeostasis and proliferation<sup>42, 43, 70, 71</sup>. IL-7 is produced by stromal cells in the BM and epithelial cells in the periphery<sup>43, 66, 116</sup>. For IL-7 signaling to occur, IL-7R $\alpha$  (CD127) and common  $\gamma_c$  chain pair together to form IL-7 receptor (IL-7R) to permit responsiveness to IL-7<sup>69</sup>. Upon the binding of IL-7 to its receptor, Jak1 and Jak3 are recruited to the receptor for phosphorylation. This event then recruits STAT1, STAT3 and STAT5 to the receptor for their

phosphorylation. Once STAT proteins become phosphorylated, they can enter the nucleus and modulate transcription.

It is still undetermined how IL-7 regulates ILC2 development and establishment in peripheral tissues. Previous research has shown that ILC2 progenitor (ILC2p) numbers are significantly reduced in IL-7R-deficient mice in bone marrow and small intestine, however, early progenitors were unaffected<sup>15, 70, 117</sup>. A recent publication from our lab showed that bone marrow ILC2s and their GATA3 expression increases when IL-7 is supplemented<sup>51</sup>. Conversely when IL-7 signaling was disrupted, a loss of ILC2s and GATA3 expression was observed<sup>51</sup>. Finally, IL-7 signaling was also found to be critical for proper ILC2 immune responses to Influenza infection<sup>51</sup>.

Here, I propose IL-7 signaling regulates GATA3 expression which in turn controls ILC2 development and function. Using various IL-7 mutant mouse models, I showed that when IL-7 signaling was interrupted, a significant loss of ILC2s, *Gata3* transcripts, and GATA3 protein expression in adult BM was observed. Additionally, I observed that loss of IL-7 signaling only affected ILC2s, leaving ILC1s and ILC3s untouched. Lastly, the role of maternal-fetal IL-7 was found to have a minimal effect on ILC2 development and lung establishment in offspring mice. Together, these data indicate that IL-7 is a specific regulator of ILC2 development and function as well as their GATA3 expression.

### **3.2 IL-7R $\alpha$ <sup>Y449F</sup> knock-in signaling mutation affects bone marrow ILC2 marker transcripts and ILC2 numbers**

IL-7 is critical for the development of ILC2s, where it has been shown that loss of IL-7 resulted in reduced ILC2 populations<sup>70, 118</sup>. I hypothesized that IL-7 signaling regulates ILC2 development through the transcriptional regulation of ILC2 lineage factors. To assess whether

transcriptional regulation has a role, RNA was isolated from ILC2-enriched bone marrow samples from WT and IL-7R $\alpha$ <sup>Y449F</sup> mice for qRT-PCR analysis of key ILC2 genes: *Gata3*, *Rora*, and *Il13*. *Tbx21* (gene for Tbet) was also included to examine if key ILC1 gene expression was also affected in IL-7R $\alpha$ <sup>Y449F</sup> mice. IL-7R $\alpha$ <sup>Y449F</sup> mice have a hypomorphic, homozygous knock-in mutation at tyrosine (Y) residue 449 to phenylalanine (F) which impedes STAT5 signaling but does not result in as severe impairments to ILC2 development as IL-7-KO mice, which permits for the isolation of ILC2s for qRT-PCR analysis. The results showed that *Gata3* and *Rora* transcripts were downregulated in IL-7R $\alpha$ <sup>Y449F</sup> ILC2s in comparison to WT (Figure 3.1). The reduction in *Rora* can be attributed to it being a key regulator of GATA3. *Il13* and *Tbx21* transcripts were also shown to be downregulated in IL7R $\alpha$ <sup>Y449F</sup> ILC2s (Figure 3.1).

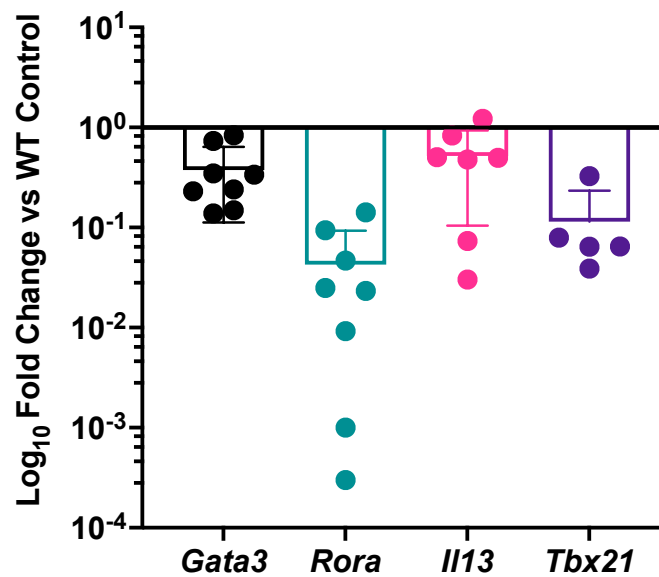


**Figure 3.1 Key ILC2 marker transcripts are downregulated in IL-7R $\alpha^{Y449F}$  bone marrow ILC2s.**

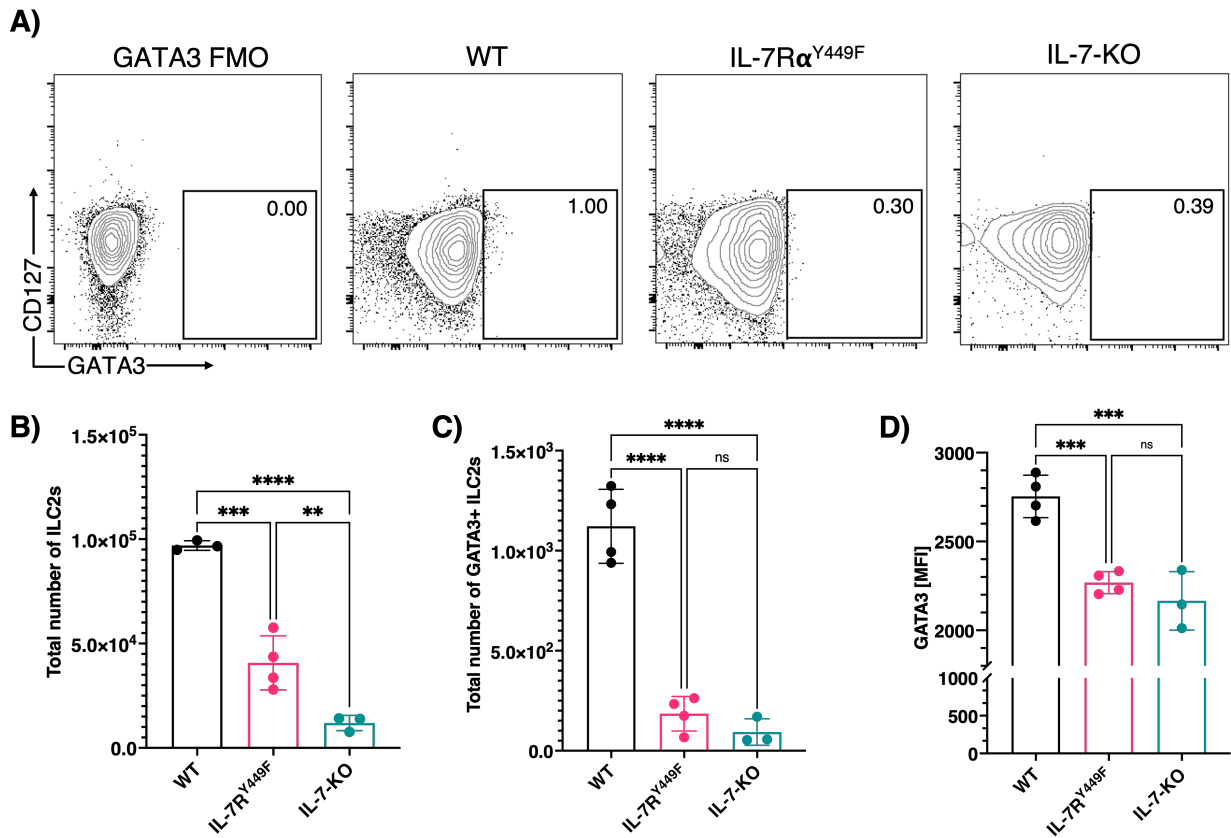
Log<sub>10</sub> scale of normalized expression values for *Gata3*, *Rora*, *Il13*, and *Tbx21* in IL-7R $\alpha^{Y449F}$  ILC2s compared to WT ILC2s. All genes were normalized to *Gapdh* reference gene. Graph shows mean + SEM from 5-8 samples.

Since canonical ILC2 marker transcripts were downregulated in IL7R $\alpha^{Y449F}$  ILC2s, I next examined whether these effects correlated with protein expression and cell numbers as detected by flow cytometry. Bone marrow from WT, IL-7R $\alpha^{Y449F}$ , and IL-7-KO mice were isolated and stained for BM ILC2 surface and intracellular markers as indicated in Table 3.1. It was observed that both IL-7R $\alpha^{Y449F}$  and IL-7-KO BM ILC2 numbers were significantly reduced compared to WT (Figure 3.2). GATA3 expression was also significantly reduced in IL-7R $\alpha^{Y449F}$  ILC2s which was predicted by qRT-PCR analysis showing *Gata3* transcripts were downregulated in these cells. IL-7-KO mice have the fewest detectable BM ILC2s and GATA3 expression.

<i>Lineage</i>	<i>Surface markers</i>	<i>ILC2 transcription factor</i>
<b>CD3</b> –CD8+ and CD4+ T cells (T cell co-receptor)	<b>Thy1.2/CD90.2</b>	<b>GATA3</b>
<b>CD4</b> – T-helper cells, monocytes, macrophages, dendritic cells	<b>ST2</b> - IL-33 receptor	
<b>CD11b</b> – monocytes, granulocytes, macrophages, NK cells	<b>CD127IL-7R<math>\alpha</math></b>	
<b>B220</b> – B-cells, some T and NK cells	<b>CD45.2</b>	
<b>NK1.1</b> – NK cells		
<b>Gr1</b> – granulocytes		
<b>Ter119</b> – red blood cells/erythrocytes		
<b>TCR<math>\beta</math></b> - T cells		
<b>TCR<math>\gamma\delta</math></b> - T cells (mainly $\gamma\delta$ T cells)		

**Table 3.1 Flow cytometry staining panel for bone marrow ILC2s.**



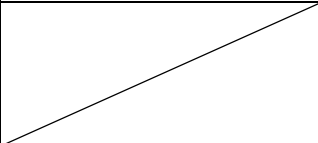
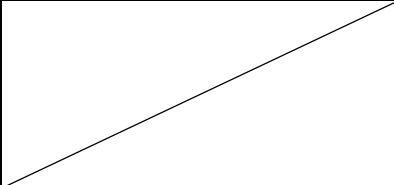


**Figure 3.2 Impaired IL-7 signaling reduces adult BM ILC2 population and their GATA3 expression.**

WT, IL-7R $\alpha^{Y449F}$ , and IL-7-KO adult BM ILC2s were stained for surface ILC2 markers and GATA3 for flow cytometry analysis. **A)** GATA3+ ILC2s in each representative flow cytometry plot is gated on the following criteria: single, live, CD45+, lineage-, ICOS+, CD127+, and GATA3+. GATA3 fluorescence minus one (FMO) was included as a gating control. **B)** Total number of BM ILC2s (ILC2ps) in each mouse strain indicated. **C)** Total number of BM GATA3+ ILC2s in each mouse strain indicated. **D)** GATA3 MFI of ILC2ps in each mouse strain indicated. Multiple Student's *t*-test and one-way ANOVA was performed for this data.

### 3.2.1 ILC1s and ILC3s are unaffected by the IL-7R $\alpha^{Y449F}$ knock-in signaling mutation

With the findings that impaired IL-7 signaling reduced adult BM ILC2 populations, I examined whether the signaling defect in IL-7R $\alpha^{Y449F}$  mice was specific to ILC2s or broadly affected all ILC subsets since IL-7 is required in early ILC development. BM cells were isolated from WT, IL-7R $\alpha^{Y449F}$ , and TSLPR $^{-/-}$  mice and stained for ILC1, ILC2, and ILC3 surface and intracellular markers as indicated in Table 3.2. TSLPR $^{-/-}$  BM served as a negative control since TSLP has minimal effects on ILC development<sup>43, 69</sup>. As shown in Figure 3.3A, there was a slight reduction in the Tbet $^{+}$  ILC1 population in IL-7R $\alpha^{Y449F}$  BM. However, absolute cell numbers and Tbet MFI showed there was no difference between all three genotypes (Figure 3.3B). It should be noted that earlier qRT-PCR analysis of the Tbet transcript, *Tbx21*, showed it was downregulated in IL-7R $\alpha^{Y449F}$  ILC2s. Similarly, ILC3s showed no difference in absolute cell numbers and ROR $\gamma$ t expression among the samples (Figure 3.3C, E). The population of ROR $\gamma$ t $^{+}$  cells was relatively large compared to ILC1s and ILC2s but likely due to the omission of CD4 and CD3 in the lineage cocktail used to identify ILCs. A portion of these ROR $\gamma$ t $^{+}$  cells are likely T<sub>H</sub>17 CD4 $^{+}$  cells as they also share the same transcription factor as ILC3s for development<sup>119</sup>. It is plausible that there may also be ILC3 subpopulations that are less dependent on IL-7 masking rarer ILC3 subpopulations that are affected by the knock-in mutation. Among all ILC subsets, only ILC2s were affected by the IL-7R $\alpha^{Y449F}$  signaling defect, with absolute cell numbers significantly reduced compared to the other two genotypes (Figure 3.3C, D). These results show that the IL-7R $\alpha$  knock-in mutation only affects ILC2, demonstrating their dependence on IL-7 for development and function.

<i>Lineage</i>	<i>Surface markers</i>	<i>ILC transcription factor</i>
<b>CD11b</b> – monocytes, granulocytes, macrophages, NK cells	<b>CD45.2</b>	<b>Tbet</b> – ILC1 marker
<b>CD11c</b> – dendritic cells, monocytes, macrophages, neutrophils, and B cells	<b>Thy1.2/CD90.2</b>	<b>GATA3</b> – ILC2 marker
<b>B220</b> – B-cells, some T and NK cells	<b>NK1.1</b>	<b>RORγt</b> – ILC3 marker
<b>Gr1</b> – granulocytes		
<b>Ter119</b> – red blood cells/erythrocytes		
<b>TCRβ</b> - T cells		
<b>TCRγδ</b> - T cells (mainly γδ T cells)		

**Table 3.2 Flow cytometry staining panel for ILC1, ILC2, and ILC3 populations.**

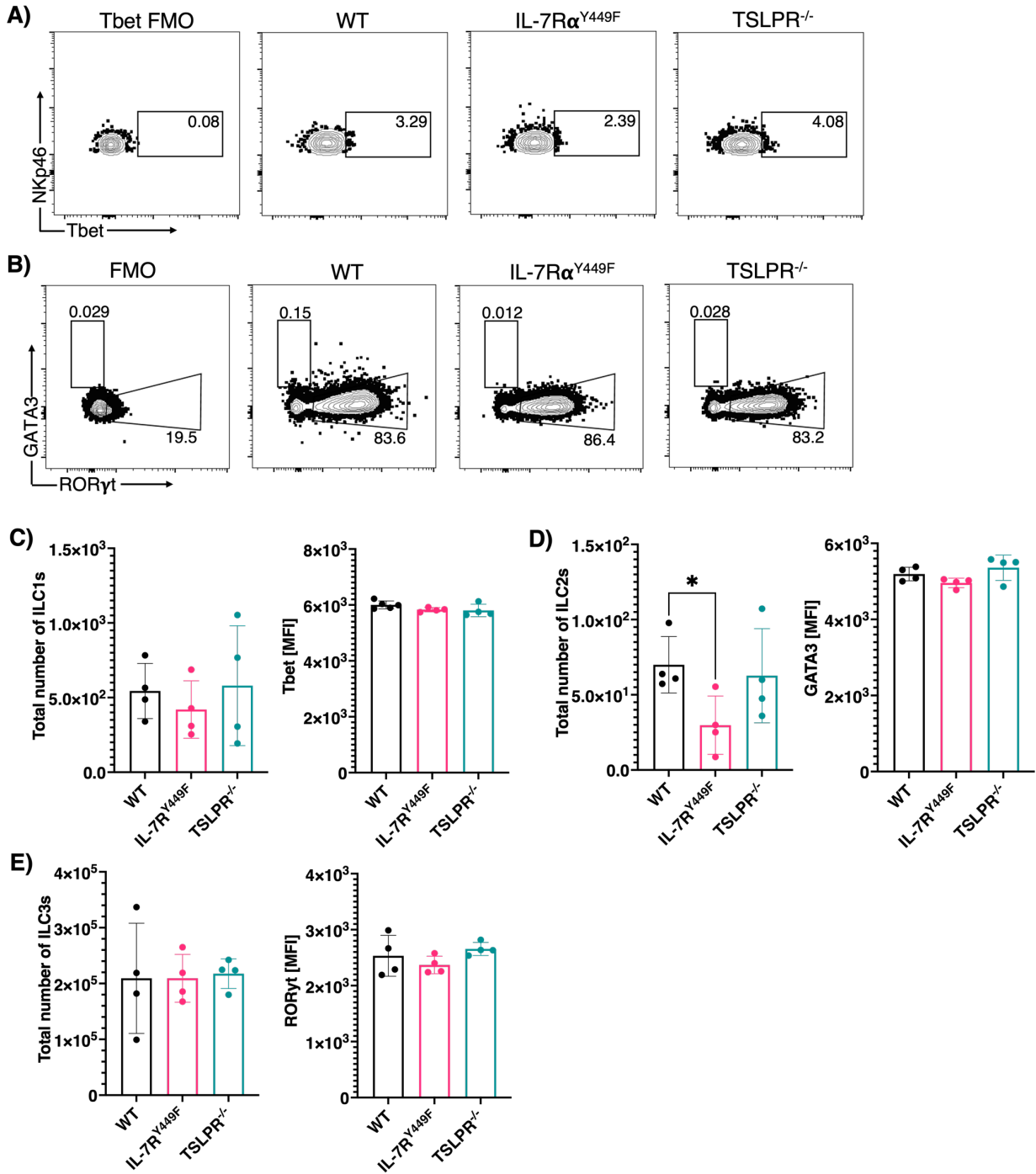


**Figure 3.3** The IL-7 signalling defect in IL-7R $\alpha^{Y449F}$  mice only affects ILC2 numbers.

Bone marrow cells were isolated from IL-7R $\alpha^{Y449F}$ , and TSLPR $^{-/-}$  mice for cell surface and intracellular marker analysis by flow cytometry (n=5 for WT, one outlier is excluded, n=4 for IL-

7R $\alpha^{Y449F}$  and TSLPR $^{-/-}$ ). **A)** ILC1s are identified as single, live, CD45 $^{+}$ , lineage $^{-}$ , NK1.1 $^{+}$ , NKp46 $^{+}$ , and Tbet $^{+}$  in representative flow plots. **B)** ILC2s are identified as single, live, CD45 $^{+}$ , lineage $^{-}$ , NK1.1 $^{-}$ , NKp46 $^{-}$ , and GATA3 $^{+}$ , while ILC3s are identified as single, live, CD45 $^{+}$ , lineage $^{-}$ , NK1.1 $^{-}$ , NKp46 $^{-}$ , and ROR $\gamma$ t $^{+}$  in representative flow plots. **C)** Total number of Tbet-expressing cells and Tbet MFIs are calculated from the data obtained by flow cytometry analysis. **D)** Total number of GATA3-expressing cells and GATA3 MFIs are calculated from the data obtained by flow cytometry analysis. **E)** Total number of ROR $\gamma$ t-expressing cells and ROR $\gamma$ t MFIs are calculated from the data obtained by flow cytometry analysis. Multiple Student's *t*-tests and one-way ANOVAs were performed for all this data.

### 3.3 IL-7R $\alpha$ <sup>Y449F</sup> knock-in effects are independent of IL-7 receptor recycling

I established that IL-7R $\alpha$ <sup>Y449F</sup> mice have impaired BM ILC2 development but it is unclear whether this observation is due to the inability of ILC2s to engulf the receptor and recycle it back to the cell surface, or solely due to incomplete or insufficient signaling cascade from the knock-in mutation<sup>69</sup>. To answer the former question, a 10-day *in vitro* IL-7 stimulation assay was done with WT and IL-7R $\alpha$ <sup>Y449F</sup> BM cells.

At each specified time point, cells were stained for ILC2 surface and intracellular markers as indicated in Table 3.1 for flow cytometry. In the stimulated WT condition, CD127 expression in ILC2s decreased after IL-7 was added to the media when compared to unstimulated condition (Figure 3.4A). GATA3 expression in unstimulated and IL-7 stimulated WT ILC2s began to increase at day 2 and peaked by day 4 (Figure 3.4B). I observed a downregulation of mutated CD127 in stimulated IL-7R $\alpha$ <sup>Y449F</sup> ILC2s similar to WT ILC2s, however, these cells failed to respond to IL-7 stimulation throughout the time course as detected through GATA3 expression (Figure 3.4C, D). It should be noted that unstimulated cells also expressed GATA3 in increasing levels as time progressed (Figure 3.4B, D). To determine whether there might be endogenous IL-7 that may be skewing the results, an IL-7 ELISA was done. Media conditions and TgIL7 spleen lysates were included as controls for the assay. From the IL-7 ELISA results, no endogenous IL-7 was detected indicated the absence of IL-7 released by the cultured cells (Figure 3.4E). This suggests it is likely that there are other stimulating cytokines and factors stimulating ILC2s, or enabling ILC2 differentiation, inducing GATA3 independently of IL-7. Combining the results in this section, the Y449F knock-in mutation in IL-7R $\alpha$  mice does not alter CD127 receptor internalization.

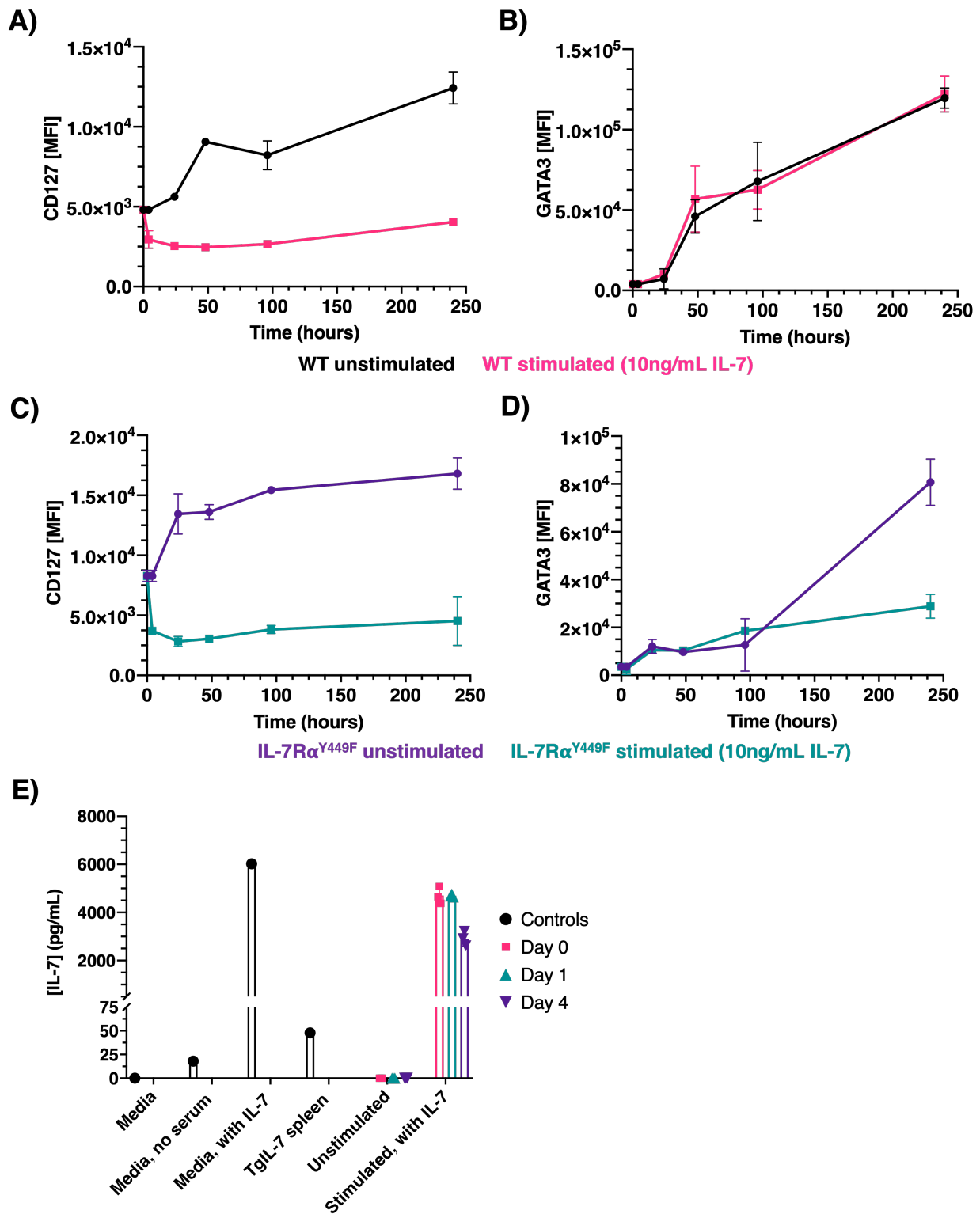


**Figure 3.4 CD127 receptor recycling in IL-7R $\alpha^{Y449F}$  bone marrow ILC2s is similar to WT during a 10-day IL-7 stimulation.**

BM cells were cultured with or without IL-7 then GATA-3 was measured at 4 hours, 1, 2, 4, and 10 days post-stimulation (n=3). **(A)** Summarized CD127 MFI plots of IL-7 stimulated WT BM ILC2s over 10-day time-course stimulation with IL-7. **(B)** Summarized GATA3 MFI plots of IL-7 stimulated WT BM ILC2s over 10-day time-course stimulation with IL-7. **(C)** Summarized CD127 MFI plots of IL-7 stimulated IL-7R $\alpha^{Y449F}$  BM ILC2s over 10-day time-course stimulation with IL-7. **(D)** Summarized GATA3 MFI plots of IL-7 stimulated IL-7R $\alpha^{Y449F}$  BM ILC2s over 10-day time-course stimulation with IL-7. **(E)** Endogenous IL-7 concentrations in unstimulated supernatants measured by an IL-7 ELISA assay. Supernatant samples were diluted 1:2 prior to analysis to ensure read-out values were within the detection range of the kit (8.23–6000 pg/mL IL-7). The IL-7 stimulated samples decrease in IL-7 concentrations over the 4-day time-course as expected but there is no increase in IL-7 in the unstimulated conditions.



### 3.4 Impaired IL-7 signaling may impede fetal liver ILC2 development

Having observed a reduction in adult BM ILC2s in impaired IL-7 signaling mouse models, I asked whether this phenomenon also presents itself in fetal liver (FL) ILC2s. This is important because Schneider *et al.*<sup>20</sup> reported that FL ILC2s have a large contribution to peripheral ILC2 pools during adulthood unlike adult BM ILC2s. I hypothesized that IL-7 signaling was required for development of all ILC2s regardless of development site.

Due to the rarity of ILC2s, we utilized the PLZF<sup>GFPcre</sup> mouse model which tags developing ILCs with GFP to assist in flow cytometry analysis. PLZF<sup>GFPcre</sup> mice were mated with IL-7R $\alpha$ <sup>Y449F</sup> mice to produce homozygous PLZF<sup>GFPcre</sup>/IL-7R $\alpha$ <sup>Y449F</sup> mice, an IL-7R $\alpha$  loss of function model that tags PLZF+ ILCs with GFP. Both PLZF<sup>GFPcre</sup> and PLZF<sup>GFPcre</sup>/IL-7R $\alpha$ <sup>Y449F</sup> timed mating pairs were set up, pregnancies were confirmed on E14.5, then FLs were isolated on E15.5 for flow cytometry analysis. As shown in the flow cytometry plots in Figure 3.5A, there was a noticeable loss of PLZF-GFP+ ILC2s from PLZF<sup>GFPcre</sup>/IL-7R $\alpha$ <sup>Y449F</sup> FLs when compared to PLZF. However, the reduction in ILC2 numbers was not significant (Figure 3.5B). It should be noted that PLZF-GFP expression is unchanged between PLZF<sup>GFPcre</sup> and PLZF<sup>GFPcre</sup>/IL-7R $\alpha$ <sup>Y449F</sup> cells (Figure 3.5C).

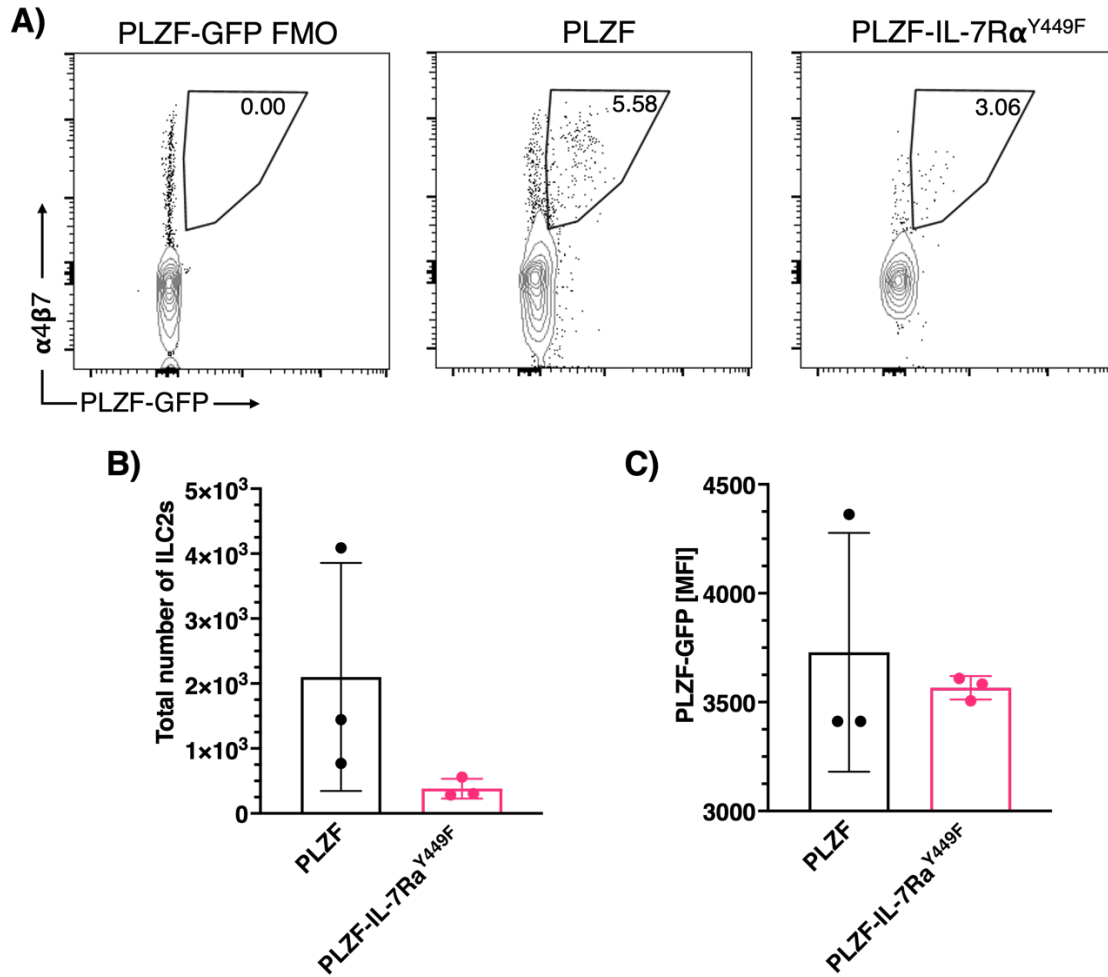


**Figure 3.5 Fetal liver ILC2s appear to be reduced in PLZF<sup>GFPcre</sup>/IL-7R $\alpha$ <sup>Y449F</sup> mice.**

PLZF<sup>GFPcre</sup> and PLZF<sup>GFPcre</sup>/IL-7R $\alpha$ <sup>Y449F</sup> fetal liver ILC2s from E15.5 were stained for flow cytometry analysis. **A)** PLZF-GFP<sup>+</sup> ILC2s in each representative flow cytometry plot is gated on the following criteria: single, live, CD45<sup>+</sup>, lineage<sup>-</sup>, Thy1<sup>+</sup>,  $\alpha 4\beta 7$ <sup>+</sup>, and PLZF-GFP<sup>+</sup>. **B)** Total number of PLZF-GFP<sup>+</sup> BM ILC2s. **C)** PLZF-GFP MFI calculated from flow cytometry data. **C)** PLZF-GFP MFI. Student *t*-tests were performed for this data.

<i>Lineage</i>	<i>Surface markers</i>	<i>ILC2 transcription factor</i>
<b>CD3</b> –CD8+ and CD4+ T cells (T cell co-receptor)	<b>CD45.2</b>	GATA3
<b>CD19</b> – B cells and dendritic cells	<b>CD127/IL-7R<math>\alpha</math></b>	
<b>CD11c</b> – dendritic cells, monocytes, macrophages, neutrophils, and B cells	<b><math>\alpha</math>4<math>\beta</math>7/LPAM/integrin-<math>\beta</math>7</b> – migration receptor for ILCps	
<b>B220</b> – B-cells, some T and NK cells		
<b>NK1.1</b> – NK cells		
<b>Ter119</b> – red blood cells/erythrocytes		

**Table 3.3 Flow cytometry staining panel for fetal liver ILC2s.**

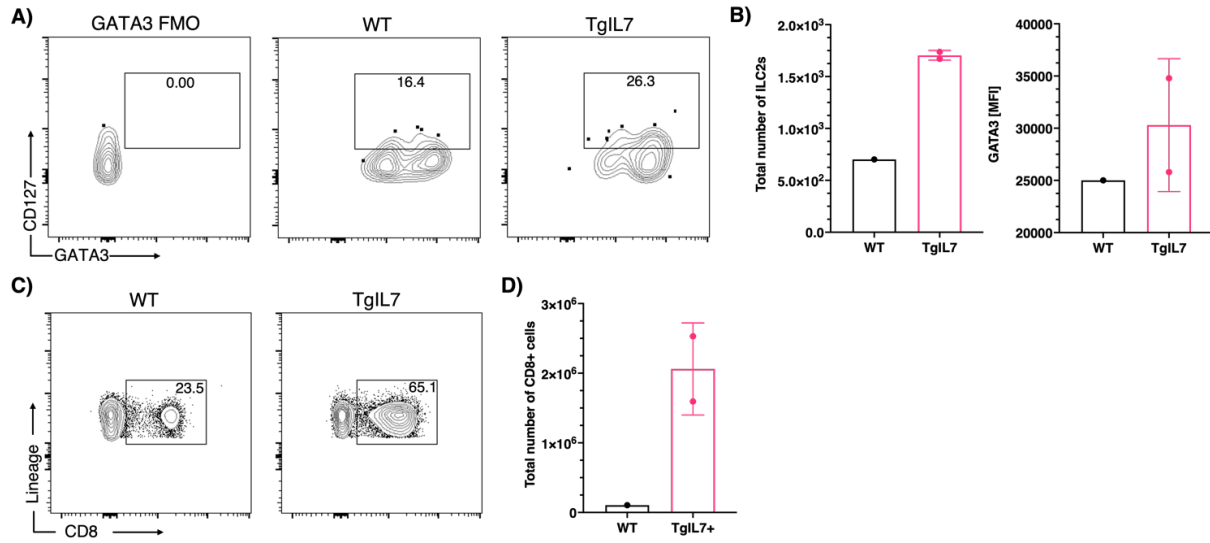


**Figure 3.6 E16.5 fetal liver ILC2s isolated from TgIL7 mothers appear to have higher cell counts and GATA3 expression compared to WT cells.**

**A)** Fetal livers were isolated from E16.5 fetuses for cell surface and intracellular marker analysis by flow cytometry. Cells in each representative flow cytometry plot is gated on the following criteria: single, live, CD45+, lineage-,  $\alpha 4\beta 7$ +, ICOS+, CD127+, and GATA3+. **B)** Total number of GATA3 expressing ILC2s (left) and GATA3 MFI (right) of ILC2s identified in flow cytometry plots. **C)** CD8+ cell staining of Lin+ maternal splenocytes as positive control. Cells in each representative flow cytometry plot is gated on the following criteria: live, CD45+, lineage+, CD8+. **D)** Total number of CD8-expressing cells calculated from the flow cytometry data.

### 3.5 Maternal-fetal IL-7 effects on fetal liver ILC2 development

After observing that IL-7 signaling disruptions may have effects on FL ILC2 development in IL-7R knock-in mice, we wanted to examine whether high concentrations of IL-7 in a gain of function model would affect developing ILC2s in the opposite manner. Due to the difficulty of delivering IL-7 directly to the fetuses, timed mating pairs of TgIL7 female mice with WT male mice were set up instead (refer to Section 2.1.1.1). This model would answer two questions: (1) does maternal-fetal IL7 exchange occur? and (2) if this exchange occurs, what impact does it have on FL ILC2 development? Regarding the first question, since it has been documented that IL-7 has a crucial role at the maternal-fetal interface of the placenta in humans and results in adverse pro-inflammatory responses at the interface when IL-7 levels are elevated, I postulated the same may occur in mouse models<sup>120</sup>.

Fetal livers were collected on E16.5 for flow cytometry analysis and stained for markers listed in Table 3.3. On two separate occasions, only 1 WT and 2 TgIL7 females became pregnant after the timed mating set-up, hence, statistical analysis could not be performed on the following data. I observed that FL ILC2 cell numbers and GATA3 expression from TgIL7 mothers trend higher than that from WT mothers (Figure 3.6A, B). GATA3 expression in FL ILC2s with fetal IL-7 exposure appeared to be higher compared to WT (Figure 3.6B). Maternal splenocytes were analyzed for CD8+ T cells to confirm each mother's genotype (Figure 3.6C, D). TgIL7 mothers had elevated CD8 T cells compared to WT which is consistent with the genotype. Due to persistent breeding issues in the animal facility, none of the subsequent timed matings resulted in more than one female becoming pregnant so these experiments could not be repeated for statistical analyses.

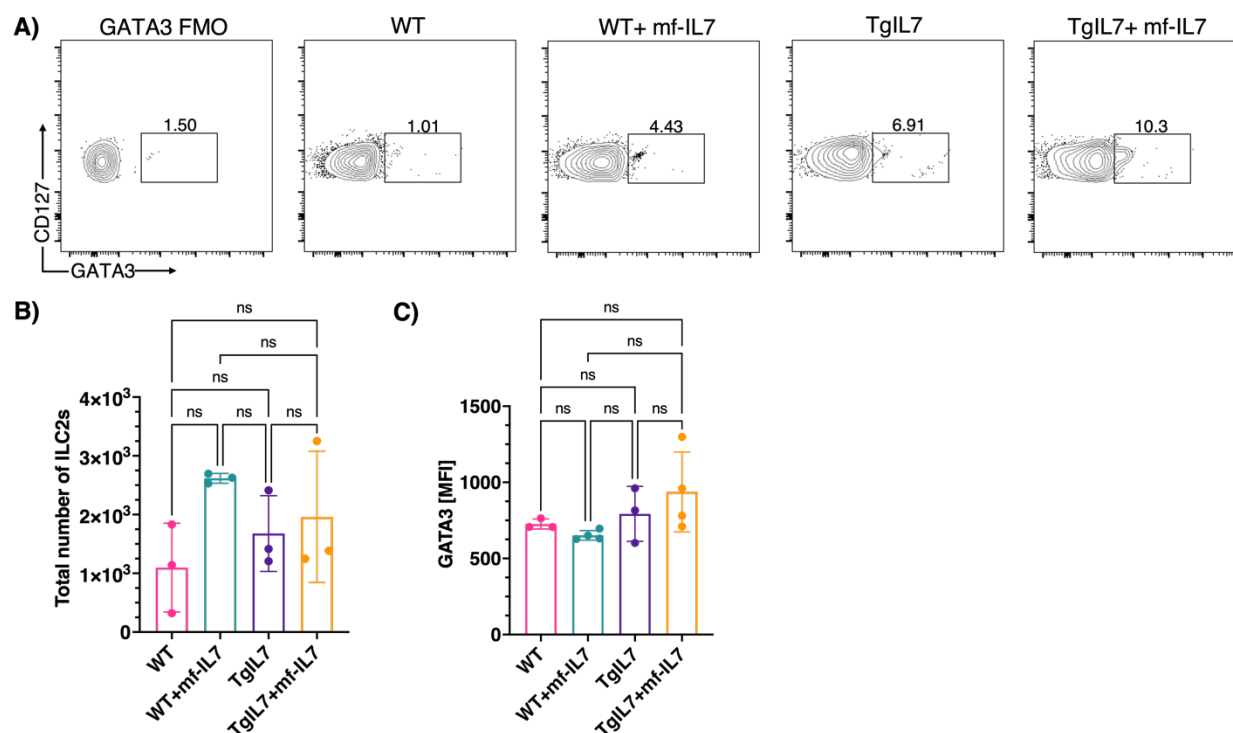


**Figure 3.7 Fetal exposure to high concentrations of maternal IL-7 shows trends towards elevated offspring adult bone marrow ILC2 development.**

Bone marrow cells were isolated from 7-week-old, litter-matched WT, WT+mfIL7, TgIL7, TgIL7+mfIL7 mice for ILC2 cell surface markers and GATA3 analysis by flow cytometry. **(A)** Representative flow plots of bone marrow ILC2s isolated from different strains/conditions. Cells are identified as single, live, CD45<sup>+</sup>, lineage<sup>-</sup>, Thy1.2<sup>+</sup>, ICOS<sup>+</sup>, Sca1<sup>+</sup>, CD127<sup>+</sup>, and GATA3<sup>+</sup>. **(B)** GATA3 MFI histogram of bone marrow ILC2s obtained by flow cytometry. **(C)** Total number of bone marrow ILC2s and GATA3 MFIs calculated the data obtained by flow cytometry. Multiple Student's *t*-test and one-way ANOVA was performed for this data.

### 3.6 Maternal-fetal IL-7 effects on adult offspring bone marrow ILC2s

With the findings that fetal liver ILC2 development appeared to have been positively impacted by high concentrations of IL-7 in TgIL7 fetal livers, I wanted to assess if this early life exposure to high concentrations of IL-7 had effects that carry into adulthood. In humans, “trained immunity” is a topic of growing interest which proposes that the maternal immune system and responses during pregnancy dictates fetal hematopoietic stem cell development and adult immune function<sup>121</sup>. I posited that maternal-fetal IL-7 exposure had lifelong effects on ILC2 development in the BM.

Offspring from TgIL7 females were matured into adulthood before BM isolation for ILC2 analysis by flow cytometry. Cells were stained for markers listed in Table 3.1. Comparing WT with maternal-fetal IL-7 (mf-IL7) exposure to WT controls, there is a pronounced GATA3+ ILC2 population that developed but their GATA3 expression is unchanged compared to WT controls (Figure 3.7A, C). Similarly, BM from TgIL7 with mf-IL7 exposure also have a distinct population of GATA3+ ILC2s that is not observed in the respective control (Figure 3.7A). The appearance of this distinct GATA3+ ILC2 population in mice with mf-IL7 exposure suggests high concentrations of IL-7 during fetal development may have life-long effects.

Besides analyzing BM ILC2s, CD4 and CD8 T cells from the thymus were also analyzed in these mice since these cells are dependent on IL-7 for their development<sup>122</sup>. Moreover, *in vivo* IL-7 treatment in mice has been shown to enhance CD4 and CD8 populations<sup>122</sup>. Should there be a long-term effect of mf-IL7 exposure, I wanted to assess whether post-natal thymic CD4 and CD8 T cells would also be enriched in addition to BM ILC2s. Strikingly there were no discernable differences in CD4 or CD8 T cell numbers in thymi isolated from mice with mf-IL7 exposure (Figure 3.8A, B). However, phospho-STAT5 was abrogated in the CD8 T cell

population. Comparing WT control to TgIL7 control, it appears that phospho-STAT5 is lower in TgIL7 than WT (Figure 3.8C, D). When comparing either control to their respective mf-IL7 exposed thymic cells, there was no signal for phospho-STAT5 indicating an impairment to steady-state STAT5 signaling in mf-IL7 exposed CD8 T cells.



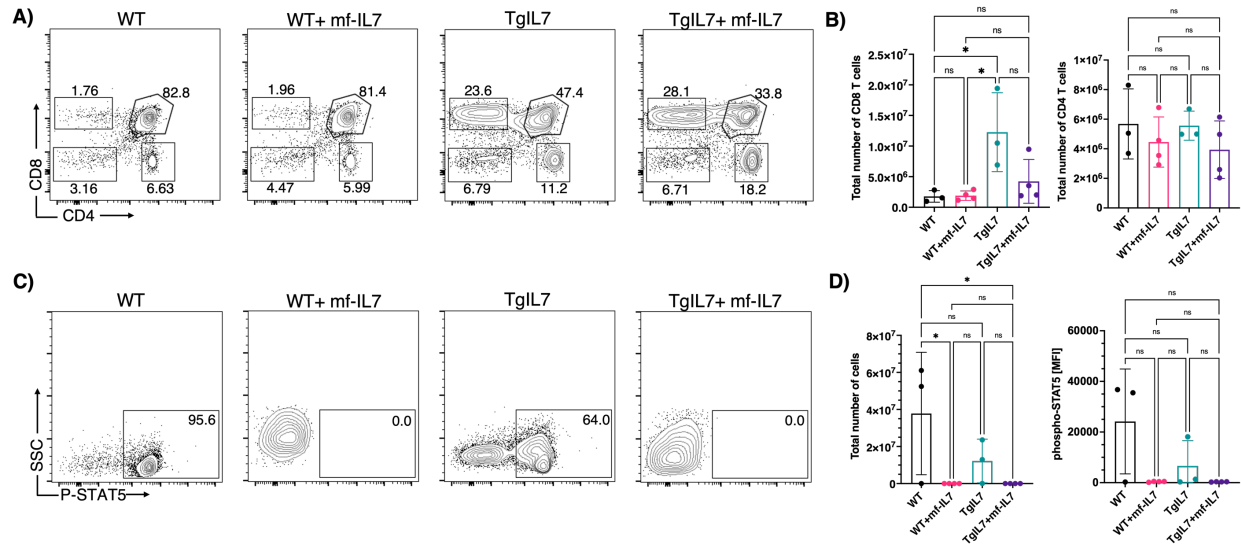


**Figure 3.8 Maternal-fetal IL-7 exposure does not impact adult thymic CD4 and CD8 T cells.**

**A)** Representative flow cytometry plots and quantification of CD4 and CD8 T cells from 7-week-old, litter-matched mice with mf-IL7 exposure. **B)** Total number of CD8 and CD4 T cells from 7-week-old, litter-matched mice with mf-IL7 exposure. **C)** Representative flow cytometry plots of phospho-STAT5 in CD8 T cells from 7-week-old, litter-matched mice with mf-IL7 exposure. **D)** Total number of CD8 T cells expressing phospho-STAT5 and phospho-STAT5 expression calculated from MFI. Multiple Student's *t*-test and one-way ANOVA was performed for this data.

### **3.7 Maternal-fetal IL-7 effects on lung ILC2 establishment and immune response**

After observing an increase in BM ILC2s in adult offspring that were exposed to high concentrations of IL-7 during fetal development, I next examined if there were functional effects on ILC2s in the lungs. It had been shown that lung ILC2s were needed for proper tissue repair and homeostasis following Influenza challenge<sup>18</sup>. I hypothesized that mf-IL7 exposure would affect lung ILC2 responses during Influenza infection.

Lung ILC2s from mice with mf-IL7 exposure were first analyzed during resting conditions to assess whether there were effects on ILC2 establishment in the lungs. Lung tissues were isolated from adult mice then prepared for flow cytometry analysis following the staining panel in Table 3.4. As shown in Figure 3.9A and B, there were no detectable changes in ILC2 numbers between mice with mf-IL7 exposure and their respective control. Additionally, I did not observe a distinct GATA3<sup>+</sup> ILC2 population that was observed in BM samples from mice with mf-IL7 exposure (Figure 3.7A, 3.9A). When comparing GATA3 expression in lung ILC2s with mf-IL7 exposure, there were no observable differences between the conditions (Figure 3.9C).

<i>Lineage</i>	<i>Surface markers</i>	<i>ILC2 transcription factor</i>
<b>CD3</b> –CD8+ and CD4+ T cells (T cell co-receptor)	<b>Thy1.2/CD90.2</b>	<b>GATA3</b>
<b>CD4</b> – T-helper cells, monocytes, macrophages, dendritic cells	<b>ST2</b>	
<b>CD11b</b> – monocytes, granulocytes, macrophages, NK cells	<b>CD45</b>	
<b>B220</b> – B-cells, some T and NK cells	<b>CD127/IL-7R<math>\alpha</math></b>	
<b>NK1.1</b> – NK cells	<b>Nrp1</b>	
<b>Gr1</b> – granulocytes		
<b>Ter119</b> – red blood cells/erythrocytes		
<b>TCR<math>\beta</math></b> - T cells		
<b>TCR<math>\gamma\delta</math></b> - T cells (mainly $\gamma\delta$ T cells)		

**Table 3.4 Flow cytometry staining panel for naïve lung ILC2s and *in vivo* stimulated**

**ILC2s.**

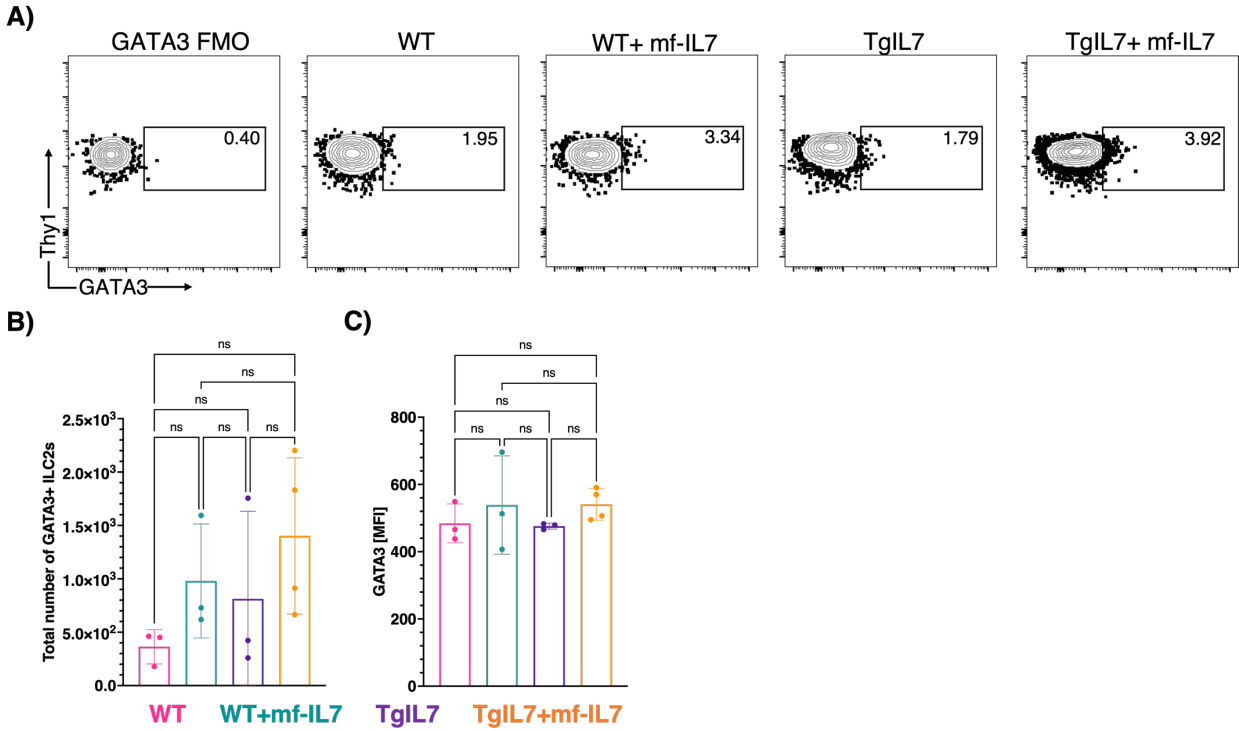


**Figure 3.9 Fetal exposure to high doses of maternal IL-7 does not impact offspring adult lung ILC2 maintenance.**

Lungs were isolated from 6- to 8-week-old WT, WT+mf-IL7, TgIL7, TgIL7+mf-IL7 mice for ILC2 cell surface markers and GATA3 analysis by flow cytometry. **A)** Representative flow plots of lung ILC2s isolated from different strains/conditions. Cells are identified as single, live, CD45+, lineage-, Thy1.2+, ICOS+, Sca1+, CD127+, and GATA3+. **B)** Total number of lung ILC2s and their GATA3 MFI calculated from flow cytometry data. Multiple Student's *t*-test and one-way ANOVA was performed for this data.

Next, mice with mf-IL7 exposure were infected with 500 HAU of Influenza PR8 for 6 days prior to ILC2 quantification. The 6-day timepoint was selected based on published data showing highest IL-13 response 6 days post-infection<sup>19</sup>. Due to poor breeding, TgIL7 mice could not be included in this experiment as a control for TgIL7 with mf-IL7 exposure. Lung ILC2s were stained for the markers listed in Table 3.5 for flow cytometry. Similar to results in naïve lung ILC2s, there were no observable differences between control mice and mf-IL7 exposed mice (Figure 3.10A, B, C). However, there was a significant elevation of ILC2 numbers and their GATA3 expression when TgIL7+ mf-IL7 samples were compared to the WT control (Figure 3.10B, C). Lung ILC2s from infected mice were also stimulated with phorbol myristate acetate (PMA) and ionomycin for 4 hours to induce IL-5 and IL-13 production. There were no observable differences in IL-5 and IL-13 production between WT and WT+ mf-IL7 (Figure 3.10D, E). Conversely, TgIL7+mf-IL7 lung ILC2s produce significantly more IL-5 and IL-13 in comparison to WT and WT+mf-IL7 cells.

<i>Lineage</i>	<i>Surface markers</i>	<i>ILC2 transcription factor</i>
<b>CD3</b> –CD8+ and CD4+ T cells (T cell co-receptor)	<b>Thy1.2/CD90.2</b>	<b>GATA3</b>
<b>CD4</b> – T-helper cells, monocytes, macrophages, dendritic cells	<b>ICOS</b>	
<b>CD11b</b> – monocytes, granulocytes, macrophages, NK cells	<b>Sca-1</b>	
<b>B220</b> – B-cells, some T and NK cells	<b>CD127/IL-7R<math>\alpha</math></b>	
<b>NK1.1</b> – NK cells	<b>CD45</b>	
<b>Gr1</b> – granulocytes		
<b>Ter119</b> – red blood cells/erythrocytes		
<b>TCR<math>\beta</math></b> - T cells		
<b>TCR<math>\gamma\delta</math></b> - T cells (mainly $\gamma\delta$ T cells)		

**Table 3.5 Flow cytometry staining panel for Influenza infected lung ILC2s.**

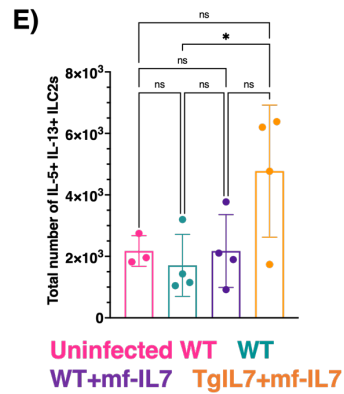
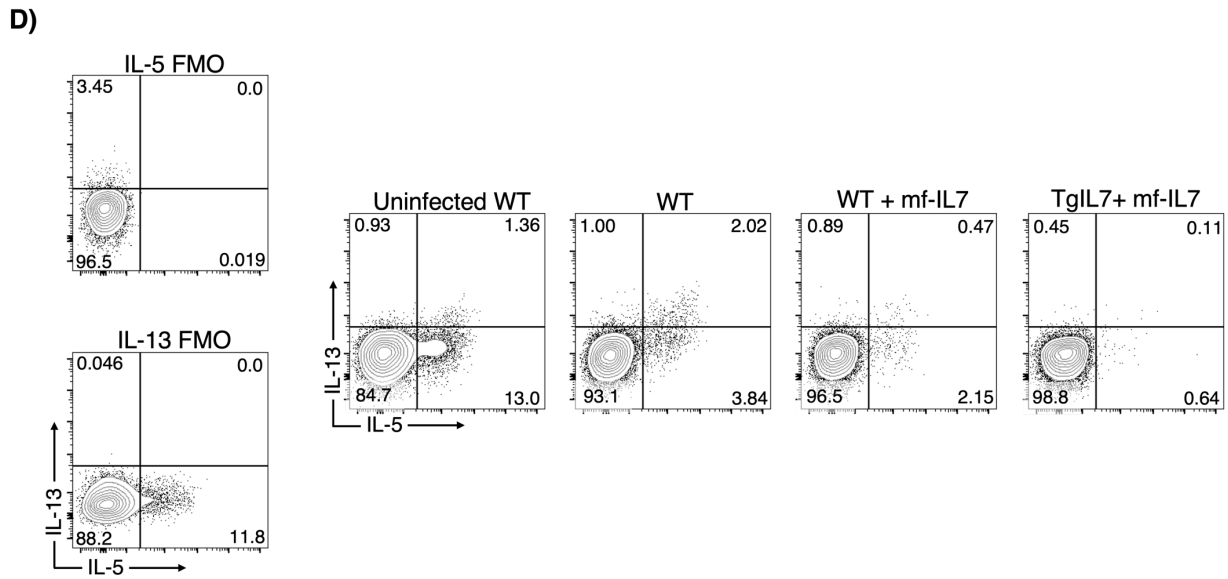
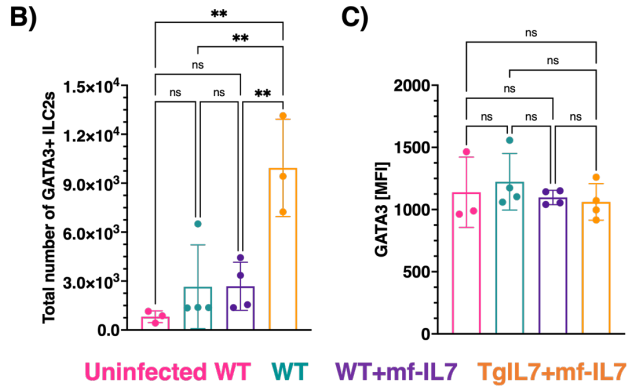
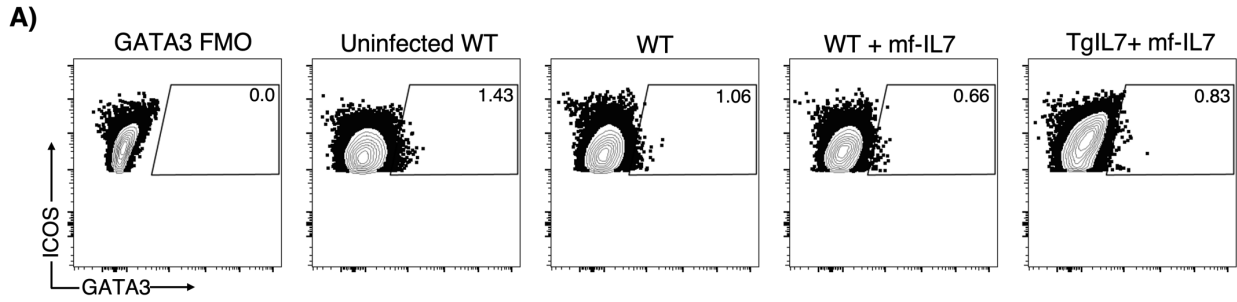


**Figure 3.10 Lung ILC2 response to PR8 Influenza challenge is unaffected by fetal exposure to high doses of maternal IL-7.**

9-week-old mice were infected with 500 HAU PR8 Influenza for 6 days before analyzing lung ILC2s for their key cell markers and IL-5 and IL-13 expression by flow cytometry. **(A)**

Representative flow plots of lung ILC2s isolated from different strains/conditions. Cells are identified as single, live, CD45<sup>+</sup>, lineage<sup>-</sup>, Thy1.2<sup>+</sup>, ICOS<sup>+</sup>, Sca1<sup>+</sup>, CD127<sup>+</sup>, and GATA3<sup>+</sup>. **(B,**

**C)** Total number of lung ILC2s and their GATA3 MFI are calculated from flow cytometry data.

**(D)** Representative flow plots of lung ILC2 IL-5 and IL-13 expression in different

strains/conditions. Cells are identified as single, live, CD45<sup>+</sup>, lineage<sup>-</sup>, and Thy1.2<sup>+</sup> before

analyzing IL-5 and IL-13. **(E)** Total number of IL-5 and IL-13 lung ILC2s are calculated from

flow cytometry data. Multiple Student's *t*-test and one-way ANOVA was performed for this data.



### 3.8 Summary and Discussion

#### 3.8.1 Summary

In this chapter, I showed that IL-7 signaling was critical for FL and BM ILC2 development using different IL-7 signaling mouse models. Through qRT-PCR, it was observed there was a reduction in *Gata3*, *Rora*, *Il13*, and *Tbx21* mRNA expression in IL-7R $\alpha^{Y449F}$  adult BM ILC2s. When IL-7 signaling was impaired, either through knock-in mutation in IL-7R $\alpha^{Y449F}$  mice or complete knock-out in IL-7-KO mice, there was a significant reduction in BM ILC2s and their GATA3 expression. This was also observed in IL-7R $\alpha^{Y449F}$  timed mating experiments where fetal livers show reduced ILC2 numbers. In adult BM ILC2s, it was established that IL-7R $\alpha^{Y449F}$  impaired signaling defects were independent of IL-7 receptor recycling as CD127 surface detection by flow cytometry after IL-7 stimulation was similar to WT ILC2s.

Additionally, I demonstrated for the first time in a mouse model that there is evidence indicative of maternal-fetal exchange of IL-7 and these effects can be observed in the fetal liver and offspring adult bone marrow environment with trends of elevated ILC2 numbers. I also found that thymic CD8 and CD4 numbers in mice with mf-IL7 exposure were unchanged compared to controls, but CD8 phospho-STAT5 signals were absent in both WT and TgIL7 mice when compared to their respective controls. Lastly, lung ILC2 numbers and their functional responses to Influenza challenge were not impacted by mf-IL7 exposure.

#### 3.8.2 Discussion

To determine whether transcriptional regulation by IL-7 governs ILC2 development, I did a qRT-PCR analysis of key ILC2 genes including *Gata3*, *Rora*, and *Il13* in WT and IL-7R $\alpha^{Y449F}$  BM ILC2s then assessed ILC2 numbers and their GATA3 expression. Both methods of analysis

showed reduced expression of *Gata3* mRNA and GATA3 transcription factor expression. IL-7-KO mice showed the greatest reduction in ILC2 numbers and GATA3 expression. Combining these results, I conclude that ILC2 development and their GATA3 expression requires intact IL-7 signaling. The severity of impaired IL-7 signaling on BM ILC2 development correlates to the severity of the IL-7 signaling loss-of-function mouse models used. The fewest ILC2s were detected in IL-7-KO mice which was due to them lacking IL-7 entirely, unlike IL-7R $\alpha^{Y449F}$  which still expresses IL-7 but experiences weaker IL-7 signaling as STAT5 is not phosphorylated. I also showed that mutated IL-7R $\alpha^{Y449F}$  receptors on ILC2s respond to IL-7 stimulation identically to WT receptor with comparable downregulation. This further supports the idea that defects in ILC2 development in these models are due to weakened signaling and downstream transcriptional regulation.

Since IL-7 is required by all ILC subsets during their earliest development stages, I examined whether impaired IL-7 signaling in IL-7R $\alpha^{Y449F}$  mice broadly affects all ILC subsets or is exclusive to ILC2 development. The findings showed that BM ILC1s and ILC3s were unaffected by the impaired IL-7 signaling which can be attributed to these cells relying on other cytokines and growth factors to receive the same development and maintenance signals as ILC2s<sup>43</sup>. Tbet and ROR $\gamma$ t expression was also unaffected. As there were no observable effects on BM ILC1s and ILC3s, I conclude that IL-7R $\alpha^{Y449F}$  mice are a reliable model to study the effects of impaired IL-7 signaling on ILC2 development. It would be worth analyzing all ILC subsets in these mice during fetal development and peripheral tissue function to see if IL-7 signaling effects are seen there.

After evaluating the importance of IL-7 for BM ILC2 development, I examined its importance for FL ILC2 development. Two different models were used to evaluate this: (1) loss-of-function with IL-7R $\alpha^{Y449F}$  timed matings, (2) gain-of-function with TgIL7 timed matings. Starting with the loss-of-function model, FL IL-7R $\alpha^{Y449F}$  ILC2s numbers were reduced but were not statistically significant in difference. These results somewhat mirror what was observed in adult BM which suggests that IL-7 signaling influences ILC2 development during adulthood and possibly, in early life, since there was a reduction in ILC2 numbers when IL-7 signaling was disrupted. Additionally, PLZF expression was unchanged between WT and IL-7R $\alpha^{Y449F}$  cells. This indicates that PLZF is a reliable marker for ILC2s when used in conjunction with other ILC2p markers such as Thy1, CD45, ICOS and  $\alpha 4\beta 7$  as it is expressed independent of IL-7 signaling.

In the gain-of-function model using TgIL7 mice, I showed that maternal-fetal IL-7 exposure can influence FL ILC2 development as there was an increase in cell numbers that was not observed in the WT FLs. A potential concern for immunopathology at the maternal-fetal interface causing premature termination as described in humans by Vilsmaier *et al.* (2021) did not manifest in these experiments. A slight increase in GATA3 expression was also observed but due to lack of biological replicates, no statistical inferences could be made. Once mouse facility breeding issues are resolved, repeating TgIL7 timed mating experiments with enough biological replicates would be needed to validate the current findings.

I further extended the maternal-fetal IL-7 experiments by examining whether adult BM ILC2s from mice that had mf-IL-7 exposure experienced similar effects as FL ILC2s. WT and TgIL7 mice with mf-IL7 exposure developed a distinct GATA3<sup>+</sup> ILC2 population that is not seen in their respective controls; however, this change was not statistically significant.

Additionally, their GATA3 expression did not change from the respective controls. Although the results were not statistically significant, replicate experiments showed the development of the distinct GATA3<sup>+</sup> population which suggests mf-IL7 exposure may have lifelong effects on BM ILC2 development. When analyzing CD4 and CD8 T cells in the thymus of these mice, no observable changes in cell numbers were observed. It was also observed that phospho-STAT5 is reduced in mice with maternal-fetal IL-7 exposure. However, there was a strong phospho-STAT5 signal in WT and TgIL7 control cells although these cells were rested and not stimulated. This indicates that there was a non-IL-7 activator of STAT5 may be present in the samples during tissue collection and cell preparation. Combining these findings, it is likely that either (1) maternal-fetal IL-7 exposure does not occur, (2) maternal-fetal IL-7 exposure does not have lifelong effects and are temporary in the fetal environment, or (3) maternal-fetal IL-7 exposure effects are limited to ILC2s. To determine which is occurring, IL-7 concentrations at the maternal-fetal interface and fetal environment should be measured using IL-7 ELISA to determine if IL-7 crosses the placenta. If the results show IL-7 crosses the placenta, then these experiments should be repeated in the adult offspring with an acid wash and full rest of thymic T cells to eliminate the effects of non-specific cytokine stimulation of phospho-STAT5. Alternatively, fluorescently tagged recombinant IL-7<sup>123</sup> could be delivered intravenously to the mother before assessing whether the tagged IL-7 appears in the fetal tissues a few days after injection. Should the new findings show BM ILC2s and thymic CD4/CD8 T cells impacted by maternal-fetal IL-7 exposure, it would complement the IL-7R $\alpha$ <sup>Y449F</sup> results showing that when IL-7 signaling is lost, ILC2 development is impaired while when IL-7 is supplemented, ILC2 development is enriched.

Both resting and Influenza-infected lung ILC2s showed no differences when mf-IL7 exposure occurred during fetal development indicating maternal IL-7 does not have long term effects in offspring ILC2 functional responses. However, it was observed that TgIL7+mf-IL7 ILC2 population was expanded and was more responsive during Influenza challenge when compared to WT cells. Since there are no differences between WT and WT+mf-IL7 immune responses, it can be assumed that overexpression of IL-7 gives an advantage to lung ILC2s in TgIL7 mice, not mf-IL7 effects. To confirm this, a repeat experiment including TgIL7 mice as a control would be necessary. It would also be interesting to analyze whether mf-IL7 exposure has effects on tissue homeostasis post-Influenza infection. Maternal-fetal IL-7 effects on lung ILC2 immune responses during papain-induced allergic reactions should also be assessed as it initiates a known  $T_H2$  response in ILC2s.

My findings in this chapter indicate that IL-7 is a critical regulator of ILC2 development and their GATA3 expression since when IL-7 signaling is disrupted, I observed a significant reduction in ILC2s, their *Gata3* transcript levels, and their GATA3 expression. Although all ILC populations depend on IL-7 for early development, I clearly showed that the signaling defect in IL-7R $\alpha^{Y449F}$  mice specifically impairs ILC2 development in adult BM. Maternal-fetal IL-7 exposure appears to impact adult ILC2 development, but more studies need to be conducted to show significant effects.

## Chapter 4: Transcriptomic analysis of IL-7 and TSLP signaling in lung ILC2s

### 4.1 Introduction

Type 2 innate lymphoid cells (ILC2s) are a rare but crucial immune cell subset with important roles in releasing IL-5 and IL-13 during viral infections, and amphiregulin to promote tissue repair<sup>2</sup>. For ILC2s to perform these functions and maintain their population, interleukin-7 (IL-7) must be present in the environment to provide homeostasis and proliferation signals<sup>124</sup>. IL-7 is also required by T cells and B cells for their development<sup>69, 116</sup>. Because of the importance of IL-7 to immune cell development and function, when IL-7 expression is significantly elevated or depleted, it leads to severe immunopathologies. When IL-7 levels are elevated in humans, it can result in the development of inflammatory conditions such as atherosclerosis, psoriasis, rheumatoid arthritis, multiple sclerosis, and inflammatory bowel disease<sup>64</sup>. Conversely, IL-7 or IL-7R deficiencies results in severely impaired immune cell development and poor immune responses to infections<sup>63</sup>. Congenital IL-7 deficiencies result in severe combined immunodeficiency (SCID), which can be fatal if bone marrow transplants are not done during early life stages<sup>125, 126</sup>.

For ILC2s to be responsive to IL-7, these cells must express the receptor for IL-7 consisting of IL-7R $\alpha$  (CD127) and common  $\gamma_c$  chain. Upon IL-7 ligand engagement with its receptor, Jak1/3 become activated which results in the recruitment of STAT1/3/5 proteins for phosphorylation.<sup>116</sup> Phosphorylated STAT proteins will enter the nucleus and modulate cellular transcription. Thymic stromal lymphopoietin (TSLP) is a cytokine similar to IL-7 in which it too uses IL-7R $\alpha$ , however, is paired with TSLPR instead of the common  $\gamma_c$  chain<sup>67, 68</sup>. Once TSLP binds this heterodimeric receptor, it triggers Jak1 and Jak2 activation, which then recruits STAT5 for its activation and entry into the nucleus.

Although IL-7 and TSLP share IL-7R $\alpha$  in their receptors, these cytokines have strong opposing effects in ILC2s. IL-7 is conventionally thought to promote ILC2 proliferation, homeostasis, and function<sup>124</sup>. In contrast, TSLP is an activating alarmin that results in pro-inflammatory immune responses<sup>124</sup>. In the lungs, ILC2s encounter both IL-7 and TSLP since airway epithelial cells can produce either cytokine depending on the context<sup>43, 124, 127</sup>. TSLP is most associated as being a master regulator of allergic inflammation and eliciting the development of autoimmunity<sup>124, 128</sup>. In the clinical setting, elevated TSLP levels are usually found in patients with atopic dermatitis, allergic asthma, or inflammatory bowel disease. Since TSLP is associated with these pro-inflammatory diseases, it is often underappreciated for its crucial role in stimulating protective immune responses to parasitic helminth infections in the gut<sup>129-131</sup>.

Since ILC2s require IL-7R $\alpha$  to be responsive to IL-7 or TSLP, IL-7R $\alpha$  (CD127) is one of the many markers used to identify lung ILC2s. Several markers are used to identify lung ILC2s because only 0.4-1% of the total live lung cells in a mouse are ILC2s and they share markers with larger immune cell populations such as T cells which may mask the presence of ILC2s<sup>41, 132</sup>. The most common markers used in combination to identify ILC2s in mice are Lineage- (see Table 2.1 for full list), CD45+, ST2+, Thy1.2+, CD127+, and ICOS+<sup>12, 133</sup>. Recently, there was a breakthrough finding that showed neuropilin-1 (Nrp1) as a robust, tissue-specific marker of lung ILC2s and has yet to be identified to be expressed on other immune cell populations in a tissue-dependent manner. Due to these findings, Nrp1 has become an invaluable marker for studying this rare population of immune cells within the lungs.

While IL-7 and TSLP share a common receptor subunit, these cytokines induce distinctly different immune responses as outlined above. I hypothesized that IL-7 and TSLP would induce

different transcriptional landscape changes in lung ILC2s. I predicted that IL-7 stimulation would result in the upregulation of immune regulation genes such as *Gata3* and *Rora*. Conversely, TSLP stimulation would upregulate pro-inflammatory genes such as *Il5* and *Il13*. I also predicted that there would be some overlap of genes expressed in both IL-7- and TSLP-stimulated lung ILC2s since both cytokines signal through IL-7R $\alpha$  and STAT5. To delineate the transcriptional changes that occurred when lung ILC2s were stimulated with either IL-7 or TSLP, unbiased RNA sequencing (RNAseq) was performed.

## **4.2 Optimizing ILC2 surface markers for cell sorting**

Nrp1 was shown to be a tissue-specific marker of lung ILC2s as identified through RNAseq data mining and adoptive transfer experiments, making it a prime candidate marker for isolating lung ILC2s<sup>21</sup>. However, it was unclear whether Nrp1 expression was dependent on IL-7 signaling, given the potential importance of this surface protein in ILC2 development and function. To assess whether impaired IL-7 signaling affected Nrp1 expression, lung cells were isolated from adult WT and IL-7R $\alpha^{Y449F}$  mice then stained for ILC2 markers to perform flow cytometry analysis as detailed in Table 3.4. The results showed that Nrp1 expression did not change when IL-7 signaling was impaired (Figure 4.1). Although there was a reduction in total ILC2s gated using Nrp1 as a criterion of identification, the qualitative cell distribution and Nrp1 expression on a per cell basis was comparable between WT and IL-7R $\alpha^{Y449F}$  cells (Figure 4.1A–C). In contrast, GATA3 expression within Nrp1+ lung ILC2s were still reduced in IL-7R $\alpha^{Y449F}$  cells (Figure 4.1D–F). These results indicate that Nrp1 expression is independent of IL-7 signaling and can be used to identify lung ILC2s in various IL-7 signalling genetic models available.



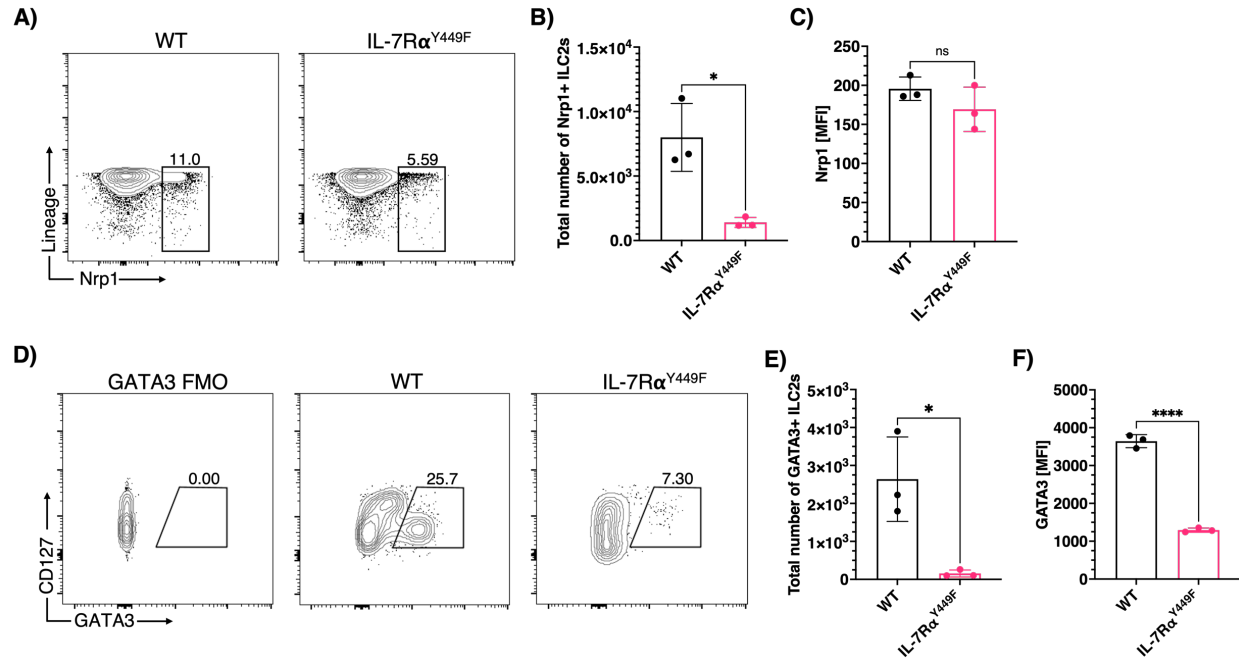


**Figure 4.1 Nrp1 expression in lung ILC2s is independent of IL-7 signaling.**

Lungs were isolated from 7- to 9-week-old mice then stained for ILC2 surface and intracellular markers for flow cytometry analysis. **(A)** Representative flow plots of Nrp1 expression in lung ILC2s. ILC2s were identified as single, live, CD45<sup>+</sup>, lineage<sup>-</sup>, Thy1.2<sup>+</sup>, and Nrp1<sup>+</sup>. **(B)** Total number of Nrp1<sup>+</sup> lung ILC2s calculated from flow cytometry data. **(C)** Nrp1 MFI expression on lung ILC2s calculated from flow cytometry data. **(D)** Representative flow plots of Nrp1<sup>+</sup> GATA3<sup>+</sup> lung ILC2s. ILC2s were identified as single, live, CD45<sup>+</sup>, lineage<sup>-</sup>, Thy1.2<sup>+</sup>, ST2<sup>+</sup>, Nrp1<sup>+</sup> and GATA3<sup>+</sup>. **(E)** Total number of GATA3<sup>+</sup> lung ILC2s are calculated from flow cytometry data. **(F)** GATA3 MFI expression on lung ILC2s are calculated from flow cytometry data. Multiple Student's *t*-tests and one-way ANOVA were performed for this data (repeated in triplicate).

### 4.3 Transcriptional profiling of *in vivo* IL-7- and TSLP-stimulated lung ILC2s

To determine the transcriptional landscape that is regulated by IL-7 versus TSLP, a 4-day *in vivo* stimulation with either 2 $\mu$ g IL-7 or 500ng TSLP was done with adult WT mice. The cytokines were delivered intranasally to each mouse. Treated lungs were isolated then stained with antibodies for flow cytometric cell sorting as indicated in Table 4.1. The 4-day time-point was selected based on the results of a 4-day *in vivo* intranasal IL-7 stimulation time-course assessment of GATA3 expression in lung ILC2s (see Appendix). At 4-days post-stimulation, I observed the greatest number of GATA3<sup>+</sup> ILC2s which would maximize the number of sorted cells. With earlier results showing that lung ILC2 Nrp1 expression was independent of IL-7 signaling, Nrp1 was one of the markers used to sort for lung ILC2s. *In vivo* cytokine stimulation experiments were performed with 4 to 5 mice per treatment condition (control/unstimulated, IL-7 stimulated, or TSLP stimulated) and pooled prior to cell sorting and RNAseq preparation. This was done thrice in total for experimental repeats. Cells for this analysis were sorted for Lineage-CD45<sup>+</sup> Thy1.2<sup>+</sup> ST2<sup>+</sup> and Nrp1<sup>+</sup> expression. Total number of sorted cells ranged from 4,000 to 11,000 depending on experiment and treatment condition.

<i>Lineage</i>	<i>Surface markers</i>
<b>CD3</b> –CD8+ and CD4+ T cells (T cell co-receptor)	<b>CD45.2</b>
<b>CD4</b> – T-helper cells, monocytes, macrophages, dendritic cells	<b>Thy1.2/CD90.2</b>
<b>CD11b</b> – monocytes, granulocytes, macrophages, NK cells	<b>ST2</b>
<b>B220</b> – B-cells, some T and NK cells	<b>Nrp1</b>
<b>NK1.1</b> – NK cells	
<b>Gr1</b> – granulocytes	
<b>Ter119</b> – red blood cells/erythrocytes	
<b>TCR<math>\beta</math></b> - T cells	
<b>TCR<math>\gamma\delta</math></b> - T cells (mainly $\gamma\delta$ T cells)	

**Table 4.1 Flow cytometry staining panel for sorting lung ILC2s for RNA isolation.**

Samples were sequenced following the method described in Section 2.6. Briefly, RNA sample quality was assessed using Bioanalyzer Nano chip before library preparation and sequencing on Illumina NextSeq platform. Output datasets were put through 10 different pipelines for read alignment, gene annotations and differential gene expression. The results showed that reads from all 9 samples were evenly distributed from 5' to 3' end after alignment, with no indication of degraded RNA in the input material (Figure 4.2A). In Figure 4.2B, kallisto sample correlation values are displayed as a matrix and the results indicated that there was poor correlation between samples TSLP\_1, TSLP\_2, and Control\_2 with the remaining samples. A total of 10,162 genes were shown to be expressed in all treatment conditions and 146, 192, and 410 genes to be exclusively expressed in control, IL-7-stimulated, and TSLP-stimulated lung ILC2s respectively (Figure 4.2C). The RNAseq dataset obtained in this study was then compared to a comprehensive published RNAseq dataset of mouse BM, fat, gut, lung, and skin ILC2s<sup>134, 135</sup> to determine how closely the lung ILC2s isolated in this thesis were to those in published data (Figure 4.2D). PCA comparison showed that the stimulated lung ILC2 dataset I acquired clusters closely with published fat and lung ILC2 data and are distinct from gut and skin ILC2s (Figure 4.2D).

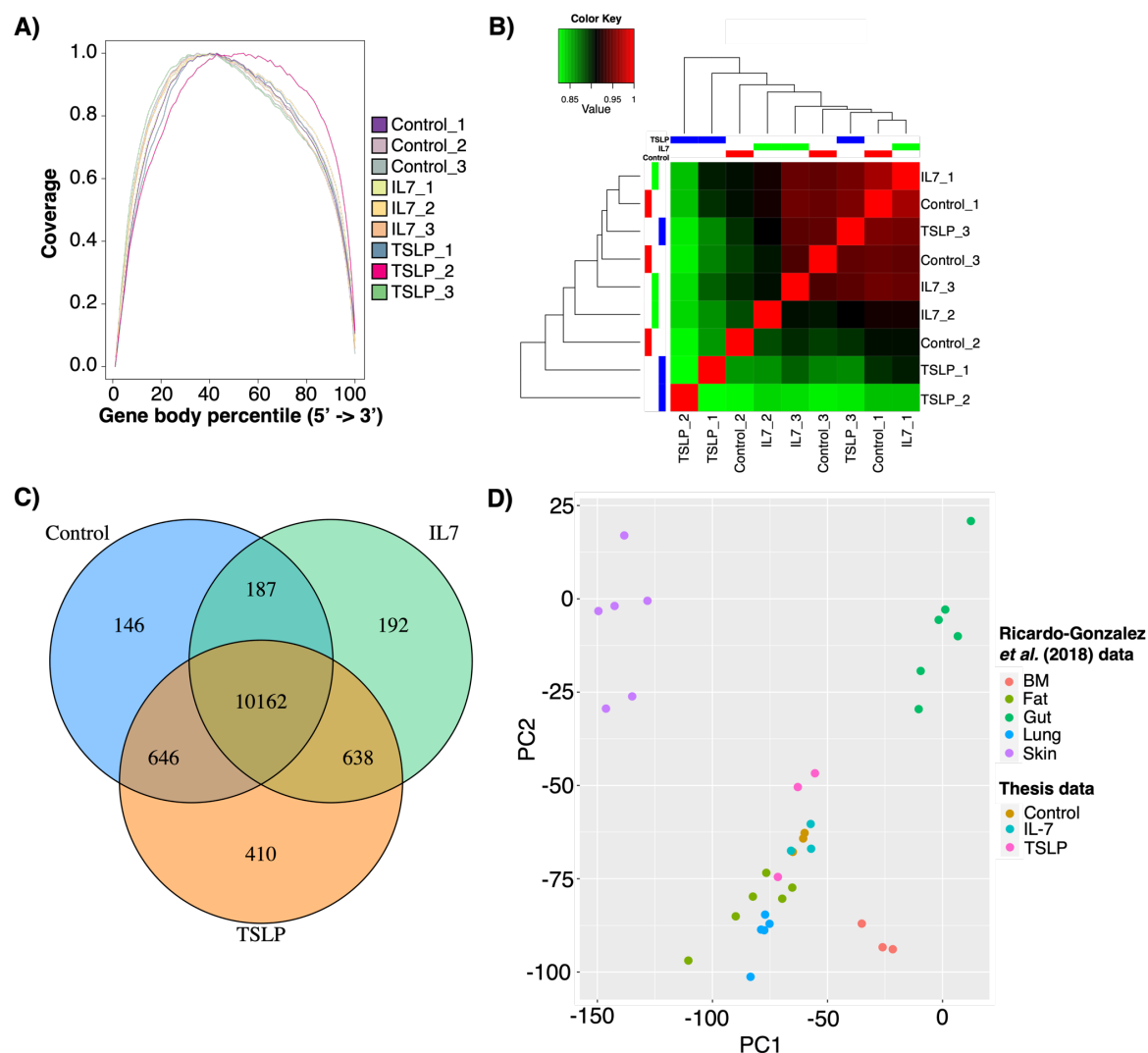
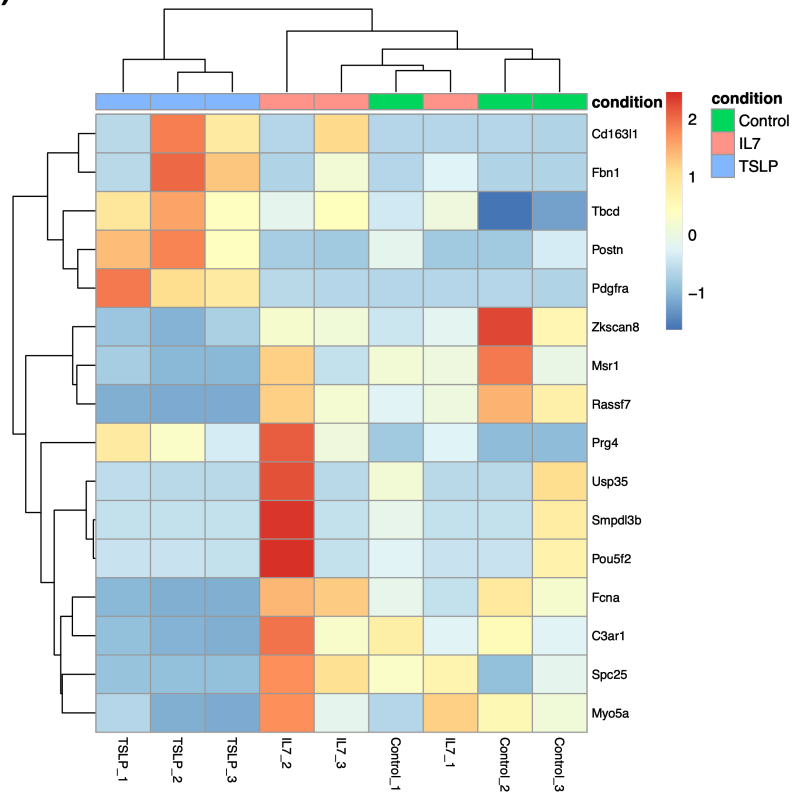


**Figure 4.2 IL-7- and TSLP-stimulated lung ILC2s RNAseq dataset has good read coverage and clustered closely to published lung and fat ILC2 RNAseq datasets.**

**A)** Read coverage across all transcripts based on mapping of sequencing reads to mouse reference genome (NCBI mm10). **B)** Sample correlation matrix using values calculated by kallisto. **C)** Total number of genes expressed in each treatment condition and total number of commonly expressed genes between conditions. **D)** PCA comparison of published mouse ILC2 RNAseq dataset<sup>134, 135</sup> to RNAseq dataset from this thesis. Published mouse ILC2 RNAseq dataset can be obtained from Gene Expression Omnibus (Series ID: GSE117568).

Although there was poor correlation with 3 samples, differential gene expression analysis was still performed. A total of 16 genes were identified to be differentially expressed in these samples, but most are not relevant to immune cells (Figure 4.3). These 16 genes were identified as *Cd163l1*, *Fbn1*, *Tbcd*, *Postn*, *Pdgfra*, *Zkscan8*, *Msr1*, *Rassf7*, *Prg4*, *Usp35*, *Smpd3b*, *Pou5f2*, *Fcna*, *C3ar1*, *Spc25*, and *Myo5a* (Table 4.2). *Postn* and *C3ar1* were previously associated with asthma and allergic airway inflammation<sup>136, 137</sup>. A notable observation is that TSLP-stimulated samples were transcriptionally distinct from control and IL-7-stimulated samples (Figure 4.3A). When normalized read counts are presented in a scatterplot, some genes were identified as differentially expressed due to one sample group showing less than 5 read counts (Figure 4.3B). Key genes used to identify ILC2s were selected from published papers (see Table 4.3)<sup>21, 134</sup> then assessed in the RNAseq dataset collected. None of the ILC2-relevant genes were differentially expressed after IL-7 or TSLP stimulation by edgeR or DESeq2 pipelines (Figure 4.4A). The read counts for these genes are reliable as none were reported to be below 5 (Figure 4.4B).

A)



B)

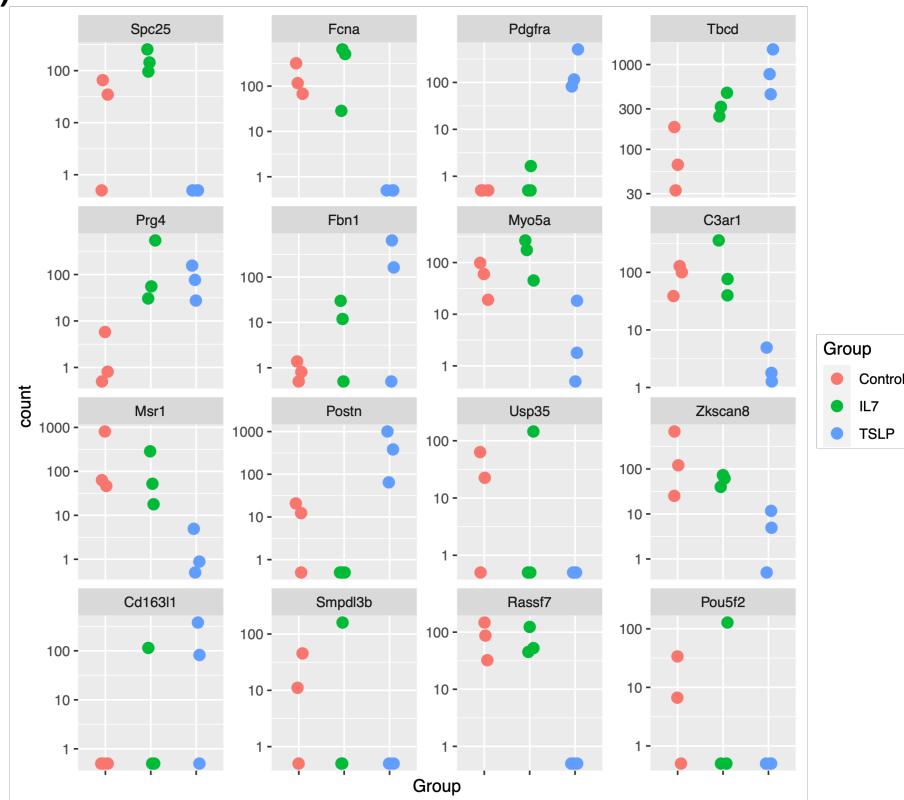


**Figure 4.3 TSLP-stimulated lung ILC2s have a distinct transcriptional landscape compared to control or IL-7-stimulated lung ILC2s.**

**A)** Heatmap displaying  $z$ -scores of key ILC2 genes in control, IL-7-stimulated, and TSLP-stimulated lung ILC2 samples. DESeq2 pipeline did not find these genes to be differentially expressed. **B)** Scatterplot of normalized read counts for key ILC2 genes in control, IL-7-stimulated, and TSLP-stimulated samples as calculated by DESeq2.



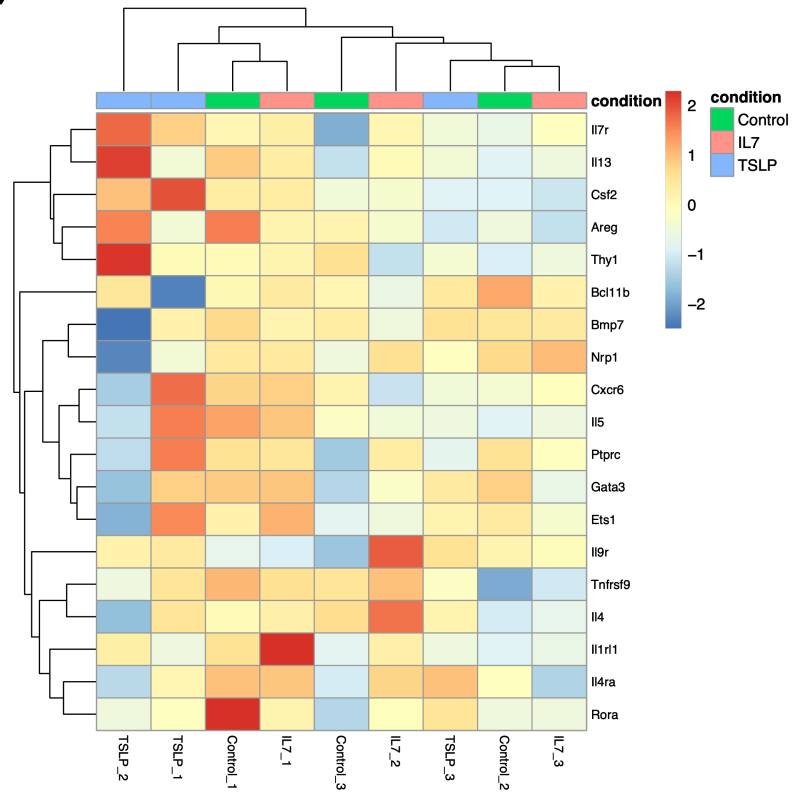
Gene	Brief description
<i>Spc25</i>	One of four subunits for Ndc80 complex; important in kinetochore-microtubule interaction and spindle checkpoint activity <sup>138</sup> .
<i>Fcna</i>	Ficolin A; enables carbohydrate derivative binding activity upstream of complement activation <sup>139</sup> .
<i>Pdgfra</i>	Surface tyrosine kinase receptor for platelet derived growth factor receptor alpha <sup>140</sup> .
<i>Tbcd</i>	Tubulin-specific chaperone D; needed for beta-tubulin folding intermediates <sup>141</sup> .
<i>Prg4</i>	Proteoglycan 4; large proteoglycan made by chondrocytes in cartilage to lubricate joints <sup>142</sup> .
<i>Fbn1</i>	Fibrillin-1; these proteins complex together to make microfibrils and provide structure to nerves, muscles, and eye lenses; carrier for TGFβ <sup>143</sup> .
<i>Myo5a</i>	Myosin Vα; transports molecules intracellularly and are important for neurons <sup>144</sup> .
<i>C3ar1</i>	Complement C3a receptor 1; anaphylatoxin released by complement system; C3a is required for ILC2 allergic inflammation <sup>137</sup> .
<i>Msr1</i>	Macrophage scavenger receptor 1; associated with macrophage-associated atherosclerosis, Alzheimer's disease, and host immune defense <sup>145-147</sup> .
<i>Postn</i>	Periostin; extracellular matrix proteins important for tissue development and regeneration; overexpression results in T2-high asthma <sup>136, 148</sup> .
<i>Usp35</i>	Ubiquitin Specific Peptidase 35l; required for the removal of ubiquitin from proteins; reduced expression found in tumours <sup>149</sup> .
<i>Zkscan8</i>	Zinc finger protein 192; predicted to be involved in transcriptional regulation through interactions with RNAPolIII <sup>150, 151</sup> .
<i>Cd163l1</i>	Scavenger receptor family member expressed on T cells 1; receptor for cysteine-rich superfamily <sup>152</sup> .
<i>Smpdl3b</i>	Sphingomyelin Phosphodiesterase Acid Like 3B; required for phosphoric diester hydrolase activity <sup>153</sup> .
<i>Rassf7</i>	Ras Association Domain Family Member 7; predicted to be involved in apoptosis and regulation of cytoskeleton organization <sup>141, 154</sup> .
<i>Pou5f2</i>	POU Domain Class 5 Transcription Factor 2; predicted to enable DNA binding transcription activity <sup>150</sup> .

**Table 4.2 Annotations of differentially expressed genes found in control, IL-7-stimulated, and TSLP-stimulated lung ILC2s.**

Gene	Brief description
<i>Il7r</i>	IL-7 receptor $\alpha$ chain; pairs with common $\gamma_c$ chain to form IL-7 receptor. Permits for IL-7 signaling and supports the development and survival of lymphocytes. <sup>116</sup>
<i>Il13</i>	IL-13 cytokine; induces airway hyperresponsiveness, goblet cell metaplasia, and glycoprotein hypersecretion which contributes to airway obstruction <sup>155</sup> .
<i>Csf2</i>	Colony-stimulating factor 2, or GM-CSF; released by BM ILC2s to aid hematopoietic recovery after BM injury <sup>156</sup> .
<i>Areg</i>	Amphiregulin; a member of the EGF family of growth factors that regulates tissue remodelling and repair after acute epithelial injury and asthma by ILC2s <sup>18</sup> .
<i>Thy1</i>	Thymus cell antigen 1; controls of inflammatory cell recruitment and expressed by ILCs <sup>157</sup> .
<i>Bcl11b</i>	B cell leukemia/lymphoma 11B; acts directly upstream of transcription factor Gfi1 to maintain mature ILC2 genetic and functional phenotype <sup>158</sup> .
<i>Bmp7</i>	Bone morphogenetic protein 7; released by ILC2s to promote adipocyte differentiation and lipid accumulation <sup>159</sup> .
<i>Nrp1</i>	Neuropilin-1; transmembrane glycoprotein that acts as a co-receptor for extracellular ligands (Sema3, TGF $\beta$ , VEGF) and expressed on lung ILC2s <sup>21</sup> .
<i>Cxcr6</i>	C-X-C chemokine receptor 6; expressed on all ILCs and deficiencies result in reduced ILC1 and ILC2 numbers and function <sup>160</sup> .
<i>Il5</i>	IL-5; produced by ILC2s for eosinophil recruitment and pro-inflammatory responses <sup>161</sup> .
<i>Ptpcr</i>	Protein tyrosine phosphatase receptor type C, or CD45; transmembrane protein found on all nucleated hematopoietic cells and precursors <sup>72, 162</sup> .
<i>Gata3</i>	Gata binding protein 3; required for ILC2 survival, proliferation, and immune responses; promotes expression of IL-7R $\alpha$ on ILCs and T cells <sup>119</sup> .
<i>Ets1</i>	ETS1 transcription factor; regulates <i>Id2</i> transcription in NK cells and promotes fitness of ILC progenitors. Critical regulator of ILC2 expansion and cytokine production <sup>163</sup> .
<i>Il9r</i>	IL-9 receptor; functional IL-9 receptor complex permits responsiveness to IL-9 which is important for ILC2 responses to lung infections and tissue repair <sup>164</sup> .
<i>Tnfrsf8</i>	TNF receptor superfamily member 8, or CD30; important role in the induction of T <sub>H</sub> 2 cell-mediated allergic asthma and expressed on ILC2s <sup>165, 166</sup> .
<i>Il4</i>	IL-4; produced by ILC2s to promote T <sub>H</sub> 2 cell differentiation during helminth infection <sup>167</sup> . Can also block regulatory T cell function and promote food allergy <sup>168</sup> .
<i>Il1rl1</i>	ST2, IL-33 receptor; promotes ILC2 inflammatory responses after injury <sup>169, 170</sup> .
<i>Il4ra</i>	IL-4 receptor $\alpha$ ; permits for IL-4 signaling and important for eosinophil recruitment <sup>171</sup> .
<i>Rora</i>	RAR-related orphan receptor $\alpha$ ; critical checkpoint for T cell and ILC2 lineage bifurcation <sup>172</sup> .

**Table 4.3 Annotations of key genes associated with ILC2s for their development, homeostasis, and immune responses.**

A)



B)

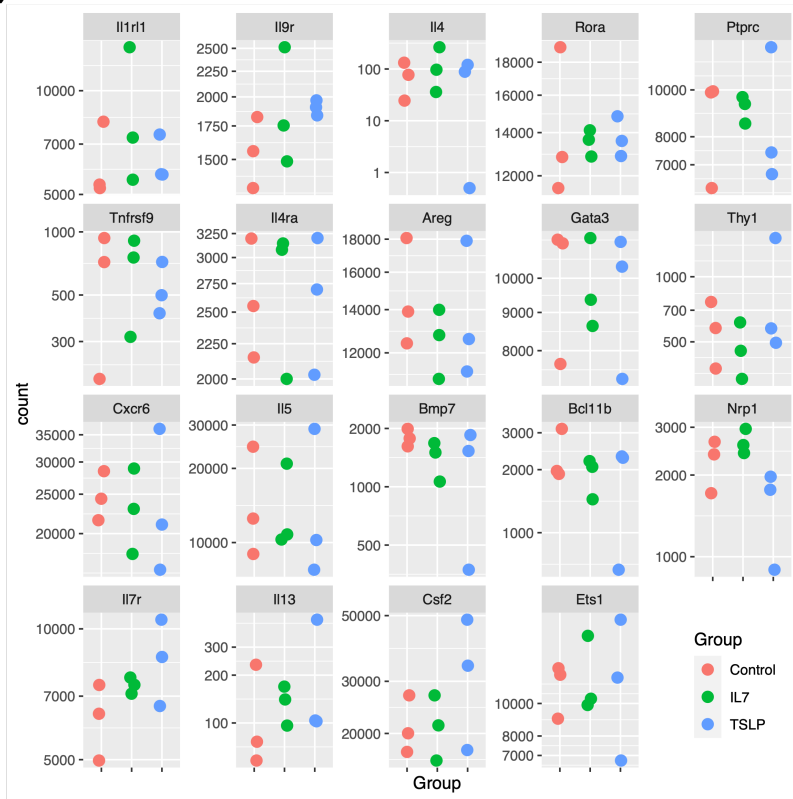
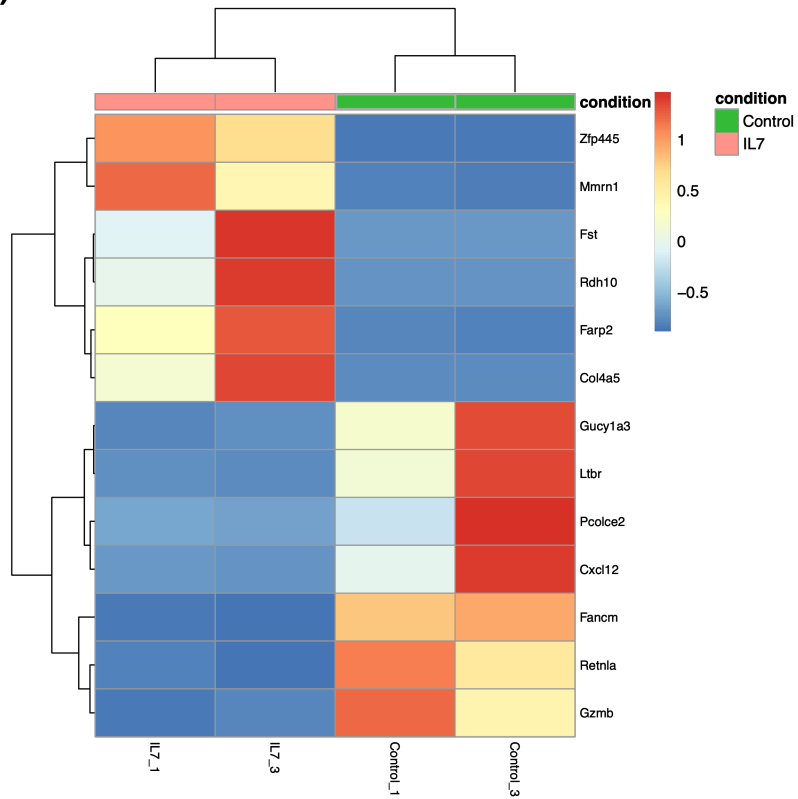


**Figure 4.4 Key ILC2 genes were not found to be differentially expressed in IL-7- or TSLP-stimulated lung ILC2s.**

**A)** Heatmap displaying  $z$ -scores of differentially expressed genes found in control, IL-7-stimulated, and TSLP-stimulated lung ILC2 samples. **B)** Scatterplot of normalized read counts for key ILC2 genes in control, IL-7-stimulated, and TSLP-stimulated samples.

Due to low correlation between TSLP\_1, TSLP\_2, and Control\_2 with the remaining samples, with read counts skewing differential gene expression analysis, Control\_1, Control\_3, IL7\_1, and IL7\_3 sequencing reads were put through the 10 different pipelines again to avoid skewing of results. Differential gene expression analysis showed a more defined output, and some immune-relevant genes were identified (Figure 4.5A). A total of 13 genes were identified as differentially expressed: *Zfp445*, *Mmrn1*, *Fst*, *Rdh10*, *Farp2*, *Col4a5*, *Gucyl1a3*, *Ltbr*, *Pcolce2*, *Cxcl12*, *Fancm*, *Retnla*, and *Gzmb* (Table 4.4). There still appears to be skewing of differential gene expression from normalized read counts below 5, but *Retnla*, *Gzmb*, and *Rdh10* appeared to have reliable counts (Figure 4.5B). However, no ILC2-specific genes were differentially expressed in this re-analysis (Figure 4.6).

A)



B)

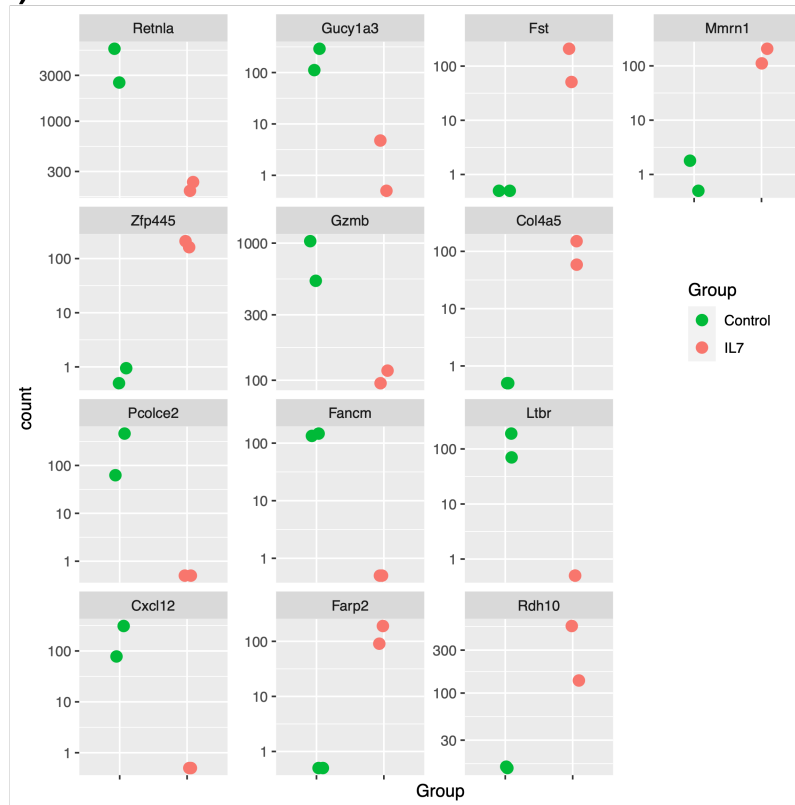


**Figure 4.5 Intranasal IL-7-stimulated lung ILC2s downregulate *Retnla* and *Gzmb* transcripts in comparison to control lung ILC2s.**

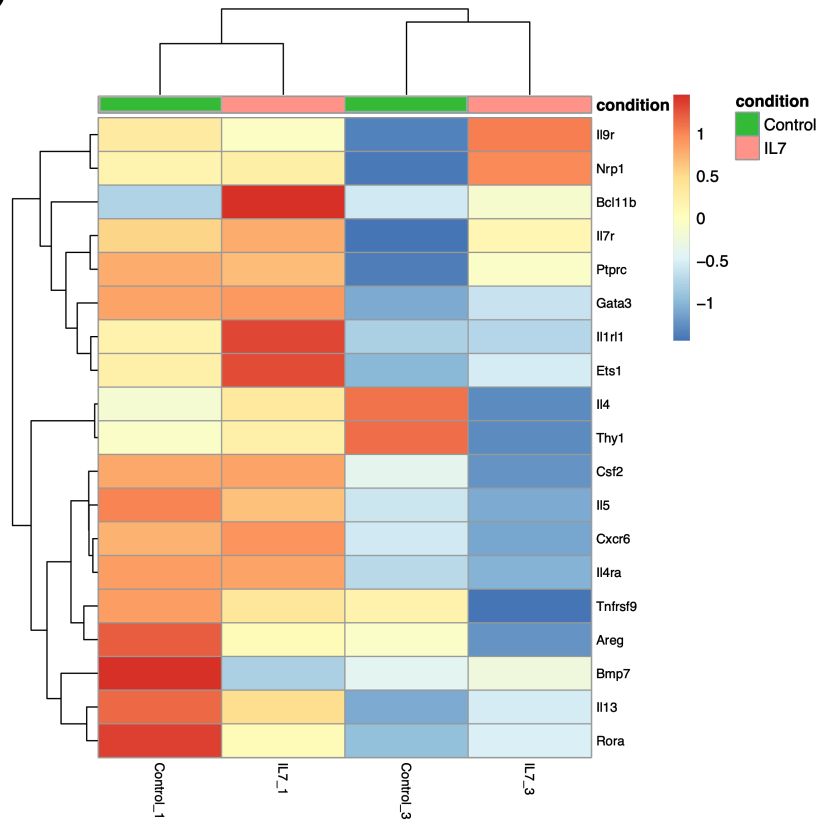
**A)** Heatmap displaying *z*-scores of differentially expressed genes in control and IL-7-stimulated lung ILC2 samples, calculated by DESeq2. **B)** Scatterplot of normalized read counts for genes identified as differentially expressed in control and IL-7-stimulated lung ILC2s, calculated by DESeq2.

Gene	Brief description
<i>Retnla</i>	RELMa protein; involved in pulmonary vascular remodeling and negatively regulates T <sub>H</sub> 2 immunity during helminth infections to limit fibrosis <sup>173</sup> .
<i>Gucy1a3</i>	Guanylate cyclase 1 soluble subunit alpha 1; catalyzes GTP to 3'5'-cyclic GMP and pyrophosphate <sup>174</sup> .
<i>Fst</i>	Follastatin; single-chain gonadal protein that inhibits follicle-stimulating hormone release and myostatin <sup>175</sup> .
<i>Mmrn1</i>	Multimerin 1; homopolymeric protein that platelet and endothelial proteins bind to and enhances platelet adhesion to collagen <sup>176</sup> .
<i>Zfp445</i>	Zinc finger protein 445; enabled chromatin binding activity and double stranded methylated DNA binding activity <sup>150, 177</sup> .
<i>Gzmb</i>	Granzyme B; produced by in NK cells and cytotoxic T cells to induce targeted cell apoptosis <sup>178</sup> .
<i>Col4a5</i>	Subunit of type IV collagen <sup>179</sup> .
<i>Pcolce2</i>	Procollagen C-endopeptidase Enhancer 2; enabled collagen binding activity. predicted to have positive regulation of peptidase activity <sup>180</sup> .
<i>Fancm</i>	Fanconi anemia complementation Group M; DNA-dependent ATPase component of Fanconi anemia core complex, important for male fertility <sup>181</sup> .
<i>Ltbr</i>	Lymphotoxin Beta Receptor; member of TNF receptor superfamily, ligand includes lymphotoxin alpha/beta and TNF superfamily 14 <sup>182</sup> .
<i>Cxcl12</i>	C-X-C motif chemokine ligand 12; antimicrobial factor, potent chemoattractant for lymphocytes and monocytes <sup>183</sup> .
<i>Farp2</i>	FERM/Pleckstrin Domain Protein 2/RhoGEF; enabled guanyl-nucleotide exchange factor activity, important for neuronal development and morphology <sup>184</sup> .
<i>Rdh10</i>	Retinol Dehydrogenase 10; converts all-trans-retinol to all-trans-retinal, needed for embryonic retinoid acid synthesis <sup>185</sup> .

**Table 4.4 Annotations of differentially expressed genes found in control and IL-7-stimulated lung ILC2s.**



A)



B)

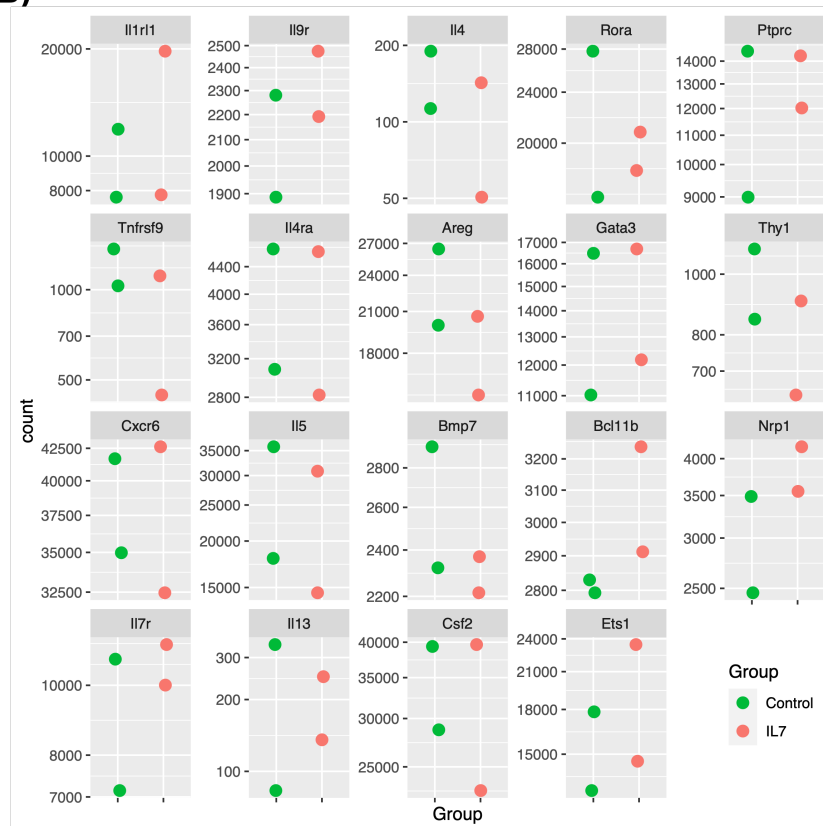


**Figure 4.6 Key ILC2 genes were not differentially expressed in IL-7-stimulated lung ILC2s when compared to unstimulated controls.**

**A)** Heatmap displaying  $z$ -scores of key ILC2 genes in control and IL-7-stimulated lung ILC2 samples, calculated by DESeq2. **B)** Scatterplot of normalized read counts for key ILC2 genes in control and IL-7-stimulated, calculated by DESeq2.

## 4.4 Summary and Discussion

### 4.4.1 Summary

In this chapter, I showed that *Nrp1* expression in lung ILC2s was independent of IL-7 signaling as *Nrp1* surface expression was not altered between WT and IL-7R $\alpha^{Y449F}$  mice. I also showed that IL-7-stimulated and TSLP-stimulated lung ILC2s were transcriptionally distinct from each other but common ILC2 markers such as *Gata3* and *Rora* were apparently not differentially expressed.

### 4.4.2 Discussion

In the RNAseq transcriptional profiling of IL-7- and TSLP-stimulated lung ILC2s, the RNAseq results were relatively poor as determined by low sample correlation between most TSLP-stimulated samples to control and IL-7-stimulated samples. Additionally, many of the differentially expressed genes had low normalized read counts (<5 read counts). The RNAseq results may have also been affected by the lack of positive controls to indicate optimal stimulation conditions. The expected internal control transcripts such as *Gata3*, *Rora*, and *Bcl11b* were not determined to be differentially expressed after IL-7 stimulation suggesting poor stimulation. However, PCA comparison showed close clustering of this RNAseq dataset to published lung and fat ILC2 RNAseq datasets which indicated a relatively pure lung ILC2 population was isolated for the analysis. Due to these reasons, the RNAseq results were interpreted cautiously with the exclusion criteria as follows: **(1)** the gene identified should be expressed in at least two samples, **(2)** the normalized read counts must be at least 5. Overall, the results showed that IL-7 and TSLP stimulation in lung ILC2s induced distinct transcriptional landscapes. This may be due to TSLP being an alarmin that promotes pro-inflammatory responses and IL-7 promoting hematopoietic processes<sup>66, 67</sup>.

*Postn* is the gene for periostin, a protein associated with asthma pathogenesis<sup>136, 186</sup>, and was found to be increased in expression in TSLP-stimulated ILC2s. A small number of published articles have shown a link between periostin and lung ILC2s in promoting pulmonary fibrosis and periostin modulating IL-13 and IL-5 release by innate immune cells<sup>187, 188</sup>. Periostin has also been shown to be a surrogate biomarker for the development of chronic obstructive pulmonary disease (COPD), a disease that ILC2s are also associated with<sup>148</sup>. The other gene that was differentially expressed in this RNAseq dataset was *C3ar1* which was downregulated in TSLP-stimulated lung ILC2s. This gene encodes for complement C3a receptor, which is needed for the induction and regulation of T<sub>H</sub>2-mediated inflammatory responses to viruses, allergens, and fungi<sup>137</sup>. It has been shown that ILC2 recruitment during IL-33 or allergen stimulation were C3a-dependent, which permitted stronger ILC and T cell interactions<sup>137</sup>. Additionally, it was discovered that C3a induced IL-13 and GM-CSF production in ILC2s while inhibiting IL-10 production<sup>137</sup>. Combining these findings that TSLP-stimulated lung ILC2s upregulated *Postn* and downregulated *C3ar1*, it appeared to be contradictory since both genes are associated with inflammatory responses. However, IL-33 and TSLP induce distinct phenotypic profiles in human ILC2s<sup>189</sup> so the upregulation of *Postn* and downregulation of *C3ar1* could be a unique feature to TSLP stimulation in mouse lung ILC2s. Other genes found to be differentially expressed and matched the exclusion criteria described earlier (*Tbcd*, *Fnb1*, *Myo5a*, *Rassf7*) are associated with cell cycle regulation and motility, suggesting that IL-7- and TSLP-stimulated ILC2s may become more active and proliferative in response to cytokine stimulation.

Additional transcript and protein analysis would be required to determine the exact immune phenotypes of IL-7- and TSLP-stimulated lung ILC2s. For instance, measuring *Postn* transcripts in IL-7- and TSLP-stimulated lung ILC2s using qRT-PCR would provide a more

concise measurement for mRNA expression changes. If *Postn* transcripts were found to be elevated in qRT-PCR analysis, further measuring periostin protein expression in TSLP-stimulated ILC2s using flow cytometry or ELISA would determine whether increased gene expression translates to increased protein expression.

Since I found that most TSLP-stimulated samples were poorly correlated to control and IL-7-stimulated samples, re-analysis of control and IL-7-stimulated samples alone was performed to assess what transcriptional changes occur with IL-7 stimulation. A more defined gene expression profile was observed after these adjustments were made and a handful of immune relevant genes were identified including *Retnla* and *Gzmb*. Following a thorough literature review, only *Retnla* was found to be relevant to ILC2 and lung biology. *Retnla* was first identified as FIZZ1 and encodes for secreted protein resistin-like molecule alpha (RELM $\alpha$ ), which suppresses T<sub>H</sub>2 cytokine immune responses in the lungs, particularly during helminth infections<sup>173, 190, 191</sup>. More recent research has shown that IL-10-producing lung ILC2s downregulate their expression of pro-inflammatory genes and have high *Retnla* expression, giving them an anti-inflammatory phenotype<sup>192</sup>. In my dataset, IL-7-stimulated lung ILC2s downregulated *Retnla* expression in comparison to control samples suggesting that IL-7 stimulation may stimulate T<sub>H</sub>2 skewing in ILC2s. The other relevant gene found to be differentially expressed in IL-7-stimulated lung ILC2s was *Gzmb*, the gene for Granzyme B (GzmB). GzmB is a potent protease secreted by NK cells and cytotoxic T cells to induce apoptosis of target cells, which includes tumours and virus-infected cells<sup>178</sup>. This was an interesting finding because ILC2s are known to release IL-4, IL-5, IL-13, and amphiregulin upon their activation to promote immune cell recruitment and tissue repair<sup>2, 54</sup>. While no studies to date have shown ILC2s as a source of GzmB, there are studies that have shown mouse liver

ILC1s expressing Granzyme A<sup>193</sup> and human gut ILC1s expressing GzmB<sup>194</sup>. It is possible that lung ILC2s may express GzmB. Due to the limitations of this RNAseq dataset, further validation of *Retnla* and *Gzmb* transcript expression by qRT-PCR is required. Protein expression should also be measured using flow cytometry or ELISA assay.

With the flow cytometry and qRT-PCR data from Chapter 3 showing a link between IL-7 signaling and GATA3 expression in ILC2s, I predicted that *Gata3* would also be differentially expressed in the RNAseq datasets. However, the transcriptional profiling did not show differential expression of *Gata3* or other ILC2-related genes between the treatments. Factors that may have resulted in these negative results include treatment duration, cytokine dosages, and dosage frequency. It is possible that the day 4 timepoint was too early or too late to detect changes in ILC2-related transcripts, so performing a 10-day time-course analysis of IL-7- and TSLP-stimulated lung ILC2s with positive controls would aid in narrowing the appropriate stimulation duration. This could be done using qRT-PCR to measure transcripts of genes identified in Table 4.3 as a more cost-effective method. Regarding dosage and dosage frequency, I did a single dose of 2µg IL-7 or 500ng TSLP per mouse for this RNAseq analysis. The dose for IL-7 was selected based on previous protocols in our lab; 10µg IL-7 is used for intraperitoneal (IP) injections and 1µg IL-7 for intranasal phospho-STAT5 activation. I presumed 2µg IL-7 would be sufficient to induce a potent response intranasally since it was twice of what was previously used for intranasal delivery and a fraction of what is needed for IP delivery, which requires a higher dose to account for diffusion in tissues and metabolism by tissue enzymes<sup>195</sup>. As for TSLP dosage, I followed the protocol described in Headley *et al.* (2009)<sup>196</sup> and Han *et al.* (2013)<sup>197</sup> which both used a single dose of 500ng TSLP intranasally to induce immune cell recruitment. To improve the immune responses generated by lung ILC2s after IL-7 or TSLP

stimulation, different dosages of IL-7 (2µg, 4µg, 8µg, and 12µg) and TSLP (500ng, 1µg, 5µg, 10µg, and 20µg) should be tested as well as the frequency of doses (one dose every day, one dose every second day).

It may also be possible that having low-input RNA resulted in key ILC2 genes not identified in differential gene expression analysis due to low read coverage and shallow sequencing depth. Read counts for 19 selected ILC2 genes were assessed, and the results showed reliable high read counts for these genes ( $\geq 500$  read counts), thus increasing sequencing depth would not be of any benefit to the analysis. If this experiment was repeated, it would be crucial to increase the amount of input RNA to alleviate the challenges of library preparation, increase read coverage and reduce noise in the output read files. *Nrp1* should be kept as a surface marker used for cell sorting for RNAseq since I showed that *Nrp1* expression on lung ILC2s was independent of IL-7 signaling when comparing WT and IL-7R $\alpha^{Y449F}$  lung ILC2s.

To summarize, I showed that IL-7 stimulation of lung ILC2s induced a distinct transcriptional landscape in comparison to TSLP stimulation of the same cell population. However, common ILC2 genes were not found to be differentially expressed after IL-7 or TSLP stimulation due to the limitations of the RNAseq dataset generated. I proposed performing extended treatment duration, cytokine dosage, and frequency of dosage analyses to improve the outcomes of a repeat RNAseq analysis.

## Chapter 5: Conclusion

### 5.1 Summary of main findings

The goals of this thesis were to examine how IL-7 regulates ILC2 development in fetal liver and adult bone marrow, and its role in regulating lung ILC2 responses to Influenza infection. Current literature suggests that IL-7 is needed for the development and function of all ILC subsets, however, the data in this thesis shows it is vital for ILC2s.

In Chapter 3, I showed evidence that BM ILC2s are dependent on IL-7 signaling for their development and when IL-7 signaling is disrupted, there was a reduction in *Gata3* transcripts and a loss of ILC2 numbers and their GATA3 expression. I further established that impaired IL-7 signaling only impacts ILC2s as ILC1s and ILC3s were unaffected by this disruption in both cell numbers and respective transcription factor expression. Interestingly, the results of the 10-day IL-7 stimulation of bone marrow ILC2s showed that IL-7R $\alpha$ /CD127 on IL-7R $\alpha^{Y449F}$  ILC2s were able to properly respond to IL-7 stimulation through its downregulation on the surface. This finding indicated that disruptions to ILC2 development and GATA3 expression in IL-7R $\alpha^{Y449F}$  mice were most likely due to impaired downstream signaling effects and not the impaired dynamics of the receptor. These findings mirror those reported in Sheikh *et al.* (2022)<sup>51</sup> and further examined IL-7 dynamics in IL-7R $\alpha^{Y449F}$  ILC2s.

Maternal-fetal IL-7 exposure effects on ILC2 development and function were also examined in Chapter 3. Fetal livers from TgIL7 mice demonstrated a trend of increased ILC2s and GATA3 expression compared to WT samples. Additionally, in adult WT and TgIL7 offspring that had mf-IL-7 exposure, a distinct GATA3<sup>+</sup> ILC2 population developed in the bone marrow that was not observed in the respective controls. To examine the potential long-term



effects of mf-IL-7 exposure, adult offspring that had mf-IL-7 exposure were challenged with a 6-day Influenza infection. No differences were observed between control WT and WT+mf-IL-7 mice. However, there was a significant increase in ILC2 numbers and IL-5 and IL-13 production in TgIL7+mf-IL7 mice when compared to WT control. Since there were no differences between WT and WT+mf-IL-7 during Influenza challenge, the effects observed in TgIL7+mf-IL-7 mice were likely due to overexpression of IL-7 and not mf-IL-7.

Finally, I examined the transcriptional landscape that is regulated by IL-7 and TSLP in lung ILC2s in Chapter 4. To aid in cell sorting for RNAseq, Nrp1 was assessed for its integrity as a lung ILC2 marker in IL-7R $\alpha$ <sup>Y449F</sup> mice. Nrp1 expression was found to be independent of IL-7 signaling in lung ILC2s and was used as an added marker for cell sorting for RNAseq. Although RNAseq results were relatively poor due to low input RNA, the data suggests that IL-7 and TSLP stimulation of lung ILC2s results in 2 distinct transcriptional profiles. With TSLP stimulation, *Postn*, a gene associated with inflammatory responses in asthma, was upregulated in comparison to control and IL-7-stimulated samples. Conversely, IL-7 stimulation results in the downregulation of *Retnla*, an anti-inflammatory gene. While both IL-7 and TSLP receptors share IL-7R $\alpha$  subunit, the preliminary dataset generated here suggests that the transcriptional responses produced can elicit expression of genes that are functionally distinct from each other.

## **5.2 Implications for human health**

My findings provide strong evidence that IL-7 is required for the development of ILC2s in adult bone marrow and fetal liver tissues. IL-7 was also shown to influence ILC2 responses to Influenza infection in the lungs of TgIL7+mf-IL7 mice. Since IL-7 plays a key role in immune cell development, and recent research showed the involvement of ILC2s in severe immune-

driven diseases such as asthma and inflammatory bowel disease<sup>54, 198</sup>, these findings are highly relevant to developing new therapeutic strategies to control these diseases.

I identified two genes relevant to human health, *Postn* and *Retnla*, independently regulated by IL-7 and TSLP in lung ILC2s. *Postn* is the gene for periostin and its transcript levels were found to be significantly elevated in TSLP-stimulated lung ILC2s suggesting a pro-inflammatory phenotype. Periostin protein and *Postn* transcripts are elevated in asthma and COPD patients and is used as a novel biomarker for these conditions. Lung ILC2s are involved in these two diseases, so targeting *Postn* using a gene suppressor or sequestering periostin to prevent receptor binding may alleviate pro-inflammatory symptoms and improve current treatments. Currently, there is a clinical trial for lebrikizumab in asthma patients, where this monoclonal antibody blocks IL-13 signaling to inhibit periostin expression<sup>199</sup>. *Retnla* was the other gene found to be differentially expressed in the transcriptional analyses. This gene is known to stimulate anti-inflammatory responses by innate immune cells. Stimulators for *Retnla* or administration of RELM- $\alpha$  (protein encoded by *Retnla*) to the lungs could be beneficial in controlling inflammation during asthma exacerbation or airway allergic reaction. There is also potential for combining *Postn* inhibitors with *Retnla* stimulators to drive a strong anti-inflammatory response during flare-ups and limit tissue damage.

In addition to targeting the downstream target of TSLP, directly targeting of TSLP in the lungs can help prevent or reduce the severity of symptoms in asthmatic and airway allergy-prone patients. Tezepelumab is a first-in-class human monoclonal antibody against TSLP and has been shown to be effective in controlling severe asthma and airway allergen-induced asthma<sup>200, 201</sup>. TSLP blockade was also found to be effective in COPD patients<sup>202</sup>. In a murine model of asthma, it was found that a combined blockade of IL-33, IL-25 and TSLP was the most effective in

inhibiting inflammation, T<sub>H</sub>2 cytokine expression, airways fibrosis and IgE production when compared to single blockage treatments<sup>203</sup>. Depending on the patient and severity of asthma, TSLP blockades can be combined with other pro-inflammatory inhibitors for a personalized treatment.

The effect of maternal IL-7 on offspring ILC2 development was also examined and the data showed a distinct GATA3<sup>+</sup> ILC2 population that developed. I then tested whether maternal-fetal IL-7 exposure had long term effects. When adult mice with maternal-fetal IL-7 exposure were infected with Influenza, there was no evidence of long-term effects as determined by lung ILC2 numbers and IL-5 and IL-13 production. It may be possible that maternal-fetal IL-7 exposure affects lung tissue repair post-Influenza infection, so ILC2 amphiregulin production and lung tissue histology should be tested. Although I did not observe changes in thymic CD8 and CD4 T cells, long term exposure to high doses of IL-7 may lead to lymphopenia-induced proliferation (LIP) and result in the development of severe inflammation diseases<sup>204</sup>. It has been shown that an abundance of IL-7 in IL-7R<sup>-/-</sup> and IL-7R $\alpha$ <sup>Y449F</sup> mice supports LIP of T cells transferred from WT mice<sup>205</sup>. With clinical research showing links between high IL-7 levels and inflammatory diseases such as multiple sclerosis, rheumatoid arthritis, and type 1 diabetes<sup>206-208</sup>, early life exposure to excessive IL-7 levels may accelerate the manifestation of disease symptoms or increase the severity of disease through inducing the development of T<sub>H</sub>2-driven cells. In the event an allograft transplant is required during early life, residual maternal IL-7 may result in rapid allograft rejection and lead to further complications<sup>209</sup>.

Although long-term genetic or therapeutic exposure to excess IL-7 can lead to immune-driven diseases, short-term uses of IL-7 may be beneficial and a promising option for treatments. For example, IL-7 treatments were found to improve the recovery of hospitalized, severe

COVID-19 patients by boosting lymphocyte counts<sup>80</sup>. The administration of IL-7 may also be used to boost NKG2D<sup>+</sup> ILC2 numbers within the lungs, which were found to be protective in severe COVID-19 patients by releasing anti-inflammatory cytokines<sup>210</sup>. Additionally, new research showed that using modified non-propagative vaccinia virus Ankara to deliver IL-7 allowed for more potent delivery of IL-7. This approach was better able to stimulate innate and adaptive immune responses and provided a broader mechanism of action compared to intravenous IL-7<sup>211</sup>. ILC2s have been reported to respond to vaccinia virus Ankara with greater IL-13 release in the lungs<sup>212</sup>. It is speculated that when vaccinia virus Ankara is combined with Influenza vaccines, it will strengthen ILC2 interactions with DCs leading to improved vaccine efficacy<sup>212</sup>.

In addition to the relevance to human health, the findings presented in this thesis further bolsters the current understanding that ILC2 development is dependent on IL-7, and that ILC1 and ILC3 populations are less reliant on IL-7 for development signals. Additionally, the work on maternal-fetal IL-7 exposure emphasizes the need for research to examine how ILC2 development and responses may be affected by cytokines and factors transferred from mother to offspring. The majority of research on maternal immunity influencing offspring immunity focuses on passive transfer of antibodies through the placenta and breastmilk, or genetic aspects such as inherited genes or epigenetics. Expanding research to cytokines and factors transferred to offspring from the mother could provide more insight on how variations in immune responses between individuals occur. For example, while it is known there are genetic predispositions to developing asthma, does exposure to elevated levels of alarmins during fetal development influence the development and severity of asthma? Research studying the pathogenesis of asthma has become more complex over the past decades and has identified the microbiome as an

important environmental factor to the development of asthma<sup>213, 214</sup>. Maternal-fetal exchange of cytokines should be another environmental factor to be considered in this disease model.

### **5.3 Future Directions**

#### **5.3.1 Transcriptional effects of IL-7 signaling on fetal liver ILC2s**

Fetal liver ILC2 populations from TgIL7 mothers appeared to be expanded compared to WT FL ILC2s. It has been shown that majority of mature ILC2s in peripheral tissues are seeded in early life and originate from the fetal liver, with minimal seeding from the adult BM<sup>20</sup>. It would be crucial to examine the transcriptional landscape in FL ILC2s under IL-7 loss of function and gain of function models, then compare to adult BM ILC2s to see if any differences exist between early life and adult ILC2 development. This data could explain why mature ILC2s are mostly from fetal origins and why they are a long-living immune cell population.

#### **5.3.2 Genetic imprinting from maternal IL-7 on offspring bone marrow ILC2s**

As an extension to RNAseq analysis of fetal liver ILC2s in loss of function and gain of function models, transcriptional analysis of adult BM ILC2s with mf-IL-7 exposure should be performed. This may address why a unique GATA3<sup>+</sup> ILC2 population forms in both WT and TgIL7 mice with mf-IL-7 exposure but not their respective controls. Epigenetic analysis by chromatin immunoprecipitation sequencing (ChIP-Seq) can also be done to examine whether genetic imprinting occurs in these cells.

#### **5.3.3 *Postn* and *Retnla* transcripts and protein expression in lung ILC2s**

In the RNAseq analysis of IL-7- and TSLP-stimulated lung ILC2s, *Postn* and *Retnla* were identified to be differentially expressed under these two conditions and have relevance to ILC2s. Performing qRT-PCR analysis of these two transcripts would be crucial to validate the RNAseq findings as well as quantify mRNA transcript copies<sup>215</sup>. It would also be important to quantify

periostin (*Postn* gene) and RELM- $\alpha$  (*Retnla* gene) protein expression to determine whether IL-7 or TSLP stimulation affects both transcription and protein expression. If any changes are observed for *Postn*/periostin or *Retnla*/RELM- $\alpha$ , measuring IL-5 and IL-13 production in treated lung ILC2s would provide further support for a pro-inflammatory or anti-inflammatory phenotype.

#### **5.3.4 Transgenic IL-7 ILC2 immune responses to Influenza infections and airway irritants**

With the observation that TgIL7+mf-IL-7 mice have elevated IL-5 and IL-13 release in response to Influenza challenge and no differences were observed in WT and WT+mf-IL-7 mice, I proposed that the effects observed in TgIL7+mf-IL-7 mice are solely caused by overexpression of IL-7. This should be further examined by thorough analysis of TgIL7 and TgIL7+mf-IL-7 mice during a 6-day Influenza challenge. TgIL7 lung ILC2 immune responses should also be assessed under stimulation with airway irritants such as house dust mite or papain since these stimulants invoke T<sub>H</sub>2 responses in ILC2s.

#### **5.3.5 IL-7 signaling during gut ILC2 immune responses**

Lung ILC2 responses to Influenza infection were examined in this thesis, however, ILC2s are also crucial in maintaining gut homeostasis and regulating immune responses to gut helminth infections<sup>2, 7</sup>. It would be interesting to assess the role of IL-7 in ILC2s during intestinal helminth infections and colitis models to examine whether the importance of IL-7 in lung ILC2s<sup>51</sup> is tissue-specific or applies broadly to all tissue-resident ILC2s.

#### **5.3.6 Signaling pathway analyses in IL-7R $\alpha$ <sup>Y449F</sup> ILC2s**

It was determined that IL-7R $\alpha$ <sup>Y449F</sup> subunit becomes internalized and recycled to the surface like WT IL-7R $\alpha$  following *in vitro* ILC2 stimulation with IL-7, which indicates that it is

not the engulfment of the receptor that caused the defects in ILC2 development observed. Determining where the signaling impairment in these mice resides is critical to understanding this model. It is known that motif Y449 on IL-7R $\alpha$  is critical for the recruitment of STAT5 upon IL-7 binding and that T cell development and function are dependent on STAT5 recruitment<sup>89, 216</sup>. Due to the similarities between ILC2s and T cells, thorough IL-7 signaling pathway analysis could implicate which pathways in the IL-7 signaling cascade contributes the most to ILC2 biology. It would also be interesting to examine whether impaired IL-7 signaling in IL-7R $\alpha$ <sup>Y449F</sup> ILC2s affects GATA3 activation. This could be done by analyzing GATA3 phosphorylation by p38 and Akt1<sup>217, 218</sup>.

## 5.4 Conclusions

The data presented in this thesis has elements that support the hypothesis that IL-7 transcriptionally regulates ILC2 maintenance and immune responses. When IL-7 signaling was disrupted through a knock-in mutation on IL-7R $\alpha$ , a loss in *Gata3* transcripts and GATA3 expression in bone marrow and fetal liver ILC2s was observed. Conversely, when IL-7 is in abundance, there was an increase in ILC2 numbers and GATA3 expression. Transcriptional profiling of lung ILC2s after IL-7 or TSLP stimulation showed that although these two cytokines share a common receptor subunit, these cytokines invoke distinct transcriptional landscapes within the same cell population.

## References

1. Vivier, E., van de Pavert, S.A., Cooper, M.D. & Belz, G.T. The evolution of innate lymphoid cells. *Nat Immunol* **17**, 790-794 (2016).
2. Eberl, G., Colonna, M., Di Santo, J.P. & McKenzie, A.N. Innate lymphoid cells. Innate lymphoid cells: a new paradigm in immunology. *Science* **348**, aaa6566 (2015).
3. Spits, H. & Di Santo, J.P. The expanding family of innate lymphoid cells: regulators and effectors of immunity and tissue remodeling. *Nat Immunol* **12**, 21-27 (2011).
4. Vivier, E. *et al.* Innate Lymphoid Cells: 10 Years On. *Cell* **174**, 1054-1066 (2018).
5. Yoder, J.A. & Litman, G.W. The phylogenetic origins of natural killer receptors and recognition: relationships, possibilities, and realities. *Immunogenetics* **63**, 123-141 (2011).
6. Spits, H. *et al.* Innate lymphoid cells--a proposal for uniform nomenclature. *Nat Rev Immunol* **13**, 145-149 (2013).
7. Artis, D. & Spits, H. The biology of innate lymphoid cells. *Nature* **517**, 293-301 (2015).
8. Gordon, Scott M. *et al.* The Transcription Factors T-bet and Eomes Control Key Checkpoints of Natural Killer Cell Maturation. *Immunity* **36**, 55-67 (2012).
9. Fuchs, A. *et al.* Intraepithelial type 1 innate lymphoid cells are a unique subset of IL-12- and IL-15-responsive IFN- $\gamma$ -producing cells. *Immunity* **38**, 769-781 (2013).
10. Fuchs, A. ILC1s in Tissue Inflammation and Infection. *Frontiers in immunology* **7**, 104-104 (2016).
11. Fallon, P.G. *et al.* Identification of an interleukin (IL)-25-dependent cell population that provides IL-4, IL-5, and IL-13 at the onset of helminth expulsion. *The Journal of experimental medicine* **203**, 1105-1116 (2006).
12. Moro, K. *et al.* Innate production of TH 2 cytokines by adipose tissue-associated c-Kit<sup>+</sup> Sca-1<sup>+</sup> lymphoid cells. *Nature* **463**, 540-544 (2010).
13. Wilhelm, C. *et al.* An IL-9 fate reporter demonstrates the induction of an innate IL-9 response in lung inflammation. *Nature immunology* **12**, 1071-1077 (2011).
14. Halim, T.Y. *et al.* Retinoic-acid-receptor-related orphan nuclear receptor alpha is required for natural helper cell development and allergic inflammation. *Immunity* **37**, 463-474 (2012).



15. Hoyler, T. *et al.* The transcription factor GATA-3 controls cell fate and maintenance of type 2 innate lymphoid cells. *Immunity* **37**, 634-648 (2012).
16. Liang, H.-E. *et al.* Divergent expression patterns of IL-4 and IL-13 define unique functions in allergic immunity. *Nature immunology* **13**, 58 (2012).
17. Wong, S.H. *et al.* Transcription factor ROR $\alpha$  is critical for nuocyte development. *Nature immunology* **13**, 229 (2012).
18. Monticelli, L.A. *et al.* Innate lymphoid cells promote lung tissue homeostasis following acute influenza virus infection. *Nat Immunol* **12**, 1045-1054 (2011).
19. Chang, Y.-J. *et al.* Innate lymphoid cells mediate influenza-induced airway hyper-reactivity independently of adaptive immunity. *Nature immunology* **12**, 631-638 (2011).
20. Schneider, C. *et al.* Tissue-Resident Group 2 Innate Lymphoid Cells Differentiate by Layered Ontogeny and In Situ Perinatal Priming. *Immunity* **50**, 1425-1438.e1425 (2019).
21. Zhang, J. *et al.* Neuropilin-1 mediates lung tissue-specific control of ILC2 function in type 2 immunity. *Nature Immunology* **23**, 237-250 (2022).
22. Saranchova, I. *et al.* Type 2 Innate Lymphocytes Actuate Immunity Against Tumours and Limit Cancer Metastasis. *Scientific Reports* **8**, 2924 (2018).
23. Germain, R.N. & Huang, Y. ILC2s — resident lymphocytes pre-adapted to a specific tissue or migratory effectors that adapt to where they move? *Current Opinion in Immunology* **56**, 76-81 (2019).
24. Gasteiger, G., Fan, X., Dikiy, S., Lee, S.Y. & Rudensky, A.Y. Tissue residency of innate lymphoid cells in lymphoid and nonlymphoid organs. *Science* **350**, 981-985 (2015).
25. Entwistle, L.J. *et al.* Pulmonary Group 2 Innate Lymphoid Cell Phenotype Is Context Specific: Determining the Effect of Strain, Location, and Stimuli. *Frontiers in Immunology* **10** (2020).
26. Sanos, S.L., Vonarbourg, C., Mortha, A. & Diefenbach, A. Control of epithelial cell function by interleukin-22-producing ROR $\gamma$ t<sup>+</sup> innate lymphoid cells. *Immunology* **132**, 453-465 (2011).
27. Luci, C. *et al.* Influence of the transcription factor ROR $\gamma$ t on the development of NKp46<sup>+</sup> cell populations in gut and skin. *Nature immunology* **10**, 75-82 (2009).
28. Withers, D.R. & Hepworth, M.R. Group 3 Innate Lymphoid Cells: Communications Hubs of the Intestinal Immune System. *Frontiers in Immunology* **8** (2017).

29. Satoh-Takayama, N. *et al.* IL-7 and IL-15 independently program the differentiation of intestinal CD3<sup>+</sup> NKp46<sup>+</sup> cell subsets from Id2-dependent precursors. *Journal of Experimental Medicine* **207**, 273-280 (2010).
30. Vonarbourg, C. *et al.* Regulated expression of nuclear receptor ROR $\gamma$ t confers distinct functional fates to NK cell receptor-expressing ROR $\gamma$ t<sup>+</sup> innate lymphocytes. *Immunity* **33**, 736-751 (2010).
31. Huang, Y. *et al.* IL-25-responsive, lineage-negative KLRG1(hi) cells are multipotential 'inflammatory' type 2 innate lymphoid cells. *Nat Immunol* **16**, 161-169 (2015).
32. Bernink, Jochem H. *et al.* Interleukin-12 and -23 Control Plasticity of CD127<sup>+</sup> Group 1 and Group 3 Innate Lymphoid Cells in the Intestinal Lamina Propria. *Immunity* **43**, 146-160 (2015).
33. Bal, S.M., Golebski, K. & Spits, H. Plasticity of innate lymphoid cell subsets. *Nature Reviews Immunology* **20**, 552-565 (2020).
34. Silver, J.S. *et al.* Inflammatory triggers associated with exacerbations of COPD orchestrate plasticity of group 2 innate lymphoid cells in the lungs. *Nat Immunol* **17**, 626-635 (2016).
35. Cai, T. *et al.* IL-17-producing ST2<sup>+</sup> group 2 innate lymphoid cells play a pathogenic role in lung inflammation. *Journal of allergy and clinical immunology* **143**, 229-244. e229 (2019).
36. Constantinides, M.G., McDonald, B.D., Verhoef, P.A. & Bendelac, A. A committed precursor to innate lymphoid cells. *Nature* **508**, 397-401 (2014).
37. Cherrier, M., Sawa, S. & Eberl, G. Notch, Id2, and ROR $\gamma$ t sequentially orchestrate the fetal development of lymphoid tissue inducer cells. *The Journal of experimental medicine* **209**, 729-740 (2012).
38. Ebihara, T. & Taniuchi, I. Transcription Factors in the Development and Function of Group 2 Innate Lymphoid Cells. *Int J Mol Sci* **20**, 1377 (2019).
39. Walker, J.A. & McKenzie, A.N. Development and function of group 2 innate lymphoid cells. *Curr Opin Immunol*, vol. 25, 2013, pp 148-155.
40. Radtke, F. *et al.* Deficient T cell fate specification in mice with an induced inactivation of Notch1. *Immunity* **10**, 547-558 (1999).
41. Lai, D.-M., Shu, Q. & Fan, J. The origin and role of innate lymphoid cells in the lung. *Mil Med Res* **3**, 25-25 (2016).

42. Huang, Q., Seillet, C. & Belz, G.T. Shaping Innate Lymphoid Cell Diversity. *Front Immunol* **8**, 1569 (2017).
43. Sheikh, A. & Abraham, N. Interleukin-7 Receptor Alpha in Innate Lymphoid Cells: More Than a Marker. *Frontiers in Immunology* **10** (2019).
44. Ishizuka, I.E., Constantinides, M.G., Gudjonson, H. & Bendelac, A. The Innate Lymphoid Cell Precursor. *Annu Rev Immunol* **34**, 299-316 (2016).
45. Yu, Y. *et al.* The transcription factor Bcl11b is specifically expressed in group 2 innate lymphoid cells and is essential for their development. *The Journal of experimental medicine* **212**, 865-874 (2015).
46. Yagi, R. *et al.* The transcription factor GATA3 actively represses RUNX3 protein-regulated production of interferon-gamma. *Immunity* **32**, 507-517 (2010).
47. Ebihara, T. *et al.* Runx3 specifies lineage commitment of innate lymphoid cells. *Nature immunology* **16**, 1124-1133 (2015).
48. Monticelli, L.A. *et al.* Innate lymphoid cells promote lung-tissue homeostasis after infection with influenza virus. *Nat Immunol* **12**, 1045-1054 (2011).
49. Li, B.W.S. *et al.* T cells and ILC2s are major effector cells in influenza-induced exacerbation of allergic airway inflammation in mice. *Eur J Immunol* **49**, 144-156 (2019).
50. Fonseca, W., Lukacs, N.W., Elesela, S. & Malinczak, C.-A. Role of ILC2 in Viral-Induced Lung Pathogenesis. *Frontiers in Immunology* **12** (2021).
51. Sheikh, A., Lu, J., Melese, E., Seo, J.H. & Abraham, N. IL-7 induces type 2 cytokine response in lung ILC2s and regulates GATA3 and CD25 expression. *Journal of Leukocyte Biology* **n/a**.
52. Doherty, T.A. & Broide, D.H. Airway innate lymphoid cells in the induction and regulation of allergy. *Allergology International* **68**, 9-16 (2019).
53. Helfrich, S., Mindt, B.C., Fritz, J.H. & Duerr, C.U. Group 2 Innate Lymphoid Cells in Respiratory Allergic Inflammation. *Frontiers in Immunology* **10** (2019).
54. McKenzie, A.N. Type-2 innate lymphoid cells in asthma and allergy. *Ann Am Thorac Soc* **11 Suppl 5**, S263-270 (2014).
55. Nussbaum, J.C. *et al.* Type 2 innate lymphoid cells control eosinophil homeostasis. *Nature* **502**, 245-248 (2013).

56. Halim, T.Y. *et al.* Group 2 innate lymphoid cells are critical for the initiation of adaptive T helper 2 cell-mediated allergic lung inflammation. *Immunity* **40**, 425-435 (2014).
57. Holgate, S.T. *et al.* Asthma. *Nature Reviews Disease Primers* **1**, 15025 (2015).
58. Bartemes, K.R., Kephart, G.M., Fox, S.J. & Kita, H. Enhanced innate type 2 immune response in peripheral blood from patients with asthma. *J Allergy Clin Immunol* **134**, 671-678.e674 (2014).
59. Rhen, T. & Cidlowski, J.A. Antiinflammatory Action of Glucocorticoids — New Mechanisms for Old Drugs. *New England Journal of Medicine* **353**, 1711-1723 (2005).
60. Kabata, H. *et al.* Thymic stromal lymphopoietin induces corticosteroid resistance in natural helper cells during airway inflammation. *Nature Communications* **4**, 2675 (2013).
61. Liu, S. *et al.* Steroid resistance of airway type 2 innate lymphoid cells from patients with severe asthma: The role of thymic stromal lymphopoietin. *J Allergy Clin Immunol* **141**, 257-268.e256 (2018).
62. Patton, D.T., Plumb, A.W. & Abraham, N. The survival and differentiation of Pro-B and Pre-B cells in the bone marrow is dependent on IL-7R $\alpha$  Tyr449. *The Journal of Immunology* **193**, 3446-3455 (2014).
63. Chen, D., Tang, T.-X., Deng, H., Yang, X.-P. & Tang, Z.-H. Interleukin-7 Biology and Its Effects on Immune Cells: Mediator of Generation, Differentiation, Survival, and Homeostasis. *Frontiers in Immunology* **12** (2021).
64. Willis, C.R. *et al.* Interleukin-7 receptor blockade suppresses adaptive and innate inflammatory responses in experimental colitis. *Journal of Inflammation* **9**, 39 (2012).
65. Sheikh, A. *et al.* Selective dependence on IL-7 for antigen-specific CD8 T cell responses during airway influenza infection. *Scientific Reports* **12**, 135 (2022).
66. Sprent, J. & Surh, C.D. Interleukin 7, maestro of the immune system. *Semin Immunol* **24**, 149-150 (2012).
67. Ziegler, S.F. *et al.* The biology of thymic stromal lymphopoietin (TSLP). *Advances in pharmacology*, vol. 66. Elsevier, 2013, pp 129-155.
68. Zhong, J. *et al.* TSLP signaling pathway map: a platform for analysis of TSLP-mediated signaling. *Database : the journal of biological databases and curation* **2014**, bau007 (2014).
69. Carrette, F. & Surh, C.D. IL-7 signaling and CD127 receptor regulation in the control of T cell homeostasis. *Semin Immunol* **24**, 209-217 (2012).

70. Harly, C., Cam, M., Kaye, J. & Bhandoola, A. Development and differentiation of early innate lymphoid progenitors. *J Exp Med* **215**, 249-262 (2018).
71. Diefenbach, A., Colonna, M. & Koyasu, S. Development, Differentiation, and Diversity of Innate Lymphoid Cells. *Immunity* **41**, 354-365 (2014).
72. Koga, S. *et al.* Peripheral PDGFR $\alpha$ +gp38+ mesenchymal cells support the differentiation of fetal liver-derived ILC2. *Journal of Experimental Medicine* **215**, 1609-1626 (2018).
73. Garrido-Mesa, N. *et al.* T-bet controls intestinal mucosa immune responses via repression of type 2 innate lymphoid cell function. *Mucosal immunology* **12**, 51-63 (2019).
74. Pellegrini, M. *et al.* Adjuvant IL-7 antagonizes multiple cellular and molecular inhibitory networks to enhance immunotherapies. *Nature Medicine* **15**, 528-536 (2009).
75. Melchionda, F. *et al.* Adjuvant IL-7 or IL-15 overcomes immunodominance and improves survival of the CD8+ memory cell pool. *The Journal of Clinical Investigation* **115**, 1177-1187 (2005).
76. Nanjappa, S.G., Walent, J.H., Morre, M. & Suresh, M. Effects of IL-7 on memory CD8 T cell homeostasis are influenced by the timing of therapy in mice. *J Clin Invest* **118**, 1027-1039 (2008).
77. Mackall, C.L., Fry, T.J. & Gress, R.E. Harnessing the biology of IL-7 for therapeutic application. *Nat Rev Immunol* **11**, 330-342 (2011).
78. ElKassar, N. & Gress, R.E. An overview of IL-7 biology and its use in immunotherapy. *J Immunotoxicol* **7**, 1-7 (2010).
79. Barata, J.T., Durum, S.K. & Seddon, B. Flip the coin: IL-7 and IL-7R in health and disease. *Nature Immunology* **20**, 1584-1593 (2019).
80. Laterre, P.F. *et al.* Association of Interleukin 7 Immunotherapy With Lymphocyte Counts Among Patients With Severe Coronavirus Disease 2019 (COVID-19). *JAMA Network Open* **3**, e2016485-e2016485 (2020).
81. Mazer, M.B. *et al.* Interleukin-7 Reverses Lymphopenia and Improves T-Cell Function in Coronavirus Disease 2019 Patient With Inborn Error of Toll-Like Receptor 3: A Case Report. *Critical Care Explorations* **3**, e0500 (2021).
82. Cantuti-Castelvetri, L. *et al.* Neuropilin-1 facilitates SARS-CoV-2 cell entry and infectivity. *Science* **370**, 856-860 (2020).

83. Sportès, C. *et al.* Administration of rhIL-7 in humans increases in vivo TCR repertoire diversity by preferential expansion of naive T cell subsets. *J Exp Med* **205**, 1701-1714 (2008).
84. Rosenberg, S.A. *et al.* IL-7 administration to humans leads to expansion of CD8+ and CD4+ cells but a relative decrease of CD4+ T-regulatory cells. *J Immunother* **29**, 313-319 (2006).
85. Bajgain, P. *et al.* CAR T cell therapy for breast cancer: harnessing the tumor milieu to drive T cell activation. *Journal for ImmunoTherapy of Cancer* **6**, 34 (2018).
86. Dwyer, C.J. *et al.* Fueling Cancer Immunotherapy With Common Gamma Chain Cytokines. *Frontiers in Immunology* **10** (2019).
87. ClinicalTrials.gov. CYT107 After Vaccine Treatment (Provenge®) in Patients With Metastatic Castration-Resistant Prostate Cancer. [Clinical trial] 2013 2019 [cited] Available from: <https://clinicaltrials.gov/ct2/show/NCT01881867>
88. Miller, C.N. *et al.* IL-7 production in murine lymphatic endothelial cells and induction in the setting of peripheral lymphopenia. *Int Immunol* **25**, 471-483 (2013).
89. Osborne, L.C. *et al.* Impaired CD8 T cell memory and CD4 T cell primary responses in IL-7R alpha mutant mice. *J Exp Med* **204**, 619-631 (2007).
90. Rich, B.E., Campos-Torres, J., Tepper, R.I., Moreadith, R.W. & Leder, P. Cutaneous lymphoproliferation and lymphomas in interleukin 7 transgenic mice. *J Exp Med* **177**, 305-316 (1993).
91. Grosschedl, R., Weaver, D., Baltimore, D. & Costantini, F. Introduction of a  $\mu$  immunoglobulin gene into the mouse germ line: Specific expression in lymphoid cells and synthesis of functional antibody. *Cell* **38**, 647-658 (1984).
92. Carpino, N. *et al.* Absence of an essential role for thymic stromal lymphopoietin receptor in murine B-cell development. *Mol Cell Biol* **24**, 2584-2592 (2004).
93. Vuilleumier, R. *et al.* Retrograde BMP signaling activates neuronal gene expression through widespread deployment of a conserved BMP-responsive cis-regulatory activation element. *Nucleic Acids Res* **47**, 679-699 (2019).
94. Chen, S., Zhou, Y., Chen, Y. & Gu, J. fastp: an ultra-fast all-in-one FASTQ preprocessor. *Bioinformatics* **34**, i884-i890 (2018).
95. FastQC. 2015 Jun [cited] Available from: <https://qubeshub.org/resources/fastqc>

96. Andrews, S. FastQC: A Quality Control Tool for High Throughput Sequence Data [Online]. 2010 [cited] Available from: <http://www.bioinformatics.babraham.ac.uk/projects/fastqc/>
97. Dobin, A. *et al.* STAR: ultrafast universal RNA-seq aligner. *Bioinformatics* **29**, 15-21 (2012).
98. Kim, D., Paggi, J.M., Park, C., Bennett, C. & Salzberg, S.L. Graph-based genome alignment and genotyping with HISAT2 and HISAT-genotype. *Nature Biotechnology* **37**, 907-915 (2019).
99. Li, B. & Dewey, C.N. RSEM: accurate transcript quantification from RNA-Seq data with or without a reference genome. *BMC Bioinformatics* **12**, 323 (2011).
100. Bray, N.L., Pimentel, H., Melsted, P. & Pachter, L. Near-optimal probabilistic RNA-seq quantification. *Nature Biotechnology* **34**, 525-527 (2016).
101. Patro, R., Duggal, G., Love, M.I., Irizarry, R.A. & Kingsford, C. Salmon provides fast and bias-aware quantification of transcript expression. *Nature methods* **14**, 417-419 (2017).
102. Pertea, M., Kim, D., Pertea, G.M., Leek, J.T. & Salzberg, S.L. Transcript-level expression analysis of RNA-seq experiments with HISAT, StringTie and Ballgown. *Nat Protoc* **11**, 1650-1667 (2016).
103. Pertea, M. *et al.* StringTie enables improved reconstruction of a transcriptome from RNA-seq reads. *Nature Biotechnology* **33**, 290-295 (2015).
104. Love, M.I., Huber, W. & Anders, S. Moderated estimation of fold change and dispersion for RNA-seq data with DESeq2. *Genome Biology* **15**, 550 (2014).
105. Chen, Y., Lun, A. & Smyth, G. From reads to genes to pathways: differential expression analysis of RNA-Seq experiments using Rsubread and the edgeR quasi-likelihood pipeline [version 2; peer review: 5 approved]. *F1000Research* **5** (2016).
106. Robinson, M.D., McCarthy, D.J. & Smyth, G.K. edgeR: a Bioconductor package for differential expression analysis of digital gene expression data. *Bioinformatics* **26**, 139-140 (2009).
107. McCarthy, D.J., Chen, Y. & Smyth, G.K. Differential expression analysis of multifactor RNA-Seq experiments with respect to biological variation. *Nucleic Acids Research* **40**, 4288-4297 (2012).
108. Team, R. RStudio: Integrated Development for R. RStudio, PBC Boston, MA. 2020.

109. Wickham, H. *ggplot2: Elegant Graphics for Data Analysis*. Springer-Verlag New York; 2016.
110. Kolde, R. *pheatmap: Pretty Heatmaps*. 2019.
111. Spandidos, A., Wang, X., Wang, H. & Seed, B. PrimerBank: a resource of human and mouse PCR primer pairs for gene expression detection and quantification. *Nucleic Acids Research* **38**, D792-D799 (2009).
112. Spandidos, A. *et al.* A comprehensive collection of experimentally validated primers for Polymerase Chain Reaction quantitation of murine transcript abundance. *BMC Genomics* **9**, 633 (2008).
113. Wang, X. & Seed, B. A PCR primer bank for quantitative gene expression analysis. *Nucleic Acids Res* **31**, e154 (2003).
114. Chen, X. *et al.* Host Immune Response to Influenza A Virus Infection. *Frontiers in Immunology* **9** (2018).
115. Castellanos, J.G. & Longman, R.S. The balance of power: innate lymphoid cells in tissue inflammation and repair. *J Clin Invest* **129**, 2640-2650 (2019).
116. Jiang, Q. *et al.* Cell biology of IL-7, a key lymphotrophin. *Cytokine Growth Factor Rev* **16**, 513-533 (2005).
117. Robinette, M.L. *et al.* IL-15 sustains IL-7R-independent ILC2 and ILC3 development. *Nat Commun* **8**, 14601 (2017).
118. Sheikh, A., Lu, J., Melese, E., Seo, J.H. & Abraham, N. IL-7 induces type 2 cytokine response in lung ILC2s and regulates GATA3 and CD25 expression. *Journal of Leukocyte Biology* (2022 (In press)).
119. Zhu, J. GATA3 Regulates the Development and Functions of Innate Lymphoid Cell Subsets at Multiple Stages. *Front Immunol* **8** (2017).
120. Vilsmaier, T. *et al.* The decidual expression of Interleukin-7 is upregulated in early pregnancy loss. *Am J Reprod Immunol* **86**, e13437 (2021).
121. Apostol, A.C., Jensen, K.D.C. & Beaudin, A.E. Training the Fetal Immune System Through Maternal Inflammation—A Layered Hygiene Hypothesis. *Frontiers in Immunology* **11** (2020).
122. Geiselhart, L.A. *et al.* IL-7 Administration Alters the CD4:CD8 Ratio, Increases T Cell Numbers, and Increases T Cell Function in the Absence of Activation. *The Journal of Immunology* **166**, 3019-3027 (2001).



123. Aspinall, R., Prentice, A.M. & Ngom, P.T. Interleukin 7 from Maternal Milk Crosses the Intestinal Barrier and Modulates T-Cell Development in Offspring. *PLOS ONE* **6**, e20812 (2011).
124. Marković, I. & Savvides, S.N. Modulation of Signaling Mediated by TSLP and IL-7 in Inflammation, Autoimmune Diseases, and Cancer. *Front Immunol* **11**, 1557 (2020).
125. Lundström, W., Fewkes, N.M. & Mackall, C.L. IL-7 in human health and disease. *Semin Immunol* **24**, 218-224 (2012).
126. Buckley, R.H. Molecular Defects in Human Severe Combined Immunodeficiency and Approaches to Immune Reconstitution. *Annual Review of Immunology* **22**, 625-655 (2004).
127. Mitchell, P.D. & O'Byrne, P.M. Biologics and the lung: TSLP and other epithelial cell-derived cytokines in asthma. *Pharmacology & Therapeutics* **169**, 104-112 (2017).
128. Zhang, Y. & Zhou, B. Functions of thymic stromal lymphopoietin in immunity and disease. *Immunol Res* **52**, 211-223 (2012).
129. Massacand, J.C. *et al.* Helminth products bypass the need for TSLP in Th2 immune responses by directly modulating dendritic cell function. *Proc Natl Acad Sci U S A* **106**, 13968-13973 (2009).
130. Zaph, C. *et al.* Epithelial-cell-intrinsic IKK-beta expression regulates intestinal immune homeostasis. *Nature* **446**, 552-556 (2007).
131. Taylor, B.C. *et al.* TSLP regulates intestinal immunity and inflammation in mouse models of helminth infection and colitis. *J Exp Med* **206**, 655-667 (2009).
132. Mousset, C.M. *et al.* Comprehensive Phenotyping of T Cells Using Flow Cytometry. *Cytometry A* **95**, 647-654 (2019).
133. Halim, T.Y., Krauss, R.H., Sun, A.C. & Takei, F. Lung natural helper cells are a critical source of Th2 cell-type cytokines in protease allergen-induced airway inflammation. *Immunity* **36**, 451-463 (2012).
134. Ricardo-Gonzalez, R.R. *et al.* Tissue signals imprint ILC2 identity with anticipatory function. *Nat Immunol* **19**, 1093-1099 (2018).
135. Kotas, M.E. *et al.* CISH constrains the tuft-ILC2 circuit to set epithelial and immune tone. *Mucosal immunology* **14**, 1295-1305 (2021).

136. Li, W. *et al.* Periostin: its role in asthma and its potential as a diagnostic or therapeutic target. *Respiratory Research* **16**, 57 (2015).
137. Gour, N. *et al.* C3a is required for ILC2 function in allergic airway inflammation. *Mucosal immunology* **11**, 1653-1662 (2018).
138. Ciferri, C. *et al.* Implications for Kinetochore-Microtubule Attachment from the Structure of an Engineered Ndc80 Complex. *Cell* **133**, 427-439 (2008).
139. Kwon, S. *et al.* Identification of a functionally relevant signal peptide of mouse ficolin A. *J Biochem Mol Biol* **40**, 532-538 (2007).
140. Zhang, K. *et al.* A functional circuit formed by the autonomic nerves and myofibroblasts controls mammalian alveolar formation for gas exchange. *Dev Cell* **57**, 1566-1581.e1567 (2022).
141. Kawai, J. *et al.* Functional annotation of a full-length mouse cDNA collection. *Nature* **409**, 685-690 (2001).
142. Yang, D.S. *et al.* Quadruped Gait and Regulation of Apoptotic Factors in Tibiofemoral Joints following Intra-Articular rhPRG4 Injection in Prg4 Null Mice. *Int J Mol Sci* **23** (2022).
143. Wipff, J., Allanore, Y. & Boileau, C. [Interactions between fibrillin-1 and tgf-beta: consequences and human pathology]. *Med Sci (Paris)* **25**, 161-167 (2009).
144. Wada, F. *et al.* Myosin Va and Endoplasmic Reticulum Calcium Channel Complex Regulates Membrane Export during Axon Guidance. *Cell Reports* **15**, 1329-1344 (2016).
145. Kong, F.Q. *et al.* Macrophage MSR1 promotes the formation of foamy macrophage and neuronal apoptosis after spinal cord injury. *J Neuroinflammation* **17**, 62 (2020).
146. Durst, R. *et al.* Increased risk for atherosclerosis of various macrophage scavenger receptor 1 alleles. *Genet Test Mol Biomarkers* **13**, 583-587 (2009).
147. Miron, J., Picard, C., Labonté, A., Auld, D. & Poirier, J. MSR1 and NEP Are Correlated with Alzheimer's Disease Amyloid Pathology and Apolipoprotein Alterations. *J Alzheimers Dis* **86**, 283-296 (2022).
148. Konstantelou, E. *et al.* Serum periostin in patients hospitalized for COPD exacerbations. *Cytokine* **93**, 51-56 (2017).
149. Liu, C., Chen, Z., Ding, X., Qiao, Y. & Li, B. Ubiquitin-specific protease 35 (USP35) mediates cisplatin-induced apoptosis by stabilizing BIRC3 in non-small cell lung cancer. *Lab Invest* **102**, 524-533 (2022).

150. Thompson, C.L. *et al.* A high-resolution spatiotemporal atlas of gene expression of the developing mouse brain. *Neuron* **83**, 309-323 (2014).
151. Williams, A.J., Blacklow, S.C. & Collins, T. The zinc finger-associated SCAN box is a conserved oligomerization domain. *Mol Cell Biol* **19**, 8526-8535 (1999).
152. Holm, D., Fink, D.R., Grønlund, J., Hansen, S. & Holmskov, U. Cloning and characterization of SCART1, a novel scavenger receptor cysteine-rich type I transmembrane molecule. *Mol Immunol* **46**, 1663-1672 (2009).
153. Gorelik, A., Heinz, L.X., Illes, K., Superti-Furga, G. & Nagar, B. Crystal Structure of the Acid Sphingomyelinase-like Phosphodiesterase SMPDL3B Provides Insights into Determinants of Substrate Specificity. *J Biol Chem* **291**, 24054-24064 (2016).
154. Liu, Z.H. *et al.* RASSF7 expression and its regulatory roles on apoptosis in human intervertebral disc degeneration. *Int J Clin Exp Pathol* **8**, 16097-16103 (2015).
155. Corry, D.B. & Kheradmand, F. INTERLEUKINS | IL-13. In: Laurent, G.J. & Shapiro, S.D. (eds). *Encyclopedia of Respiratory Medicine*. Academic Press: Oxford, 2006, pp 382-385.
156. Sudo, T. *et al.* Group 2 innate lymphoid cells support hematopoietic recovery under stress conditions. *Journal of Experimental Medicine* **218** (2021).
157. Schubert, K. *et al.* Thy-1 (CD90) regulates the extravasation of leukocytes during inflammation. *Eur J Immunol* **41**, 645-656 (2011).
158. Califano, D. *et al.* Transcription Factor Bcl11b Controls Identity and Function of Mature Type 2 Innate Lymphoid Cells. *Immunity* **43**, 354-368 (2015).
159. Miyajima, Y. *et al.* Effects of BMP7 produced by group 2 innate lymphoid cells on adipogenesis. *Int Immunol* **32**, 407-419 (2020).
160. Meunier, S. *et al.* Maintenance of Type 2 Response by CXCR6-Deficient ILC2 in Papain-Induced Lung Inflammation. *Int J Mol Sci* **20** (2019).
161. Ikutani, M. *et al.* Prolonged activation of IL-5-producing ILC2 causes pulmonary arterial hypertrophy. *JCI Insight* **2**, e90721 (2017).
162. Penninger, J.M., Irie-Sasaki, J., Sasaki, T. & Oliveira-dos-Santos, A.J. CD45: new jobs for an old acquaintance. *Nature Immunology* **2**, 389-396 (2001).

163. Zook, E.C. *et al.* The ETS1 transcription factor is required for the development and cytokine-induced expansion of ILC2. *Journal of Experimental Medicine* **213**, 687-696 (2016).
164. Turner, J.E. *et al.* IL-9-mediated survival of type 2 innate lymphoid cells promotes damage control in helminth-induced lung inflammation. *J Exp Med* **210**, 2951-2965 (2013).
165. Polte, T., Behrendt, A.K. & Hansen, G. Direct evidence for a critical role of CD30 in the development of allergic asthma. *J Allergy Clin Immunol* **118**, 942-948 (2006).
166. Wallrapp, A. *et al.* The neuropeptide NMU amplifies ILC2-driven allergic lung inflammation. *Nature* **549**, 351-356 (2017).
167. Pelly, V.S. *et al.* IL-4-producing ILC2s are required for the differentiation of TH2 cells following *Heligmosomoides polygyrus* infection. *Mucosal immunology* **9**, 1407-1417 (2016).
168. Noval Rivas, M., Burton, O.T., Oettgen, H.C. & Chatila, T. IL-4 production by group 2 innate lymphoid cells promotes food allergy by blocking regulatory T-cell function. *J Allergy Clin Immunol* **138**, 801-811.e809 (2016).
169. Xu, H. *et al.* Interleukin-33 contributes to ILC2 activation and early inflammation-associated lung injury during abdominal sepsis. *Immunol Cell Biol* **96**, 935-947 (2018).
170. Collins, S.A., Lockett, G.A. & Holloway, J.W. 3 - The Genetics of Allergic Disease and Asthma. In: Leung, D.Y.M., Szeftler, S.J., Bonilla, F.A., Akdis, C.A. & Sampson, H.A. (eds). *Pediatric Allergy: Principles and Practice (Third Edition)*. Elsevier: London, 2016, pp 18-30.e14.
171. Patial, S. *et al.* Myeloid-IL4R $\alpha$  is an indispensable link in IL-33-ILCs-IL-13-IL4R $\alpha$  axis of eosinophil recruitment in murine lungs. *Sci Rep* **11**, 15465 (2021).
172. Ferreira, A.C.F. *et al.* ROR $\alpha$  is a critical checkpoint for T cell and ILC2 commitment in the embryonic thymus. *Nat Immunol* **22**, 166-178 (2021).
173. Pesce, J.T. *et al.* Retnla (Relma/Fizz1) Suppresses Helminth-Induced Th2-Type Immunity. *PLOS Pathogens* **5**, e1000393 (2009).
174. Wang, Q., Mergia, E., Koesling, D. & Mittmann, T. Nitric oxide/cGMP signaling via guanylyl cyclase isoform 1 modulates glutamate and GABA release in somatosensory cortex of mice. *Neuroscience* **360**, 180-189 (2017).

175. Chugh, D. *et al.* Voluntary wheel running with and without follistatin overexpression improves NMJ transmission but not motor unit loss in late life of C57BL/6J mice. *Neurobiol Aging* **101**, 285-296 (2021).
176. Leatherdale, A. *et al.* Multimerin 1 supports platelet function in vivo and binds to specific GPAGPOGPX motifs in fibrillar collagens that enhance platelet adhesion. *J Thromb Haemost* **19**, 547-561 (2021).
177. Takahashi, N. *et al.* ZNF445 is a primary regulator of genomic imprinting. *Genes Dev* **33**, 49-54 (2019).
178. Velotti, F., Barchetta, I., Cimini, F.A. & Cavallo, M.G. Granzyme B in Inflammatory Diseases: Apoptosis, Inflammation, Extracellular Matrix Remodeling, Epithelial-to-Mesenchymal Transition and Fibrosis. *Frontiers in Immunology* **11** (2020).
179. Rheault, M.N. *et al.* Mouse Model of X-Linked Alport Syndrome. *Journal of the American Society of Nephrology* **15**, 1466-1474 (2004).
180. Francone, O.L. *et al.* Disruption of the murine procollagen C-proteinase enhancer 2 gene causes accumulation of pro-apoA-I and increased HDL levels. *J Lipid Res* **52**, 1974-1983 (2011).
181. Yin, H. *et al.* A homozygous FANCM frameshift pathogenic variant causes male infertility. *Genet Med* **21**, 62-70 (2019).
182. Camara, A. *et al.* CD169(+) macrophages in lymph node and spleen critically depend on dual RANK and LTbetaR signaling. *Proc Natl Acad Sci U S A* **119** (2022).
183. Babazadeh, S. *et al.* Macrophage polarization by MSC-derived CXCL12 determines tumor growth. *Cell Mol Biol Lett* **26**, 30 (2021).
184. He, X., Kuo, Y.C., Rosche, T.J. & Zhang, X. Structural basis for autoinhibition of the guanine nucleotide exchange factor FARP2. *Structure* **21**, 355-364 (2013).
185. Klyuyeva, A.V. *et al.* Changes in retinoid metabolism and signaling associated with metabolic remodeling during fasting and in type I diabetes. *J Biol Chem* **296**, 100323 (2021).
186. Matsumoto, H. Roles of Periostin in Asthma. *Adv Exp Med Biol* **1132**, 145-159 (2019).
187. Hams, E. *et al.* IL-25 and type 2 innate lymphoid cells induce pulmonary fibrosis. *Proc Natl Acad Sci U S A* **111**, 367-372 (2014).
188. Conway, S.J. *et al.* The role of periostin in tissue remodeling across health and disease. *Cell Mol Life Sci* **71**, 1279-1288 (2014).

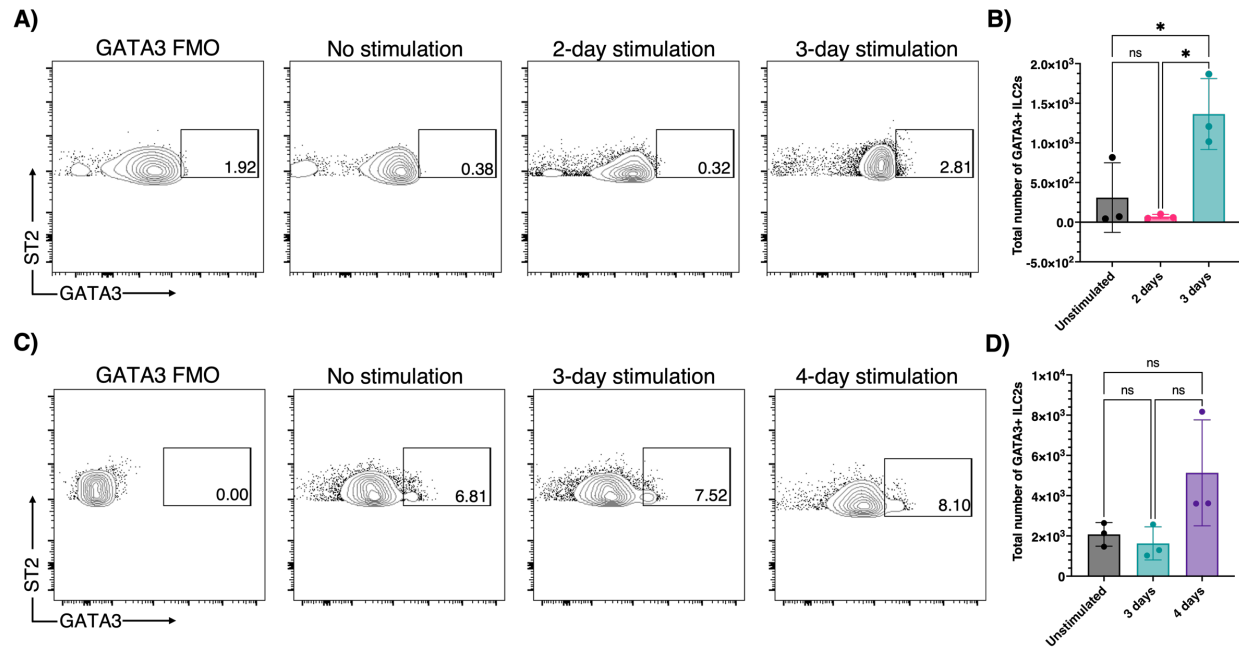
189. Camelo, A. *et al.* IL-33, IL-25, and TSLP induce a distinct phenotypic and activation profile in human type 2 innate lymphoid cells. *Blood Adv* **1**, 577-589 (2017).
190. Holcomb, I.N. *et al.* FIZZ1, a novel cysteine-rich secreted protein associated with pulmonary inflammation, defines a new gene family. *The EMBO Journal* **19**, 4046-4055 (2000).
191. Nair, M.G. *et al.* Alternatively activated macrophage-derived RELM- $\alpha$  is a negative regulator of type 2 inflammation in the lung. *Journal of Experimental Medicine* **206**, 937-952 (2009).
192. Seehus, C.R. *et al.* Alternative activation generates IL-10 producing type 2 innate lymphoid cells. *Nature Communications* **8**, 1900 (2017).
193. Di Censo, C. *et al.* Granzyme A and CD160 expression delineates ILC1 with graded functions in the mouse liver. *Eur J Immunol* **51**, 2568-2575 (2021).
194. Castleman, M.J. *et al.* Enteric bacteria induce IFN $\gamma$  and Granzyme B from human colonic Group 1 Innate Lymphoid Cells. *Gut Microbes* **12**, 1667723 (2020).
195. 5 - Intraperitoneal Drug Administration. In: Claassen, V. (ed). *Techniques in the Behavioral and Neural Sciences*, vol. 12. Elsevier, 1994, pp 46-58.
196. Headley, M.B. *et al.* TSLP Conditions the Lung Immune Environment for the Generation of Pathogenic Innate and Antigen-Specific Adaptive Immune Responses. *The Journal of Immunology* **182**, 1641-1647 (2009).
197. Han, H. *et al.* Thymic Stromal Lymphopoietin Amplifies the Differentiation of Alternatively Activated Macrophages. *The Journal of Immunology* **190**, 904-912 (2013).
198. Saez, A. *et al.* Innate Lymphoid Cells in Intestinal Homeostasis and Inflammatory Bowel Disease. *Int J Mol Sci* **22** (2021).
199. Corren, J. *et al.* Lebrikizumab treatment in adults with asthma. *N Engl J Med* **365**, 1088-1098 (2011).
200. Marone, G. *et al.* Tezepelumab: a novel biological therapy for the treatment of severe uncontrolled asthma. *Expert Opin Investig Drugs* **28**, 931-940 (2019).
201. Gauvreau, G.M. *et al.* Effects of an Anti-TSLP Antibody on Allergen-Induced Asthmatic Responses. *New England Journal of Medicine* **370**, 2102-2110 (2014).

202. De Pasquale, C., Campana, S., Bonaccorsi, I., Carrega, P. & Ferlazzo, G. ILC in chronic inflammation, cancer and targeting with biologicals. *Molecular Aspects of Medicine* **80**, 100963 (2021).
203. An, G. *et al.* Combined blockade of IL-25, IL-33 and TSLP mediates amplified inhibition of airway inflammation and remodelling in a murine model of asthma. *Respirology* **25**, 603-612 (2020).
204. Ellestad, K.K. & Anderson, C.C. Two Strikes and You're Out? The Pathogenic Interplay of Coinhibitor Deficiency and Lymphopenia-Induced Proliferation. *The Journal of Immunology* **198**, 2534-2541 (2017).
205. Osborne, L.C., Patton, D.T., Seo, J.H. & Abraham, N. Elevated IL-7 Availability Does Not Account for T Cell Proliferation in Moderate Lymphopenia. *The Journal of Immunology* **186**, 1981-1988 (2011).
206. Lundmark, F. *et al.* Variation in interleukin 7 receptor  $\alpha$  chain (IL7R) influences risk of multiple sclerosis. *Nature Genetics* **39**, 1108-1113 (2007).
207. Kelly, E.A. *et al.* Potential contribution of IL-7 to allergen-induced eosinophilic airway inflammation in asthma. *J Immunol* **182**, 1404-1410 (2009).
208. Monti, P. & Bonifacio, E. Interleukin-7 and Type 1 Diabetes. *Current Diabetes Reports* **14**, 518 (2014).
209. Schreiber, M. *et al.* Inducible IL-7 Hyperexpression Influences Lymphocyte Homeostasis and Function and Increases Allograft Rejection. *Frontiers in Immunology* **10** (2019).
210. Gomez-Cadena, A. *et al.* Severe COVID-19 patients exhibit an ILC2 NKG2D<sup>+</sup> population in their impaired ILC compartment. *Cellular & Molecular Immunology* **18**, 484-486 (2021).
211. Lélou, K. *et al.* Viral Delivery of IL-7 Is a Potent Immunotherapy Stimulating Innate and Adaptive Immunity and Confers Survival in Sepsis Models. *J Immunol* **209**, 99-117 (2022).
212. Roy, S. *et al.* Viral vector and route of administration determine the ILC and DC profiles responsible for downstream vaccine-specific immune outcomes. *Vaccine* **37**, 1266-1276 (2019).
213. Frati, F. *et al.* The Role of the Microbiome in Asthma: The Gut-Lung Axis. *Int J Mol Sci* **20** (2018).
214. Barcik, W., Boutin, R.C.T., Sokolowska, M. & Finlay, B.B. The Role of Lung and Gut Microbiota in the Pathology of Asthma. *Immunity* **52**, 241-255 (2020).

215. Carleton, K.L. Quantification of Transcript Levels with Quantitative RT-PCR. In: Orgogozo, V. & Rockman, M.V. (eds). *Molecular Methods for Evolutionary Genetics*. Humana Press: Totowa, NJ, 2011, pp 279-295.
216. Pallard, C. *et al.* Distinct Roles of the Phosphatidylinositol 3-Kinase and STAT5 Pathways in IL-7-Mediated Development of Human Thymocyte Precursors. *Immunity* **10**, 525-535 (1999).
217. Hosokawa, H. *et al.* Akt1-mediated Gata3 phosphorylation controls the repression of IFN $\gamma$  in memory-type Th2 cells. *Nat Commun* **7**, 11289 (2016).
218. Liberman, A.C., Druker, J., Refojo, D., Holsboer, F. & Arzt, E. Glucocorticoids inhibit GATA-3 phosphorylation and activity in T cells. *Faseb j* **23**, 1558-1571 (2009).



## Appendix: 4-day *in vivo* intranasal IL-7 stimulation of lung ILC2s



**4-day *in vivo* intranasal IL-7 stimulation of lung ILC2s.** WT mice were given a single 2 $\mu$ g IL-7 intranasally before lungs were collected on indicated timepoint. **A)** Representative flow cytometry plots showing GATA3 expression in IL-7 stimulated lung ILC2s at 2- and 3-days post-stimulation. **B)** Total number of GATA3+ lung ILC2s after 2- and 3-day IL-7 stimulation. **C)** Representative flow cytometry plots showing GATA3 expression in IL-7 stimulated lung ILC2s at 3- and 4-days post-stimulation. **D)** Total number of GATA3+ lung ILC2s after 3- and 4-day IL-7 stimulation. These experiments were done in duplicate and Multiple Student's *t*-test and one-way ANOVA was performed for each set of data.